2017

INVESTIGATION OF THE STRESS-INDUCED NUCLEAR

LOCALISATION OF RETINOBLASTOMA BINDING PROTEIN 6 (RBBP6)

AND ITS ROLE IN UBIQUITINATION OF Y-BOX BINDING PROTEIN-1

(YB-1)

Tephney Gladness Mahomedy

Thesis presented in fulfillment of the requirements for the degree of

Master of Science in Biotechnology

Faculty of Natural Sciences

University of the Western Cape

Supervisor   : Prof. D J. R. Pugh

Date   : December 2017

ABSTRACT

Investigation of the stress-induced nuclear localisation of

Retinoblastoma Binding Protein 6 (RBBP6) and its role in ubiquitination of

Y-Box Binding Protein-1 (YB-1)

T. G Mahomedy, MSc Biotechnology thesis, Department of Biotechnology, Faculty of

Natural Sciences, University of the Western Cape

Retinoblastoma Binding Protein 6 (RBBP6) is a 200 kDa RING finger-containing human protein known to serve as an E3 ubiquitin ligase, and to play a role in ubiquitination and suppression of the tumour suppressor p53. It also regulates the stability of mRNA transcripts by modulating 3'-polyadenylation.

The human RBBP6 gene codes for four protein products, denoted isoforms 1-4. Isoform 1 is 1792 amino acids in length and corresponds to the full-length protein, including the ubiquitin-like DWNN domain found at the N-terminus. In contrast, isoform 3 contains only 118 residues and consists predominantly of the DWNN domain, followed by a 37-residue C-terminal tail, of which the final 17 residues are not found in any of the other isoforms. At the C-terminus of the DWNN domain is a di-glycine (Gly-Gly) motif found in the equivalent position to that in ubiquitin, raising the possibility that it may play a role in the covalent attachment of the DWNN domain to other proteins, in a process analogous to ubiquitination.

RBBP6 has previously been characterized as a nuclear protein, localizing in punctate bodies known as nuclear speckles. However, previous investigations in our laboratory have suggested that isoform 3 is predominantly cytoplasmic, but accumulates in nuclear speckles following stress.

Y-Box Binding Protein-1 (YB-1) is an oncogenic transcription factor known to play an aggravating role in a number of cancers and identified as a potential target for therapeutic intervention. RBBP6 has been shown to interact with YB-1 *in vivo*, causing its ubiquitination and consequent degradation in the proteasome. *In vitro* studies have shown that the R3 fragment of RBBP6, which consists of the DWNN, zinc finger and RING finger domains, is able to poly-ubiquitinate YB-1 using UbcH1 as ubiquitin-conjugating (E2) enzyme. UbcH1 is an unusual E2 enzyme in that it contains an ubiquitin-associated domain (UBA), which is known to bind to ubiquitin, in addition to the catalytic domain. This has led to the hypothesis that an interaction between the UBA of UbcH1 and the DWNN domain of RBBP6 promotes the ubiquitination activity of RBBP6 in combination with UbcH1.

This study focused on two questions of interest: first, does the DWNN domain of RBBP6 interact with the UBA domain of UbcH1 *in vitro*? In order to do test this hypothesis, both domains were expressed in bacteria as fusions with glutathione S-transferase (GST) and GST pull-down assays were used to investigate the interaction. Surprisingly, no interaction was found between the DWNN domain and the UBA, but a clear interaction was observed between the zinc finger of RBBP6 and the UBA.

iii

The second question investigated was whether the Gly-Gly motif at the C-terminus of the DWNN domain plays a role in the localisation of isoform 3. Three mammalian expression constructs were generated and their localisations investigated using immunofluorescence microscopy. Detection was carried out using haemagglutinin (HA) immuno-tags attached to the N-termini of the exogenous proteins. The constructs were HA-DWNN13, which corresponds to wild-type isoform 3; HA-DWNN-PI, a truncation of the C-terminus immediately before the Gly-Gly motif, and HA-DWNN13-AA, a replacement of the C-terminal Gly-Gly with Ala-Ala, leaving the rest of isoform 3 intact.

Our results show that HA-tagged isoform 3 (HA-DWNN13), like the endogenous isoform 3, is predominantly cytoplasmic in resting cells but is also present in speckle-like bodies within the nucleus. Co-localisation studies with SC35, a splicing factor commonly used as a marker for nuclear speckles, confirmed that these speckle-like bodies are indeed nuclear speckles, also known as splicing speckles. Replacement of the di-glycine motif with di-alanine had no observable effect on the localisation of isoform 3, which suggests that the di-glycine motif does not play a functional role in the localisation of the protein. However removal of the GG motif and the rest of the C-terminus of isoform 3 (HA-DWNN-PI) produced a very different phenotype, in which the protein was distributed uniformly across the cytoplasm and the nucleus, with no sign of speckling in the nucleus. This suggests that the C-terminal tail plays a role in the localisation of isoform 3, in particular by causing it to be exported from the nucleus.

Keywords: RBBP6, YB-1, ubiquitination, heat shock response, nuclear speckles.

DECLARATION

I declare that *"Investigation of the stress-induced nuclear localisation of Retinoblastoma Binding Protein 6 (RBBP6) and its role in ubiquitination of Y-Box Binding protein-1 (YB-1)"* is my own work that has not been submitted for any degree or examination in any other university, and that all the sources I have used or quoted have been indicated or acknowledged by complete references.

Tephney Gladness Mahomedy

Date….…December 2017……….

Signed……………………….

v

ACKNOWLEDGEMENTS

This completed work would not have been possible without the help of my heavenly father who has equipped me with everything to overcome all challenges I faced during the course of this study triumphantly. There are a number of people who have contributed towards this work: both small and great and wish to acknowledge the following:

My supervisor Professor David Pugh, thank you for the supervision and guidance during the project. Your office door was always open and your support does not go unnoticed. Thank you for keeping me on my toes by continually asking "how are things" each time you saw me. The project would not have been a success without your constant support and timely provision of reagents. Professor Mervin Meyer, thank you for opening the doors of cell culture lab as well as provision of reagents. Your guidance with transfections does not go unnoticed, thank you.

Miss Andronica Ramalia, thank you for cell culture training. Indeed you were a help in times of need. Mr Mihlali Mlaza (my little brother), thank you for your all round assistance especially with cell culture, I cannot quantify how much, you and I both know. Miss Ania Szmyd-Potapczyk, thank you for your kind suggestions with transfections as well as preparing slides for immunofluorescence and the other tricks you shared. Dr Andrew Faro, thank you for your all round support and constant motivation. You were truly there in every challenge I faced throughout the course of the project. Thank you for listening to my whining and moaning each time my experiments

did not work. The rest of the cancer signaling laboratory members, thank you very much for your characters and personalities which made it very easy to develop working relationships and even beyond. You provided a perfect environment to work in and I appreciate your spirit of unity. To the rest of the Biotechnology department, I return a heart-felt gratitude for providing long lasting memories. The school of postgraduate studies thank you for your support especially with the thesis write-up. You made me believe that with every beginning, there is surely an end. Thank you.

My friends, Emmanuel Ameh, Zintle Kolo, Roland Missengue, Tamanda Mtotha and Chimpape Lombe. Thank you for your support. Especially Chipampe "Chips", Emmanuel "Emma" and Roland "Ro" thank you for being truly friends indeed. My parents (Mr and Mrs Mahomedy) thank you for allowing me to pursue my dreams. I know you did you fully understand my work nevertheless you believed in me. To my siblings: Success, Eucrecia and Prosperity Mahomedy. Thank you for the love and support, I will especially treasure our outings during the times of the strike. Thank you.

LIST OF ABBREVIATIONS

AIDS	Acquired immune deficiency syndrome
Akt	Serine/threonine protein kinase
CFI	Cleavage factor 1
CFII	Cleavage stimulatory factor 2
CstF	Cleavage stimulatory factor
Cys	Cysteine
BER	Base excision repair
DDR	DNA damage response
DNA	Deoxyribonucleic acid
dNTP	2'-deoxynucleoside 5'-triphosate
DTT	1,4-dithio-DL-threitol
E1	Ubiquitin-activating enzyme
E2	Ubiquitin conjugating enzyme
E3	Ubiquitin ligase
eIF2α	Eukaryotic initiation factor 2α
GFP	Green fluorescent protein
GST	Glutathione S-transferase
HECT	Homologous to E6-AP carboxyl terminus
HDM2	Human Double Minute 2
HIV	Human immunodeficiency virus
Hsp's	Heat shock proteins
HSF	Heat shock factor

HSR	Heat shock response
IPTG	Isopropyl-1-thio-D-galactoside
kb	kilo base
kDa	kilo Dalton
LB	Luria broth
MDM2	Murine double minute 2
MDR1	Multi drug resistant gene
Mpe1	mutant PCFII extrogenic suppressor 1
mRNA	messenger RNA
NaN$_3$	Sodium azide
NEDD8	Neural Precursor Cell-expressed Developmentally Down-regulated 8
NER	Nucleotide excision repair
nSG	Nuclear stress granules
N-terminus	Amino terminal
P2P-R	proliferation potential protein-related
PACT	p53-Associated Cellular protein-Testes derived
PAGE	Polyacrylamide Gel Electrophoresis
PBS	Phosphate buffered saline
PCR	Polymerase chain reaction
pRb	Retinoblastoma protein
PVDF	Polyvinyldifluoride
RBBP6	Retinoblastoma binding protein 6
RING	Really interesting new gene

ix

RNA	Ribonucleic acid
siRNA	Short interference RNA
SNAMA	Something that sticks like glue
SUMO-1	Small ubiquitin-related modifier 1
SDS	Sodium dodecyl sulphate
UBA	Ubiquitin associated domain
UBC	Ubiquitin-conjugating catalytic domain
UBL	Ubiquitin-like protein
ULM	Ubiquitin-like modifiers
UPP	Ubiquitin proteasome pathway
UV	Ultraviolet
YB-1	Y-box binding protein-1
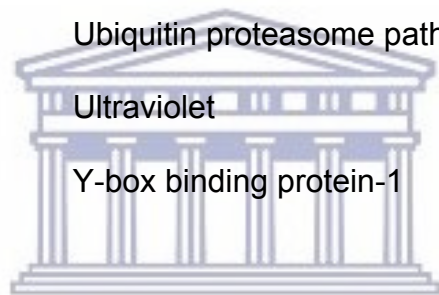
TABLE OF CONTENTS

xiii

UNIVERSITY *of the*

WESTERN CAPE

LIST OF TABLES

UNIVERSITY *of the*

WESTERN CAPE

LIST OF FIGURES

CHAPTER 1 : LITERATURE REVIEW

1.1   Introduction

Retinoblastoma Binding Protein 6 is a 200 kDa human protein that was originally identified as interacting with the tumour suppressor pRb (Sakai et al., 1995, Saijo et al., 1995) and was subsequently shown to bind p53, another tumour suppressor, as well (Simons et al, 1997). The single gene coding for RBBP6 is found in all eukaryotes but not in prokaryotes (Pugh et al., 2006). RBBP6 has been shown to be essential in mice, yeast, worms and flies (Mather et al., 2005, Huang et al., 2013).

The presence of a RING finger domain and the N-terminal ubiquitin-like DWNN domain suggested a role in ubiquitination. A knock-out mouse study conducted by Li et al. (2007) showed that RBBP6 cooperates with MDM2 in suppressing p53, making it a potential promoter of cancer. However, their study also suggests that RBBP6 may play an equally important role in keeping the activity of p53 in check during development (Li et al., 2007).

Through its ubiquitination activity, RBBP6 has also been linked to suppression of the highly tumourigenic Y-Box Binding protein-1, thereby making it anti-tumorigenic, as well promotion of DNA damage though suppression of zBTN38 (Chibi et al., 2008, Miotto et al., 2014). In addition to its role in ubiquitination, RBBP6 has what appears to be an independent set of functions related to mRNA processing: it forms part of the 3'-end polyadenylation complex in both yeast and human and plays a role in selection of 3'-

1

polyadenylation sites, leading to regulation of the expression of 4000 human genes (Vo et al., 2001, Di Giammartino et al., 2014). It interacts with elements of the spliceosome and contains an arginine-serine-rich domain (RS domain) similar to those found in splicing factors and other splicing associated proteins (Simons et al., 1997). More recently it has been shown to play a role in 3'-end processing of mRNA transcripts, positively regulating the expression of up to 4000 genes by influencing the choice of polyadenylation site (Di Giammartino et al., 2014).

The single RBBP6 gene is expressed in a number of isoforms, including the full-length protein (isoform 1) and a smaller isoform (isoform 3) consisting essentially of the N-terminal DWNN domain followed by a 40-amino acid tail. Recent reports suggest that isoform 3 may regulate the activity of isoform 1 by competing for binding to the 3'-end cleavage machinery (Di Giammartino et al., 2014). Meanwhile, unpublished reports from our laboratory suggest that whereas isoform 1 is localized to punctate bodies in the nucleus called nuclear speckles, isoform 3 is predominantly localized in the cytoplasm and translocates to the nucleus following stress.

If true, this may provide a mechanism whereby 3'-end processing can respond to cell stress. The DWNN domain adopts a structure similar to the protein modifier ubiquitin. An intriguing feature of the DWNN domain is the C-terminal Gly-Gly motif found in vertebrate orthologues at the same position as the same motif in ubiquitin, which raises the possibility that the DWNN domain may become covalently attached to other proteins and therefore play the role of an ubiquitin-like modifier.

Further unpublished results from our laboratory suggest that the DWNN domain is required for efficient poly-ubiquitination of YB-1 by RBBP6, acting in conjunction with the E2 enzyme UbcH1. UbcH1 is an unusual E2 enzyme in that it contains a domain known to associate with ubiquitin (a so-called ubiquitin associated domain, or UBA) at its C-terminus, which led us to hypothesize that the UBA may interact directly with the DWNN domain of RBBP6, thereby facilitating the ubiquitination activity of RBBP6.

It is clear from the above that RBBP6 is an important protein which may shed light on the regulation of many cellular processes. Of particular interest is the relative localisation of isoforms 1 and 3 within the cell, since that will affect the ability of the two isoforms to compete with each other for binding to the 3'-end processing machinery. Also of interest is whether the Gly-Gly motif plays any role in the localisation of isoform 3.
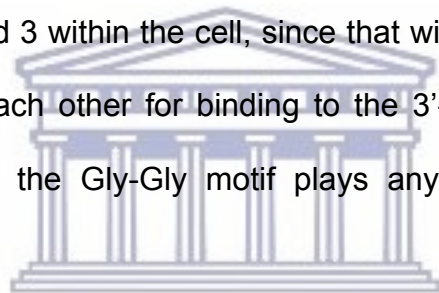
1.2   Retinoblastoma Binding Protein 6 protein family

RBBP6 is a large multi-domain protein that is implicated in a range of biological processes including ubiquitination, transcription and mRNA processing. The RBBP6 protein family exists in eukaryotic organisms and not in prokaryotes and there are three known splice variants. The mouse protein is known as p53-associated cellular protein-testes derived (PACT) or P2P-R (Witte and Scott, 1997), fruit fly (SNAMA) (Mather et al., 2005), worm (RBPL-1) (Huang et al., 2013) and in humans as RBBP6. RBBP6 was originally cloned and characterized by Simons et al. (1997) by using purified wild type p53 as a probe on mouse testes expression library. cDNA encoding a nuclear protein

3

was isolated and designated as PACT. Using the same assay, Rb was used as a probe and was found to interact with RBBP6 therefore shown to interact with tumor suppressor proteins p53 and Rb (Simons et al., 1997). The RBBP6 encoding gene is situated on chromosome 16p12.2 and codes for proteins of 1792, 1758, 118 and 952 amino acids (Pugh et al., 2006) respectively, known as isoforms 1-4. Isoforms 2 and 4 have not been the subject of much study and therefore the focus of this review will be on isoforms 1 and 3.

All RBBP6 proteins in both vertebrates and invertebrates share a common N-terminal end composed of: DWNN domain, zinc knuckle domain and RING finger, see Figure 1.1 (Mather et al., 2005, Pugh et al., 2006). Vertebrate RBBP6 also contains a number of other domains which are found at the C-terminus end and include the SR domain, Retinoblastoma binding (Rb) domain, nuclear localisation signal domain and p53 binding domain (Pugh et al., 2006).
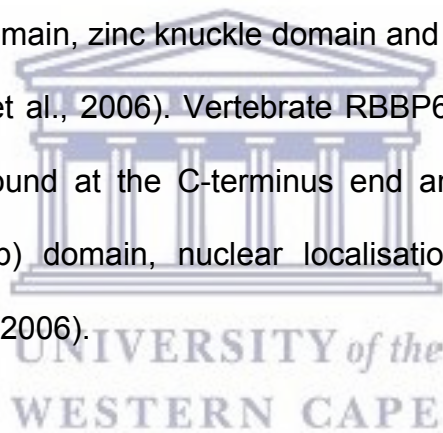
The additional sequences which are only found in vertebrates are likely to confer higher levels of regulation acquired by organisms during the course of evolution, as well as additional functions, possibly. For example, the p53 and pRb-binding domains found in the C-terminus are likely to have been added relatively late in evolutionary history, due to the need to oppose tumourgenicity in multi-cellular organisms.
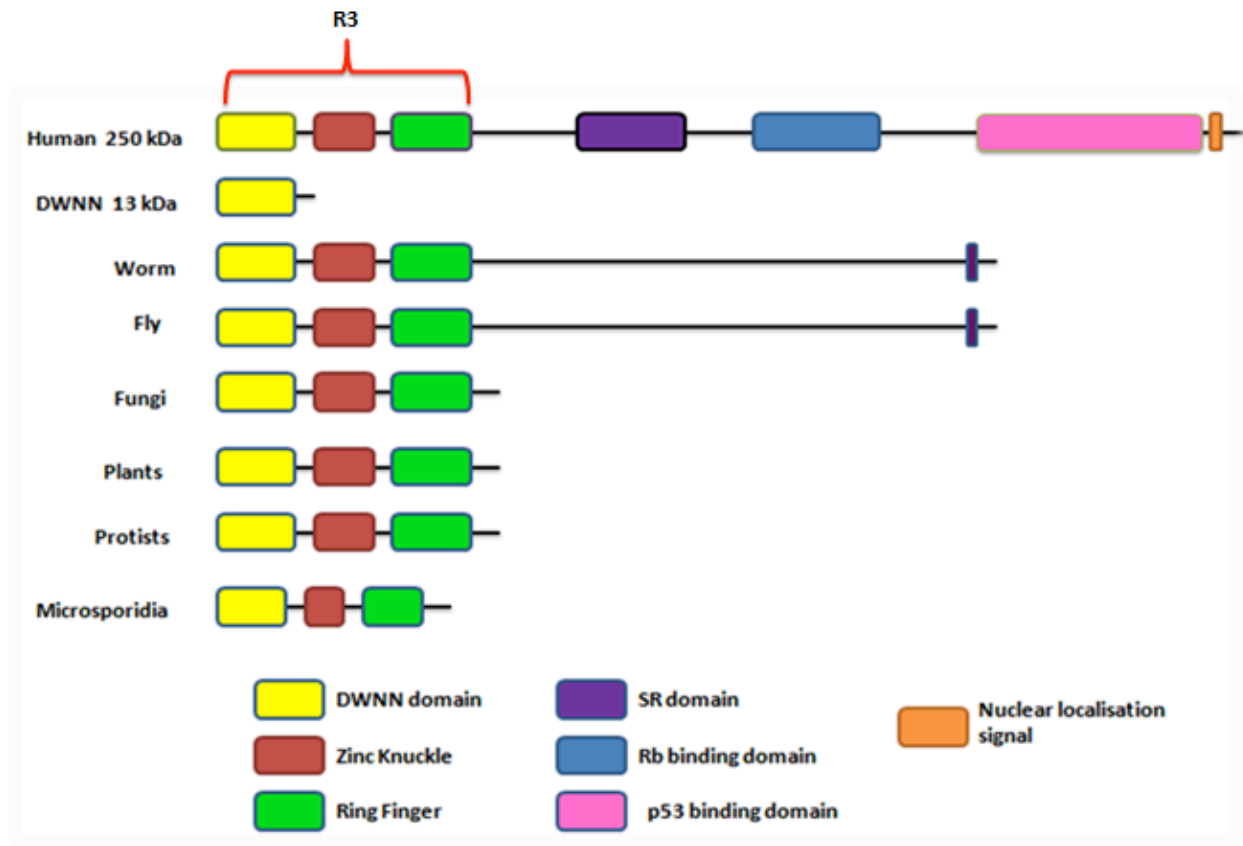
Figure 1.1: Domain organisation of RBBP6 orthologues in various eukaryotic organisms. The RING finger domain, DWNN and zinc knuckle domains are well conserved in both vertebrates and invertebrates. In humans and mice RBBP6 has an additional C-terminal extension which includes the Rb binding domain as well as the p53 binding domain. Adapted from (Pugh et al., 2006).

On the other hand, the ubiquitination activity of the protein is likely to centre on the RING finger domain, and possibly the ubiquitin-like DWNN domain, which are found in the N-terminal part of the protein, which is present in all eukaryotes and makes up the entire protein in lower organisms (denoted R3 in this study). Similarly, the fact that the yeast form of the protein, Mpe1, which contains only the equivalent of R3 in vertebrates (see Figure 1.1), is sufficient for 3'-end cleavage (Vo et al., 2001), suggests that the polyadenylation activity may be contained entirely in the N-terminus of the human protein.

The DWNN domain

The structure of the DWNN domain found at the N-terminus of all RBBP6 isoforms is most similar to that of ubiquitin, raising questions as to whether it can perform a similar function (Pugh et al., 2006). This hypothesis is supported by the fact that the DWNN domain contains a Gly-Gly motif at the same position as found in ubiquitin and other ubiquitin-like modifiers, in which it serves as the point of attachment to the substrate protein (Pugh et al., 2006)

As well as forming part of the full-length RBBP6 structure, the DWNN domain is also independently expressed along with a 40-residue C-terminal tail, making up isoform 3. In human cancers, DWNN is down-regulated while the larger isoforms tend to be up-regulated (Mbita et al., 2012). The function of the DWNN domain is still poorly understood but in 2014 a study by Di Giammartino and co-workers revealed that DWNN

6

inhibited pre-mRNA 3' cleavage by competing with full-length RBBP6 for binding to the mRNA polyadenylation core machinery (Di Giammartino et al., 2014).

The zinc finger domain

The zinc finger is a small protein domain that was first discovered in 1983 in *Xenopus* transcription factor IIIA (TFIIIA) and they are highly abundant in higher eukaryotes (Gamsjaeger et al., 2007). They are present among proteins that perform a broad range of functions in various cellular processes such as replication and repair, transcription and translation, metabolism and signaling, cell proliferation and apoptosis (Sri Krishna et al., 2003). The zinc finger is the second conserved domain of RBBP6. Zinc fingers are structurally diverse and fall into eight fold groups, which are defined based on the structural properties in the vicinity of the zinc-binding site.

RBBP6 zinc finger is CCHC (Cys-Cys-His-Cys motif) types which are known to bind both DNA and RNA. An example is the trypanosome poly-zinc finger pre-mRNA processing protein which binds both DNA and RNA (Mörking et al., 2004). CCHC zinc finger types are also known to be involved in protein-protein interactions (Matthews et al., 2000). Finally zinc fingers have recently been shown to have the ability to bind ubiquitin. A 2009 study by Cordier and co-workers revealed that the zinc finger of NF-κB essential modulator is a regulatory protein (NEMO) an essential protein NF-κB signaling is a ubiquitin binding domain (Cordier et al., 2009). The study showed furthermore that the zinc finger residues involved in ubiquitin binding are functionally important and required for NF-κB signaling response.

7

The RING finger domain

The RING domain is the third conserved domain of the RBBP6 protein family and is a characteristic feature of E3 ubiquitin ligases. E3 ligases form part of the ubiquitination proteasome pathway and they confer specificity by recognizing target substrates by mediating the transfer of ubiquitin from an E2 ubiquitin-conjugating enzyme to the substrate (Deshaies and Joazeiro, 2009). RING fingers are small domains that fold independently with the help of two Zn^{2+} ions (Krishna et al., 2003).

RBBP6 RING finger is classified as a U-box due the conserved pattern of hydrophobic residues (Chibi et al., 2008). The U-box is a domain that comprises of ~70 amino acids and has the same structure as RING fingers but without the need to bind zinc ions and is present in proteins ranging from yeast to man (Hatakeyama et al, 2001). U-Box proteins mediate poly-ubiquitination in the presence of E1 and E2 and in the absence an E3 (Cyr et al., 2002).
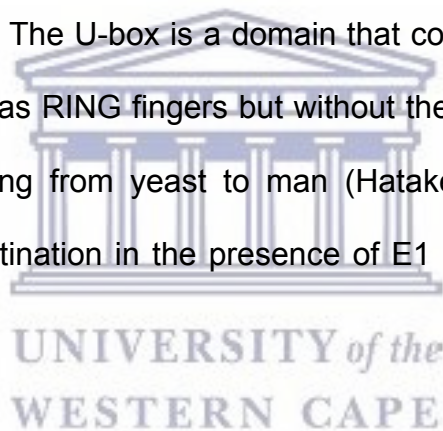
Functions of RBBP6

RBBP6 is a large multi-domain containing protein with known multiple functions. Perhaps the most well documented function is the role in maintenance of protein stability through the ubiquitin proteasome pathway. The key enzymatic function seems to lie on the RING finger and possibly the DWNN domain. The RING finger of RBBP6 has been shown to be directly implicated in the regulation of YB-1 through the ubiquitin proteasome system (UPP). Using a yeast two-hybrid library screen, RBBP6 RING was shown to interact with YB-1 and further ubiquitinate it leading to its destruction in the

8

proteasome (Chibi et al., 2008). The presence of the RING finger domain led Li et al. (2007) to speculate that RBBP6 may potentially play a role of scaffolding by facilitating the interaction between p53 and Hdm2 since it does not ubiquitinate p53 on its own. The study further revealed that PACT is an essential gene for survival and that its disruption led to embryonic death before day 7.5 (E7.5) and widespread apoptosis. Furthermore, they showed that introduction of a p53 null mutation in Pact$^{-/-}$ mice partially rescued the lethality (Li et al., 2007). The results suggest that PACT negatively regulates p53.

In 2005 a study conducted by Mather and co-workers showed that SNAMA controls nucleic acid metabolism and apoptosis (Mather et al., 2005). The study showed that deletion of SNAMA resulted in abnormal occurrence of apoptosis during embryogenesis. The worm homolog (RBPL-1) was also shown to be indispensable to worm development. Silencing of RBPL-1 gene resulted in embryonic lethality and defects in germ cell proliferation as well as intestine development (Huang et al., 2013a). Taken together RBBP6 homologs play a vital role in the development of organisms.

Finally, RBBP6 has been has been shown to play a role in the regulation of zBTB38 protein and prevention of DNA damage. A study by Miotto and co-workers showed that cells lacking RBBP6 have higher levels of zBTB38 (Miotto et al., 2014). High levels of zBTB38 were sufficient to induce DNA damage and its depletion was sufficient to prevent DNA damage in the absence of RBBP6. The data showed a direct involvement of RBBP6 in the regulation of zBTB38 through the ubiquitin proteasome pathway.

9

Interestingly, cells lacking RBBP6 were shown to have spontaneous DNA damage and that the effect was reversible by the simultaneous deletion of zBTB38 (Miotto et al., 2014).

1.3   Y-Box Binding protein-1

One of the reported functions of RBBP6 is the ubiquitination of YB-1 through its RING finger and marking it for destruction through the 26S proteasome (Chibi et al., 2008). Y-box binding protein 1 (YB-1), also known as DNA binding protein B (dbpB) (Sorokin et al., 2005), is an oncogenic transcription and translational factor that belongs to a superfamily of cold-shock domain proteins (Wolffe, 1994). YB-1 is made up of three domains the N-terminal or (A/P) domain which is rich in alanine and proline and thought to function as a transcriptional regulation domain (Eliseeva et al., 2011).

The middle portion of YB-1, termed the nucleic acid binding domain or cold shock domain (CSD), has been highly conserved throughout evolution. Lastly the C-terminal region contains alternating positively and negatively charged regions which have been implicated in protein-protein interactions, see Figure 1.2 (Izumi et al., 2001). The C-terminal domain contains alternating regions of acidic and basic amino acids (Izumi et al., 2001).
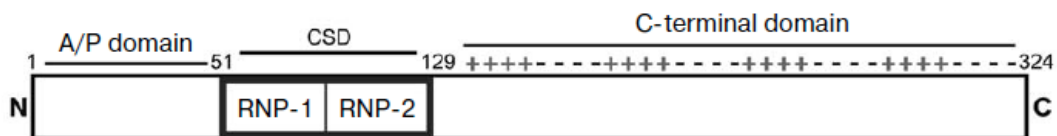
Figure 1.2 Domain organisation of YB-1 (Eliseeva et al., 2011)

10

YB-1 is involved in a number of cellular processes in the cytoplasm and nucleus (Eliseeva et al., 2011). YB-1 is involved in all DNA and mRNA-dependent processes which include DNA replication and repair, transcription, pre-mRNA splicing and mRNA translation (Matsumoto and Wolffe, 1998, Kohno et al., 2003, Silveira et al., 2011). YB-1's multiple functions are not limited to regulation of DNA and RNA processes but also the regulation of expression of the multi-drug resistance (MDR1) gene.

The MDR1 gene is overexpressed in cancer cells that are resistant to many chemotherapeutic agents. DNA damaging agents such as UV irradiation and cisplatin cause YB-1 to induce the expression of MDR1 through increased binding to a Y-Box element within the MDR1 promoter (Asakuno et al., 1994, Ohga et al., 1998). YB-1 is a predominately cytoplasmic protein which translocates to the nucleus in response to genotoxic stress (Koike et al., 1997). Mechanisms of nuclear translocation of YB-1 have sparked great interest in the scientific community.

It has been reported that phosphorylation of YB-1 by Akt is required for nuclear translocation (Sutherland et al., 2005). A study conducted by Zhang et al. (2003) showed for the first time that p53 was required for nuclear localisation of YB-1. In their study they showed that genotoxic stress induced the nuclear translocation of YB-1 but only in cells containing wild-type p53 (Zhang et al., 2003). YB-1 interacted with p53 through its C-terminus between the amino-acid residues 363-376 (Okamoto et al., 2000). The study clearly showed the requirement of functional p53 for the translocation of YB-1 into the nucleus.

In addition, the study speculated the correlation nuclear YB-1 with drug resistance and poor prognosis in some tumor types since p53 causes YB-1 to translocate to the nucleus, which is associated increased drug resistance through activation of MDR1 (Zhang et al., 2003). This effect would make cells more resistant to resistant apoptosis through inhibition of p53 activity and aid in the development of drug-resistant clones consequently promoting the survival of some tumor cells (Zhang et al., 2003).

A 2010 study conducted by Basaki and co-workers revealed that YB-1 promotes cell cycle progression through the CDC6-depependent pathway in human cancer cells (Basaki et al., 2010). They showed that depletion of YB-1 caused a marked suppression of cell proliferation and expression of the cell cycle related gene CDC6 in cancer cells. Consequently, it was concluded that YB-1 is a potent biomarker for tumour growth and cell cycle in its close association with CDC6 in cancer cells (Basaki et al., 2010).

Several lines of evidence have pointed that YB-1 is closely involved in tumour growth as well as malignant progression of cancer (Braithwaite et al., 2006). In addition, nuclear YB-1 is associated with poor prognosis in several types of human cancers including breast (To et al., 2011), prostate (Giménez-Bonafé et al., 2004), lung (Shibahara et al., 2001) and colon (Law et al., 2010) cancer. Nuclear expression of YB-1 is linked with poor survival in breast cancer patients; a study conducted by Lee et al. (2008) showed that YB-1 might be a target for therapeutic intervention. They showed that targeting YB-1 in human epidermal growth factor receptor (*her-2*) overexpressing breast cancer cells induced apoptosis through the mTOR/STAT3 pathway, thereby suppressing tumor

growth in mice. They confirmed this by inhibiting YB-1 with siRNAs both *in vitro* and *in vivo*. Out of seven breast cancer cell lines, six were suppressed in growth (Lee et al., 2008).

1.4   RBBP6 and its involvement in cancer

The interaction of RBBP6 with the tumor suppressor protein p53 has ignited great interest in evaluating it as a potential cancer biomarker. p53, a tumour suppressor commonly referred to as the "guardian of the genome" is mutated more than 50% of human cancers (Hollstein et al., 1991). In a quest to understand the correlation between mutant p53 and RBBP6 in colon cancer, Chen et al. (2013) used immunohistochemistry, western blot and real time PCR on cancerous and non-cancerous colon tissue samples (Chen et al., 2013).

They observed that RBBP6 was over-expressed in colon tumorous tissues and that there was a correlation of overexpressed RBBP6 and mutant p53 in colon cancer (Chen et al., 2013). In addition, the study showed that patients with tumours which had an accumulation of mutant p53 and overexpressed RBBP6, relapsed and died shortly after surgery. The study revealed that both RBBP6 and mutant p53 could be helpful in predicting cancer prognosis (Chen et al., 2013).

In a 2010 study employing Complementary DNA Microarray Analysis, Yoshitake and co-workers revealed that PP-RP was overexpressed in oesophageal cancer cells as compared to non-cancerous cells (Yoshitake et al., 2004). They concluded that PP-RP

13

could be an ideal target for diagnosis and immunotherapy for patients with oesophageal cancer (Yoshitake et al., 2004). RBBP6 is also overexpressed in gastric cancer cells. In a proteomic based approach study conducted by Morisaki et al. (2014) on gastric stem cells in an attempt to identify novel biomarkers which could be used to diagnose gastric cancer. The study used CSC-like SP cells, OCUM-12/SP cells, OCUM-2MD3/SP cells, and their parent OCUM-12 cells and OCUM-2MD.

 After immunohistochemical analysis of 300 gastric cancers, RBBP6 and eight other proteins were overexpressed as compared to the parent OCUM-12 cells. The study concluded that out of the eight identified potential biomarkers of gastric cancer, RBBP6 was a promising prognostic marker and a therapeutic target for gastric cancer (Morisaki et al., 2014). RBBP6 overexpression in a number of cancers makes it a promising target for therapeutic intervention.
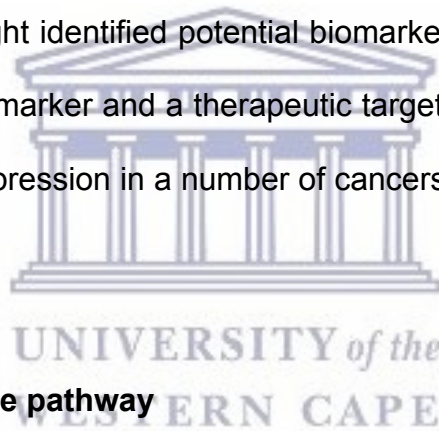
1.5   Ubiquitin proteasome pathway

The ubiquitination pathway (UPP) is an evolutionary conserved mechanism known to play a major role in the destruction of damaged, oxidised and misfolded proteins (Wang and Maldonado, 2006, Bogyo et al., 1998). To date YB-1 and zBTB38 have been identified as substrates for RBBP6 ubiquitination (Chibi et al., 2008, Miotto et al., 2014). Apart from protein destruction, UPP is known to play a role in DNA repair, regulation of the cell cycle, propagation of transmembrane signaling, protein-protein interactions, apoptosis and many others (Metzger et al., 2012).
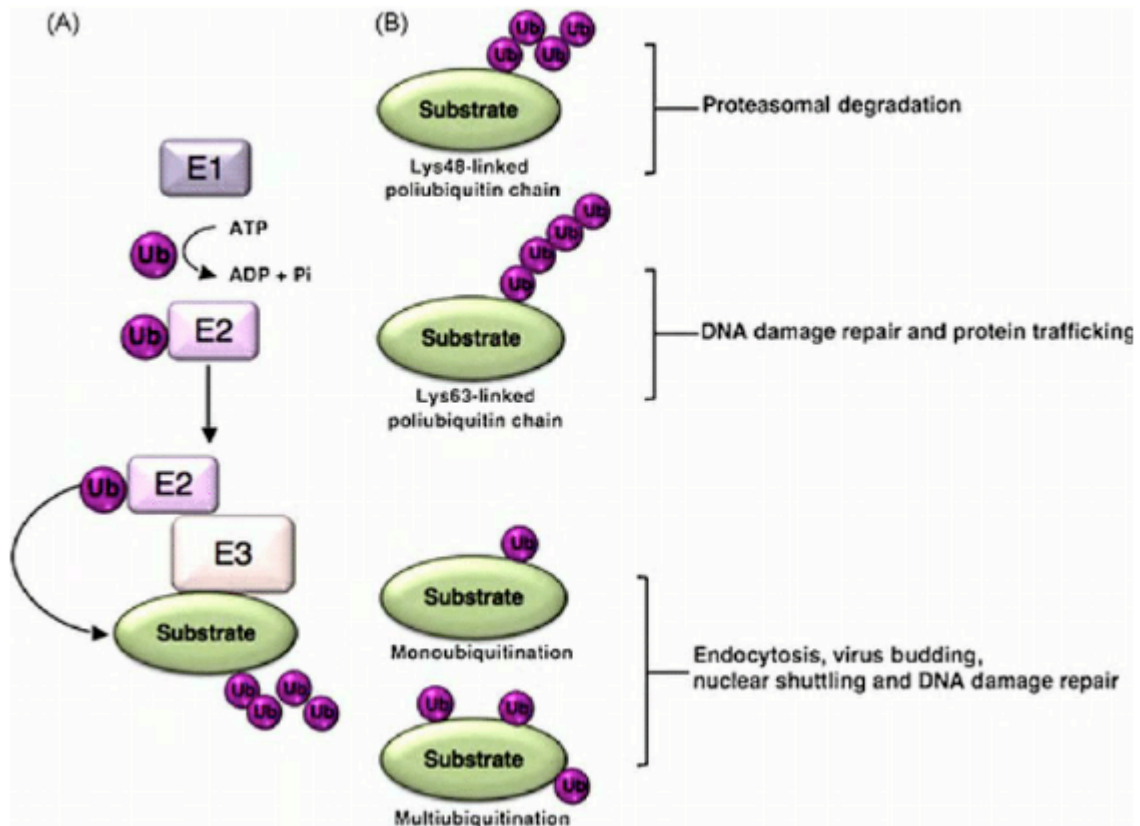
Figure 1.3 Diagrammatic representation of the ubiquitin proteasome pathway (A) ubiquitination is carried out by a cascade of three enzymes. E1 activates Ub at its C-terminus. Activated E1 is transferred from E1 to E2 and the E3 catalyses the transfer of the activated Ub from E2 to the substrate. (B) Different outcomes of modification of a substrate with Ub (Molfetta et al., 2010).

The central element to this mechanism is the covalent attachment of ubiquitin (Ub) to targeted substrates in an adenosine triphosphate (ATP) dependent manner (Wang and Maldonado, 2006). Ubiquitin is a highly conserved 76 amino acid residue protein that is found in all eukaryotes. The molecule has seven (7) internal lysine residues: K6, K11, K27, K33, K48 and K63) onto which various poly-ubiquitin chains can be attached (Walczak et al., 2012). The UPP is diagrammatically represented in Figure 1.3.

Attachment of a single ubiquitin to a substrate is called mono-ubiquitination, whereas attachment of a single ubiquitin to more than one site is known as multiple mono-ubiquitination (Deshaies and Joazeiro, 2009, Dikic and Robertson, 2012). Poly-ubiquitination results through the attachment of a chain of four or more ubiquitin molecules to a single lysine residue on the substrate (Tenno et al., 2004).

Proteins modified by K-48 poly-ubiquitination chains are targeted by the proteasome for proteolytic digestion (Pickart, 2001, Chung et al., 2001). On the other hand, proteins modified with K-63 poly-ubiquitin chains are implicated with non-proteolytic signaling (Deshaies and Joazeiro, 2009). Attachment of a ubiquitin molecule onto a substrate is catalyzed by a set of three enzymes namely ubiquitin activating enzyme (E1), ubiquitin conjugating enzyme (E2) and ubiquitin ligating enzyme (E3).

1.5.1 Ubiquitin-like proteins

Since the discovery of ubiquitin in 1970 several other proteins which share sequence and structural similarities have since been discovered. This family of proteins are

16

classified as ubiquitin-like proteins (UBL) or ubiquitin-like modifiers (ULM) (Kerscher et al., 2006). These proteins are covalently attached to substrates in an enzymatic cascade similar to that of ubiquitin with the contrast of not targeting substrates for degradation in the proteasome. Rather, modification of substrates with UBL proteins destines substrates for cellular processes such as nuclear transport, translation, autophagy and anti-viral pathways (van der Veen and Ploegh, 2012).

Included in this family are Neural Precursor Cell-expressed Developmentally Down-regulated 8 (NEDD8), small ubiquitin-related modifier 1 (SUMO-1), Apg8 and Apg12, amongst others (Herrmann et al., 2007). NEDD8, the most similar to ubiquitin, sharing 80% sequence similarity, was discovered in a set of genes that were found to be down-regulated in neural precursor cells during the development of the murine brain (Kumar et al., 1993).
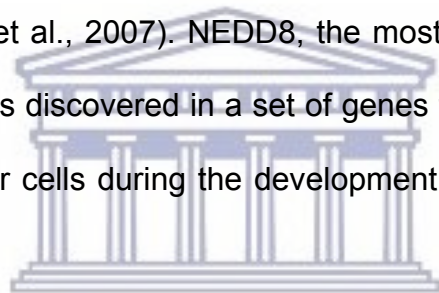
An enzymatic cascade catalyses the addition of NEDD8 to substrates in a process called Neddylation (Dye and Schulman, 2007). A similar process of conjugation takes place with SUMO-1, which is termed SUMOylation (Park-Sarge and Sarge, 2005). UBL proteins all have a 3D structure similar to ubiquitin including a C-terminal di-glycine motif (Herrmann et al., 2007). In addition to the ubiquitin-like DWNN domain, RBBP6 isoform 3 contains a di-glycine motif at an equivalent position to that fund in ubiquitin, suggesting that isoform 3 might play a similar role as UBL (Pugh et al., 2006).

17

1.5.2 The ubiquitin activating enzyme (E1)

The initial step of ubiquitination conjugation is carried out by the E1, which activates ubiquitin by forming a high-energy thiol-ester bond between E1 and the backbone carboxylic group of Gly76 (Pickart, 2001). To date, only two human ubiquitin activating enzymes have been identified as compared to an array of E2s and E3s (Jin et al., 2007). This enzyme of 110 kDa in size uses ATP to activate ubiquitin, creating a Ub thiolester intermediate. This highly reactive form of ubiquitin is transferred to catalytic cysteine on the E2, forming a thiol-ester bond between ubiquitin C-terminal carboxylate group and the ε-amino group of the substrate lysine residue (Haas and Rose, 1982).

1.5.3 Ubiquitin conjugating enzyme (E2)

While there are only two known E1 enzymes, about 40 E2s are encoded by the human genome (Sheng et al., 2012). All E2s are characterized by the presence of the conserved ubiquitin-conjugating catalytic domain (UBC), which is 15-200 amino acids in length (Burroughs et al., 2008). The aforementioned domain consists of a highly conserved active-site motif containing the Cys residue that forms a thiol ester with ubiquitin (Haldeman et al., 1997). There are three known classes of E2 enzymes: Class 1 members are the simplest and comprise of only the catalytic domain. Class II members have C-terminal extensions or a "tail", whereas class III E2 members have additional N-terminal sequences.

1.5.4 Ubiquitin conjugating enzyme 1

Human conjugating enzyme 1 (UbcH1), which is also known as E2-25K and Huntington Interacting Protein 2, is a class II E2 enzyme that is broadly expressed in mammalian tissues (Middleton and Day, 2015). UbcH1 is up-regulated in Alzheimer's disease and interacts with huntingtin, the key protein mutated in Huntington's disease (Kalchman et al., 1996). UbcH1 is a 25 kDa protein that has the ability to synthesize K48-linked chains on mono-ubiquitinated substrates *in vitro* in the absence of an E3 (Chen and Pickart, 1990).

Additional features include: unusual discrimination against noncognate E1 enzymes, resistance of the active-site Cys residue to alkalyation and the high synthesis of K48-linked poly-ubiquitin chains (Haldeman et al., 1997). Among all known E2 enzymes, UbcH1 contains a unique C-terminal ubiquitin-associated domain (UBA) in addition to the conserved ubiquitin conjugating domain found in all E2s (Chen and Pickart, 1990).

The UBA of UbcH1 is an integral part of the ubiquitin-binding surface and contains a highly conserved MGF loop (Met172, Gly173, and Phe174) which is present in most UBA domains and a primary contact surface for ubiquitin in most UBA domains (Wilson et al., 2009). Other UBA-containing proteins include HHR23A (the human homolog of yeast RDA23), which is involved in DNA repair, and p62, a protein that carries diverse cellular functions including NF-κB signaling and transcriptional activation (Watkins et al., 1993). The UBA is composed of three helices which are stabilized by a hydrophobic core (Chang et al., 2006). Initial studies conducted by Haldeman and co-workers using

19

truncated versions of E2-25K (residues 1-151 and residues 1-153 respectively) and chimeric E2 in which residues 154-200 of E2-25K were fused to yeast UBC4, suggested that the UBA was necessary for the enzyme's synthesis of K48-linked chains but not for the normal ligase activity (Haldeman et al., 1997).

This is supported by the fact that chimeric E2-25K was unable to generate poly-ubiquitin chain synthesis. The results suggested that the UBA is required for the formation of K-48 linked poly-ubiquitin chains (Haldeman et al., 1997). However the solution structure subsequently revealed that residues 151 and 153 are located within the α-helix, suggesting that the inability to synthesize poly-ubiquitin chains may have been the result of protein unfolding and rather from the truncation (Wilson et al., 2011).

1.5.5 Ubiquitin protein ligases (E3)

While there are limited E2s, there are more than 1000 E3s in the cell (Lecker et al., 2006). The role of the E3 is to confer specificity to ubiquitination by recognizing target substrates and mediating the transfer of ubiquitin from an E2 to a substrate. Substrates may however be targeted by more than one E3 (Deshaies and Joazeiro, 2009, Metzger et al., 2012).There are two types of E3 ligases in eukaryotes that play functionally distinct roles. HECT-type E3s, which contain a homologous to E6AP carboxy terminus (HECT) domain or RING-type E3s, which contain a really interesting new gene (RING) domain (Deshaies and Joazeiro, 2009). Among the E3 ligases, the RING domain constitutes the largest number and they are composed of a single subunit or multi-subunit complex (Cyr et al., 2002, Stegmuller and Bonni, 2010).

20

1.5.6 The HECT domain E3 ligases

HECT domain E3 ligases play roles in protein signaling pathways involved in the regulation of cell growth and proliferation (Sheng et al., 2012). They also play a role in protein trafficking and immune responses. There are approximately 30 HECT domain E3s in mammals and all members share a conserved HECT domain, which is roughly 350 residues (Cyr et al., 2002). The HECT domain is located at the C-terminus of E3 ligases while the N-terminus is comprised of diverse domains that mediate substrate targeting (Metzger et al, 2012). Both RING domain and HECT domain E3 ligase confer substrate specificity but they execute this role in different ways. HECT domain E3 ligases directly transfer ubiquitin to the substrate. Therefore the E3 directly catalyze the attachment of ubiquitin to the substrate (Dikic and Robertson, 2012).

1.5.7 RING domain E3 ligases

The mammalian genome encodes for more than 600 RING domain E3 ligases (Deshaies and Joazeiro, 2009). Some well-known RING domain E3 ligases are C-terminus of Hsc70-iteracting protein (CHIP) and Murine Double Minute 2 (MDM2) (Kappo et al., 2012). Members of the RING domain family have a RING finger that coordinates two zinc ions with the aid of four pairs of conserved cysteine or histidine residues in a cross-braced arrangement (Kappo et al., 2012) to create a platform for binding of E2s (Metzger et al., 2014). The conserved cysteine and histidine residues are buried within the domains core where they help maintain the overall structure through binding of two zinc ions. The zinc ions are catalytically inert hence the RING domain

21

does not form a catalytic intermediate with ubiquitin. Rather, the RING finger serves as scaffold that brings E2 and the substrate together (Dikic and Robertson, 2012).

1.6 RBBP6 and its role in mRNA processing

One of the most established functions of RBBP6 is mRNA processing (Di Giammartino et al., 2014). In eukaryotic cells, almost all mRNA is produced through a two-step process: 3'-end cleavage and polyadenylation which are both essential steps for the synthesis of functional mRNAs (Elkon et al., 2013). In a sequential process, RNA polymerase II catalyses the cleavage of primary mRNA transcript followed by the addition of a stretch of 200-300 nucleotides which are added at the 3' upstream of the cleavage product (Nevins and Darnell, 1978). The processing and regulation of polyadenylation requires a set of multiple factors which are well conserved across eukaryotic species (Lee and Moore, 2014).
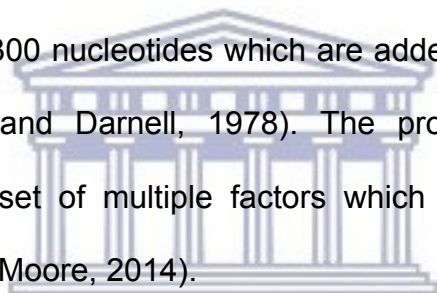
The core 3'-end processing machinery is a multisubunit complex constituting of four multisubunit complexes: cleavage/polyadenylation specificity factor (CPSF), cleavage stimulatory factor (CstF), Cleavage factor I (CFI) and CFII. Mpe1 or YKL059c, a *Saccharomyces cerevisiae* protein crucial for cell viability, contains an evolutionary conserved tripartite structure found in all RBBP6 orthologues: N-terminal ubiquitin-like domain, zinc knuckle and RING finger (R3) (Vo et al., 2001). A study conducted by Vo et al. (2001) revealed that Mpe1 is a component of the 3'-end processing machinery. The study utilized mpe1-1, a mutant of Mpe1 and immumoneutralized extracts of Mpe1, which were found to be defective in 3'-end processing. A later study conducted by Lee

and Moore. (2014) revealed interesting facts on the role of Mpe1 in mRNA processing. Using deletion techniques and examining the role of each highly conserved domain on the efficiency of 3'-end processing of mRNA precursor their findings revealed that not only are all domains of Mpe1 necessary for 3'-end processing but that ubiquitination had a direct impact on polyadenylation (Lee and Moore, 2014). Addition of inhibitors that prevented ubiquitin-mediated interactions blocked mRNA cleavage, demonstrating, for the first time, a direct role for ubiquitination on mRNA processing.

Using an Mpe1 mutant mpe1-1, it was observed that the mutation abolished the interaction of ubiquitinated substrates with Pap1 (Lee and Moore, 2014). Pap1 is a polymerase component of the cleavage and polyadenylation factor (CPF) complex and plays a role in polyadenylation-dependent pre-mRNA 3' end formation. RBBP6, the human orthologue of Mpe1, also contains the same evolutionarily-conserved tripartite structure as Mpe1. In addition to the conserved tripartite domains, RBBP6 also has a stretch of C-terminal domains which include an SR domain (Simons et al., 1997).

A study conducted by Di Giammartino et al. (2014) revealed the direct involvement of RBBP6 in regulating the human polyadenylation machinery. Analysis of nuclear extracts following RBBP6 knock down showed that they were defective in 3'-end cleavage and that the activity could be rescued by the addition of recombinant RBBP6 N-terminal derivative (DWNN, zinc knuckle and RING finger). Furthermore the study showed that RBBP6 isoform 3 negatively regulated 3'-end processing by competing with RBBP6 for binding to the core machinery. Isoform 3 also outcompeted RBBP6-N by binding to

23

CstF64 therefore implicating both RBBP6 isoform 1 and 3 as novel regulators of 3'-end processing. CstF64 forms part of the mammalian cleavage stimulation factor the 64 kDa subunit of the Cleavage Stimulation factor (Di Giammartino et al., 2014). There are also other facts that strongly suggest the involvement of RBBP6 in mRNA splicing. RBBP6 contains an SR domain of which SR proteins are reported to play a role in the regulation of mRNA splicing (Cáceres et al., 1997). Furthermore, the SR domain has been observed to precipitate from nuclear extracts with $MgCl_2$, suggesting an interaction with other SR-related proteins.

Simons et al. (1997) have supported this fact as they demonstrated that RBBP6 interacts with Sm small nuclear ribonucleoproteins (snRNPs) antigens which form part of the spliceosome (Simons et al., 1997). RBBP6 is not classified as an SR-related protein due to the absence of an RNA binding motif nevertheless, Lee and Moore. (2014) demonstrated that both the zinc knuckle and the RING finger bind RNA (Lee and Moore, 2014). These features along with speckle localisation suggest a strong of involvement of RBBP6 in mRNA processing (Simons et al., 1997).

1.7   Cellular response to stress

1.7.1 Introduction

Changes in the environment away from optimal conditions can threaten the viability of cells, requiring them to take action. For example, when the temperature is raised by as little as 5 °C above the optimal 37 °C the stability of many of the proteins making up the cell will be reduced, leading to unfolding and aggregation (Benjamin and McMillan,

24

1998). The cell responds by initiating the heat shock response which includes, among many other processes, up-regulation of chaperones and other heat shock proteins which help proteins to refold and eliminate irretrievably aggregated proteins from the cell (Kim et al., 2013). Similarly, when the cell is subjected to ionizing radiation from artificial sources such, as X-rays for medical treatments, can induce a variety of lesions on DNA which leads to the expression of non-functional proteins. The cell responds by initiating the DNA damage response that includes DNA repair pathways, which are discussed in detail in the sections following.

1.7.2 Cellular response to heat shock

1.7.2.1   The heat shock response

The heat response was first identified in *Drosophila melanogaster*, the fruit fly, after exposure to heat showed puffing on salivary gland chromosomes (Lindquist, 1986). It was later discovered that the heat-induced puffing was due to the increased synthesis of proteins with molecular masses 70 and 26 kDa (Jäättelä, 1999) which are now known as heat shock proteins. This study sparked great interest and has since has been studied from prokaryotes to eukaryotes (Lindquist, 1986).

Furthermore the cellular response to stress has proved to be an invaluable tool for investigating the mechanisms and dynamics of inducible gene expression in eukaryotes (Lindquist, 1986). The cellular stress response is triggered by a number of diverse adverse environmental and physiological conditions, including heat shock, exposure to non-native amino acid analogs, heavy metals, oxidative stress, anti-inflammatory drugs,

25

and arachidonic acid (Lindquist, 1986, Morimoto and Santoro, 1998, Causton et al., 2001). As a consequence protein homeostasis is challenged which results in an increased flux of non-native proteins which are more prone to misfolding and aggregation (Parsell and Lindquist, 1994). Cell stress affects the function of macromolecules, perhaps the most sensitive of which are proteins. In eukaryotic cells, proteins are synthesized in the cytosol before they are sorted to their various locations (Hazkani-Covo et al., 2004).

It is crucial that proteins are located in their correct subcellular localizations to execute their functions correctly (Nathan et al., 1997). Furthermore, proteins need to be conformationally flexible to perform their functions in the cell. Perturbations in temperature can lead to entangling, denaturation and aggregation which may abolish the proper function of proteins (Richter et al., 2010). Cellular responses to environmental cues require the appropriate coordination of signaling events. The heat shock response is triggered by changes in temperature of just a few degrees. In fact this is just as true for organisms that are adapted to living at very high temperatures (Richter et al., 2010).

Exposure to elevated temperatures leads to an accumulation of misfolded and aggregated proteins. Mechanisms to protect the cell against insults such as these involve the rapid induction of heat shock proteins (Hsp's) (Kim et al., 2013). Cell survival may be favoured if the damage is contained and reversible. On the other hand, irreparably damaged proteins trigger apoptotic pathways permitting cell death (Gonda et

al., 2012). The cellular response to stress provides an example of how a dynamic interplay of signaling activities can determine the fate of the cell and ultimately the organism. This dynamic signaling event is a highly conserved cellular defense mechanism characterized by the elevated synthesis of Hsp's.

1.7.2.2 Heat shock proteins

Although Heat shock proteins (Hsp's) were first identified in relation to heat shock, it is now known that Hsp's are induced by a variety of stresses including wound healing, exposure to cold or biotic stresses. Since many stresses other than heat induce the expression of Hsp genes, the term "heat shock protein" is thus a misnomer (Park and Seo, 2015). Hsp's, which are also known as molecular chaperones, are involved in the protein quality control system. They achieve this by ensuring that unfolded proteins are folded and that damaged proteins are degraded through degradation pathways including UPP, endoplasmic reticulum-associated degradation and chaperone mediated autophagy (Bozaykut et al., 2014).

Apart from being involved in the protein quality system, Hsp's are also involved in cell cycle progression and replication, (Kregel, 2002, Chowdary et al., 2004). Furthermore, a wide range of tumours have been shown to express atypical levels of one or more Hsp's, suggesting that they play a role in regulation of tumourigenicity (Ciocca and Calderwood, 2005). This observation has led to the suggestions that Hsp's could be used as biomarkers for cancer (Ciocca and Calderwood, 2005).

Hsp's are generally classified into six subfamilies based on their molecular weights in kilodaltons: Hsp100 (>100 kDa), Hsp90 (81-99 kDa), Hsp70 (65-80 kDa), Hsp60 (55-64 kDa), Hsp40 (35-54 kDa) and small heat shock proteins (< 34 kDa) (Lindquist and Craig, 1988). Each gene family includes members which are inducibly regulated in response to stress, as well as some which are constitutively expressed or are targeted to different compartments within the cell to execute their variable functions (Jolly and Morimoto, 2000). Whilst the vast majority of hsp's are located in the cytoplasm they are also located in other organelles such as the mitochondria, endoplasmic reticulum and nucleus (Jolly and Morimoto, 2000).

Hsp ≥100

The Hsp100 protein family is widely expressed from bacteria to mammals. They are characterised by an N-terminal domain that is responsible for substrate binding, two AAA nucleotide-binding domains for the 19S regulator of the 26S proteasome, a wing domain and a small C-terminal domain (Bozaykut et al., 2014). This family is highly inducible and known for its cytoprotective functions (Benjamin and McMillan, 1998). Members of this family maintain proteostasis in cells (Bakthisaran et al., 2015). Under severe thermal stress conditions, Hsp100 proteins maintain the functional integrity of key polypeptides by enabling resolubilization of non-functional protein aggregates (Jolly and Morimoto, 2000, Park and Seo, 2015). Furthermore, they also help degrade irreversibly damaged polypeptides. These activities are aided by interacting with Hsp70 (Bozaykut et al., 2014).

28

Hsp90

The Hsp90 family is highly abundant and expressed in a range of organisms from prokaryotes to eukaryotes. This family is known to play a role in DNA replication, DNA recombination, DNA repair, RNA processing and RNA transcription (Dezwaan and Freeman, 2008). Hsp90s are located both in the cytoplasm and endoplasmic reticulum (Jee, 2016). They are also known to bind steroid receptors, protein kinases, intermediate filaments as well as actin microfilaments in a specific manner (Jee, 2016, Kim et al., 2013, Mosser and Morimoto, 2004). This family is characterized by an N-terminal domain that contains an ATP and co-chaperone binding site as well as a drug binding site that binds natural compounds such as geldanamycin and radicicol. In the middle of the protein is a domain which is responsible for binding to co-chaperone and client proteins.
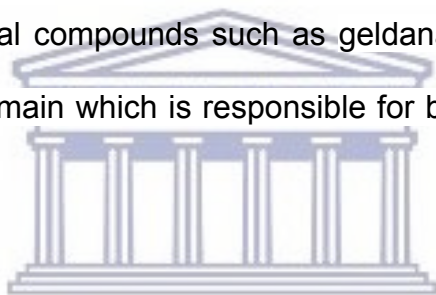
Finally a C-terminal domain contains a dimerization motif, a second drug binding site and a conserved MEEVD pentapeptide at the very C-terminus, which is recognized by the co-chaperone HSP70/HSP90 (Jackson, 2013, Scheufler et al., 2000). The activities of the Hsp90 system are regulated by ATP binding and hydrolysis. Hsp90 are involved in the folding of newly synthesized proteins. In a heat shock response, Hsp90 specializes in capturing and holding client proteins in intermediate conformations until they can be transferred to the Hsp70/Hsp40 system which promotes their folding (Mosser and Morimoto, 2004). In contrast Hsp70, proteins have the ability to hold both unfolded polypeptides and refold protein substrates to their native state (Mosser and Morimoto, 2004).

29

Hsp 70

The Hsp70 family is the most studied Hsp's and contains members that are both constitutively expressed as well as stress inducible (Bettencourt et al., 2008). Different members of the family are localized to different parts of the cell. Hsp70 and Hsp90 are localised within the cytoplasm whereas glucose regulated protein (GRP) 78 (a homologue of hsp70) is localised in the mitochondria (Jee, 2016). Hsp70 is probably the most studied member in this family. There are several Hsp70 family members in humans which include constitutively expressed heat shock cognate protein Hsc70 (Hsp73), mitochondrial Hsp75 (mtHsp75), highly stress inducible Hsp70 (which is also known as Hsp72 or Hsp70i) and Grp78 (BiP) localised in the mitochondria (Tavaria et al., 1996, Jäättelä, 1999).

Family members share a common structure which includes a 45 kDa nucleotide-binding domain, which acts as an ATPase domain, a 15 kDa substrate-binding domain (SBD) and a C-terminal lid region which covers the SBD (Yu et al., 2015). When proteins are damaged beyond repair, they are targeted for degradation by binding to carboxy terminus of Hsp70-interacting protein (CHIP) by attaching a chain of poly-ubiquitin to the substrate, thereby targeting it for proteasomal degradation (Jiang et al., 2001).

Hsp 60

The Hsp60 protein family is widely expressed from prokaryotes to eukaryotes (Kaufmann, 1990). They are especially found in abundance in prokarytotes, chloroplasts and mitochondria (Cabiscol et al., 2002). Hsp60 is constitutively expressed in the

nucleus and targeted to the mitochondria (Kaufmann, 1990). In the mitochondria, Hsp60 forms a complex with Hsp10 and functions in folding misfolded protein intermediates (Richardson et al., 1998). Hsp60 is reported to have both pro-death and pro-survival functions which are both controversial (Chandra et al., 2007). Anti-apoptotic function of Hsp60 in evident by its overexpression in several cancers—notably cervical cancer (Castle et al., 2005), Hodgkin lymphoma (Hsu and Hsu, 1998), colorectal cancer (Cappello et al., 2005) and prostate cancer (Cornford et al., 2000)—which is linked to good patient outcome. In contrast, loss of Hsp60 expression is associated with the risk of developing an infiltrating recurrent bladder cancer (Lebret et al., 2003). Consistent with the role of Hsp60 in pro-survival functions, Hsp60 helps improve the vulnerability of pro-caspase-3 to proteolytic maturation—a very important event in apoptosis (Gruber et al., 2010).
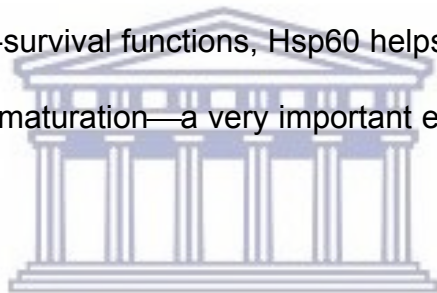
Hsp40

The Hsp40 or DNAJ family comprises more than fifty members identified in humans (Qiu et al., 2006). They are characterized by the presence of a conserved J domain which binds to the N-terminal ATPase domain of Hsp70 and the adjacent linker region. Hsp40 is a co-chaperone of the Hsp70 system which increases the affinity of binding to substrate proteins (Kampinga and Craig, 2010). The family is divided into three subfamilies based on their homology to the DNAJ protein from *E. coli* (Kampinga et al., 2009). Class I and II members function as chaperones that independently recruit Hsp70 to non-native substrates while class III members are diverse and they also combine the J domain with a variety of other functionalities (Kim et al., 2013). Hsp40 family proteins

31

have diverse functions, for example, Hsp40 functions in cell physiology (Hartl and Hayer-Hartl, 2002) whereas Hsp42 functions in the suppression of the aggregation of nonnative proteins (Tiwari et al., 2015).

Hsp 10-30

This family is also classified as the small heat shock proteins (sHps) which are found in all kingdoms. They are characterized by a conserved β-sandwich α-crystallin domain, which is flanked by variable N- and C-terminal sequences (Kriehuber et al., 2010, Chowdary et al., 2004, Bakthisaran et al., 2015). There are a total of eleven known sHsp's in the human genome (Kampinga et al., 2009). Like other Hsp's, sHsp's also function as molecular chaperones by preventing undesired protein interactions and assisting in refolding of denatured proteins (Park and Seo, 2015).

It is reported that sHsp's play an important role in muscle development and function. A critical aspect in muscle differentiation is generation of multinucleated muscle fibers through fusion of mono-nucleated myoblasts to which sHsp's are reported to play a direct role (Dubińska-Magiera et al., 2014). For example, *in vivo* studies show that HSPB5 mRNA is expressed early in myotomes or muscle differentiation (Benjamin et al., 1997). In addition, sHsp's in vertebrates maintain the clarity of the eye lens and aberrations in humans are linked to myopathies and neuropathies (Haslbeck and Vierling, 2015).

1.7.2.3   Regulation of the heat shock response (HSR)

The HSR is transcriptionally regulated by a family of heat shock transcription factors (HFs), which are activated by elevated temperatures (Cates et al., 2011, Åkerfelt et al., 2010). The key role of HSFs is to bind onto heat shock elements (HSE) which lie upstream of Hsp genes, driving increased expression of Hsp's and thereby conferring tolerance to thermal stress (Chowdary et al., 2004). The mammalian genome encodes three HSF homologues: HSF1, HSF2 and HSF4 (Wu, 1995).

It is speculated that HSF1 is the key player in the mammalian HSR. This is supported by the fact that a mouse HSF1 knockout is unable to induce the expression of hsp70 in response to thermal stress whereas HSF2 mouse knock out fibroblasts are (McMillan et al., 1998). In addition, mouse HSF1 knockout fibroblasts have defective development and growth (McMillan et al., 1998), which suggests that HSF1 also plays a key role in development. HSF2 is 35.2% identical to HSF1 and is activated by erythroid differentiation, embryogenesis and spermatogenesis (Morimoto, 1998).

HSF2 depends strictly on HSF1 for its stress-related functions and is recruited to hsp promoters only in the presence of HSF1. The cooperation between HSF1 and HSF2 require an intact HSF1 DNA binding domain (Åkerfelt et al., 2010). HSF3 has only been characterized in avian cells and is induced by high temperatures therefore both HSF1 and HSF3 are responsible for heat-induced Hsp expression (McMillan et al., 1998).
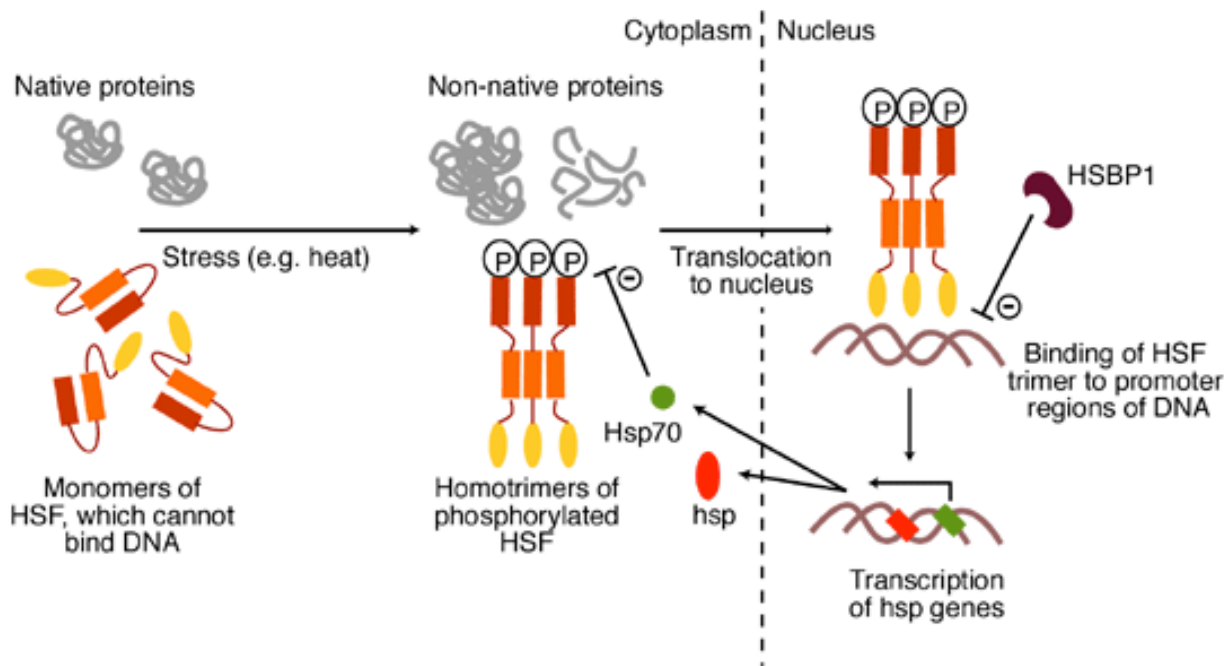
Figure 1.4 Regulation of the heat shock response. HSF1 is maintained as an inert monomer which gets activated by various stresses. Competition of unfolded substrates to bind to Hsp90 destabilizes the monomeric state of HSF1 to homo-trimers, which translocate to the nucleus. Overexpression of HSBP1 negatively regulates HSF1 DNA binding activity (Pockley, 2001).

Finally HSF4 is a novel family member that is yet to be characterized (Cotto et al., 1997, McMillan et al., 1998). The regulation of the HSR by HSF1 is diagrammatically illustrated in Figure 1.4. Under normal conditions, HSF1 is maintained as an inert monomer forming part of a multi-chaperone complex (Wu, 1995).

This complex, which includes Hsp70 and Hsp90, ensures that HSF1 is maintained in an inactive state by binding to its activation domain, thereby inhibiting activation. Stressful conditions such as heat shock lead to the accumulation of unfolded proteins which compete with HSF1 to bind Hsp90 (Shamovsky and Nudler, 2008). This destabilizes the complex, thereby causing a transition of HSF1 from an inert monomer to a homo-trimer (HSF_3) which translocates to the nucleus to bind DNA (Fulda et al., 2010). Once normal conditions are restored the HSF homo-trimer loses its activity and returns to its inert monomeric state. This attenuation is a result of over-expression of heat shock factor binding protein 1 (HSBP1) during stress, which binds to Hsp70 thereby negatively affecting HSF1 DNA binding activity (Satyal et al., 1998).

1.7.3 The cellular response to DNA damage

1.7.3.1   DNA damage and causes

DNA is the main genetic material in living organisms which contains all the genetic information required for the growth, development and reproduction of the organism (Jun, 2010). DNA is very stable and this is vital as it guarantees the maintaining and passing down of vital characters from one generation to the other (Wei-Feng et al., 2006). Damage to DNA can change or eliminate fundamental processes such as DNA

35

replication or transcription (Dexheimer, 2013). DNA damage may arise from either endogenous or exogenous factors, nevertheless the majority of DNA modifications are from an endogenous origin (De Bont and Van Larebeke, 2004). Spontaneous hydrolysis is one simple examples of endogenous DNA damage.

Formation of these lesions is estimated to occur at a rate of 100-500 times per cell per day which results from the formation of uracil from cytosine (Krokan et al., 2002). Endogenous cellular metabolism results in the accumulation of reactive molecules, which are known as reactive oxygen species. The most important of these molecules are O_2, hydrogen peroxide (H_2O_2) and nitric oxide (NO), which may cause DNA modification such as base modification, single or double-strand breakage and DNA-protein cross links (De Bont and Van Larebeke, 2004).

DNA damage can also be caused by ionizing radiation which can originate from both natural sources such as gamma radiation and artificial sources such as medical treatments involving X-rays (Ward, 1988). In addition to physical insults, DNA damage can also be caused by chemical agents such as the anticancer drugs methyl methanesulfonate and temozolomide. These drugs induce alkylation of the DNA bases and consequently induce DNA damage (Wogan et al., 2004).

1.7.3.2   DNA damage response pathway

Cells have evolved highly coordinated pathways to circumvent genotoxic stress, which are known as the DNA damage response (DDR). This response relies on the ability of

36

an organism to sense problems in its DNA and address these by arresting cell cycle progression and activation of DNA repair mechanisms (Giglia-Mari et al., 2011). Alternatively cells with irreparable genomes can be eliminated through apoptosis (Bernstein et al. 2002). The DDR pathway is a signal transduction pathway consisting of sensors, transducers and effectors. The identities of sensors are not yet known but they recognize lesions following DNA damage (Zhou and Elledge, 2000). Transducers coordinate the initiation of amplification and activation of checkpoints through phosphorylation. The central components of the signal transduction response are two related and conserved proteins kinases: ataxia-telangiectasia mutated (ATM) and ataxia telangiectasia and Rad 23 related (ATR) (Zhou and Elledge, 2000). DNA double strand breaks activate ATMs and ATR is activated by single stranded DNA regions exposed to UV or DNA replication fork stalling (Abraham, 2001). Effectors are protein kinases that execute a specific cellular response (Bartek and Lukas, 2003).
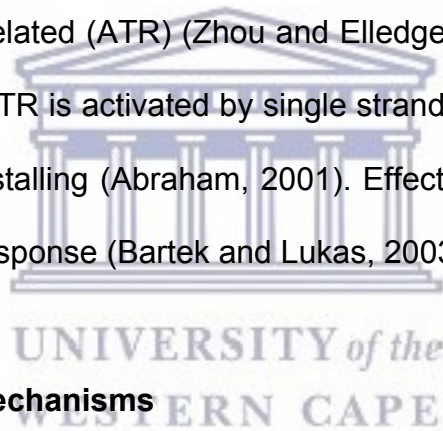
1.7.3.3 DNA repair mechanisms

Given that DNA is frequently challenged with insults at a frequency of about 10^4-10^5 impacts per cell per day, cells have developed multiple repair mechanisms wherein each corrects a different subset lesion to counter damage (Pan et al., 2016). The mammalian cell utilizes five major repair mechanisms: base excision repair (BER), mismatch repair (MMR), nucleotide excision repair (NER), and double-strand break repair, which includes both homologous recombination (HR) and non-homologous end joining (NHEJ) of which two are discussed below (Dexheimer, 2013).

Base excision repair

Base excision repair (BER) is the predominant mechanism responsible for the repair of damaged bases (Zharkov, 2008). Bases with small chemical alterations that do not distort the DNA double-helix structure are substrates for BER (Almeida and Sobol, 2007). The pathway is initiated by a lesion-specific DNA glycosylases that remove a damaged base by cleaving the *N*-glycosidic bond linking the base and its corresponding dexoyribose, leading to the production of an abasic site or AP site (Jacobs and Schär, 2012). An AP site specific endonuclease catalyses the incision of the AP site, the resultant gap is filled-in by a BER specific DNA polymerase and finally sealed by a XRCC1/ligase III complex (Giglia-Mari et al., 2011).

Nucleotide excision repair (NER)

In contrast to BER, the nucleotide excision repair (NER) pathway catalyses the removal of small base lesions that are derived from oxidation and can cause distortion of DNA helix structure (Hoeijmakers, 1993). This pathway is more complex than BER as it requires around 30 different proteins for the removal of damaged nucleotides (Tornaletti and Hanawalt, 1999). The NER system is divided into two distinct mechanisms, namely: global genome NER (GG-NER) and transcription-coupled NER (TC-NER) (Dexheimer, 2013).

The GG-NER mechanism is responsible for the elimination of lesions throughout the genome while TC-NER mechanism is responsible for the repair of lesions located on the coding strand of actively transcribing genes (Sugasawa et al., 1998). An excinuclease catalyses the formation of dual incisions on the damaged DNA strand to

38

remove an oligodeoxynucleotide-containing lesion, which are later ligated by a DNA polymerase. Defects of NER repair mechanism causes several human genetic disorders including xeroderma pigmentosum, Cockayne syndrome and trichothiodystrophy, which are all characterized by extreme sensitivity to the sun (Cleaver et al., 2009). This renders the pathway of biological importance.

1.8   Nuclear speckles

The mammalian cell nucleus is a highly dynamic environment characterized by the presence of defined structural units (Spector and Lamond, 2011). These defined structures or compartments create distinct environments within the nuclear landscape (Dundr and Misteli, 2010). There are a number of known proteinaceous nuclear bodies of varying sizes, including nuclear speckles, Cajal bodies, paraspeckles, polycomb bodies and promyelocytic leukemia bodies, as illustrated in Figure 1.5 (Dundr and Misteli, 2010, Spector and Lamond, 2011).

Nuclear speckles are amongst the most studied of nuclear bodies. They are located in the interchromatin region of the nucleoplasm, which accounts for the alternative name interchromatin granule clusters (ICGs) (Thiry, 1995). They are also referred to as SC35 domains or splicing speckles and are enriched with factors that are involved in pre-mRNA processing and RNA transport (Lamond and Spector, 2003). When observed under a fluorescence microscope, they appear as irregular beaded and immobile structures that vary in size that ranges from 2-3 μm. A typical nucleus at interphase contains 20-50 nuclear speckles (Thiry, 1995).

39
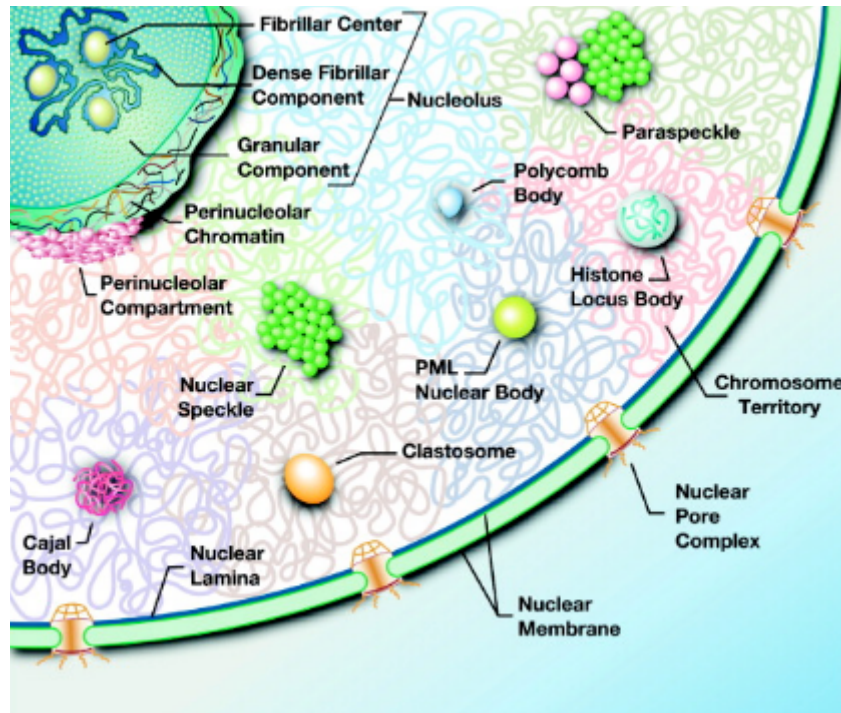
Figure 1.5 A fluorescence image depicting the internal compartmentalization of the mammalian cell nucleus. The nucleus is a very dynamic environment characterized by the presence of bodies such as nuclear speckles, Cajal bodies, and polycomb bodies (Mao et al., 2011)
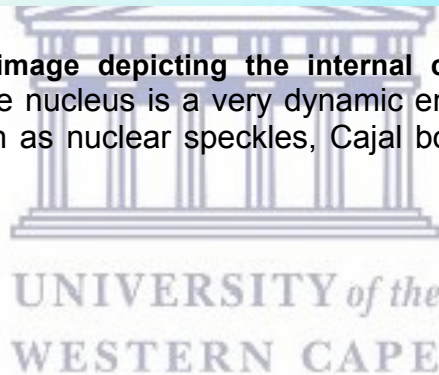
A number of studies have shown beyond doubt that there is no single signal that targets proteins to nuclear speckles. A study conducted in 2001 by Eilbracht and Schmidt-Zachmann identified the sequence element that directs SF3b[155], a spliceosomal protein, into speckles. They found it to be on the nuclear localisation signal which is rich in lysines (K) and arginines (R) (KRKRR, amino acids 196-200) and a molecular segment with multiple threonine-proline repeats (amino acids 208-513).

They also found that the amino acids 208-440 were required for correct subcellular localisation of SF3b[155] (Eilbracht and Schmidt-Zachmann, 2001). In contrast, a study

40

conducted by Salichs and co-workers revealed that a repeat of six histidine (His) residues was sufficient to direct heterologous proteins to nuclear speckles. They confirmed this by the generation of green fluorescent protein (GFP) fusion proteins with 5, 6, 7, 8 or 9 His repeats, which were analysed for subcellular localisation (Salichs et al., 2009).

They found that a positive relationship existed between the accumulation in speckles and the length of the His-tract (Salichs et al., 2009). Interestingly, GFP fusion proteins with polyproline or glutamine tracts, which are commonly found in transcription factors, showed no localisation into speckles. However a threonine-proline repeat in SF3b[155] (amino acids 208-513) has been shown to be involved in targeting the protein into speckles (Eilbracht and Schmidt-Zachmann, 2001). Indeed, nuclear speckles are dynamic and much remains to be discovered.
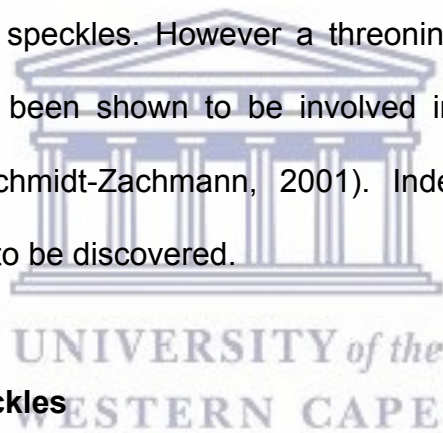
1.8.1 Composition of speckles

Nuclear speckles are a home for many pre-mRNA splicing factors, including spliceosomal small nuclear ribonucleoproteins (snRNPS), SR family proteins, as well as many other non-snRNP factor proteins which are yet to be characterized (reviewed in (Spector and Lamond, 2011)). Members of the SR family include SC35, ASF/SF2 and SRp20 (Kim et al., 2011). SR proteins are important splicing regulators which regulate alternative as well as constitutive splicing (Cáceres et al., 1997). They shuttle continuously between the nucleus and the cytoplasm, suggesting that the role of SR proteins may not be limited to nuclear pre-mRNA splicing but may also include unknown

41

cytoplasmic functions (Sanford et al., 2004). They are characterized by the presence of one or more RNA-recognition motifs (RRM) as well as a serine-arginine-rich dipeptide RS domain. In addition, there is a class of splicing factors called ~~the~~ SR-related proteins, which, unlike SR proteins, lack any RRM. Instead, SR-related proteins may contain other domains such as a DExD/H box or zinc finger.

A study using enriched IGCs from mouse liver revealed that a total of 146 known proteins were resident in speckles, in addition to a number of uncharacterized proteins (Mintz et al., 1999). Other RNA molecules such as uridine-rich small nuclear RNAs (UsnRNAs), 7SK RNA, metastasis-associated lung adenocarcinoma transcript 1 (MALATI1) and long noncoding RNA (lncRNA) have also been reported to be localised into speckles (see review (Spector and Lamond, 2011)). In an attempt to understand the role of splicing factors in the organization of nuclear speckles, Tripathi et al. (2012) showed that SRSF1 regulates the assembly of pre-mRNA processing factors in nuclear speckles.

An experiment conducted on Hela cells depleted of splicing factors in comparison to small interfering treated RNA targetting SRSF1 had mislocalization of several of the nuclear speckle components. In particular, SRF1-depletion caused a mislocalization of speckle nuclear proteins but not MALATI1. MALATI1 amongst all lncRNA is the most abundant and interacts with several splicing factors including SR proteins. The authors concluded that SRSF1, along with MALATI1, could influence the recruitment of splicing

factors into speckles (Tripathi et al., 2012). The mechanism of how speckles are formed and maintained within the cell is still poorly understood.

1.8.2 Dynamics of nuclear speckles

Nuclear speckles are very dynamic structures. This is supported by the fact that size, shape as well as number of speckles vary between cell types (Spector and Lamond, 2011). Nuclear speckles have since been speculated to be storage and assembly areas for pre-mRNA splicing machinery including spliceosome subunits, therefore play a crucial role in alternative splicing (Kim et al., 2011). Alternative splicing of mRNA provides an important means of genetic control and is a crucial step in the expression of most genes (Chen and Manley, 2009). Studies have shown that inhibition of transcriptional and/ or splicing activity causes an accumulation of splicing factors into speckles (Reddy et al., 2012).
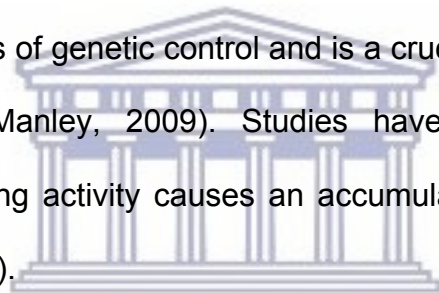
In addition, speckles were observed to be larger in size when using microscopic techniques (Melcak et al., 2000). Fluorescence microscopy with photobleaching has revealed that the rate of exchange of speckle components is very rapid (Phair and Misteli, 2000). Studies conducted on the splicing factor SF2/ASF revealed that it had a mean residence time in speckles of no more than ~50 seconds which suggests that exchange rate of speckle components is a very rapid one (Lamond and Sleeman, 2003). In addition, the dynamic events of speckles are said to be dependent in the activities of RNA polymerase II transcription (Misteli and Spector, 1999). Although,

43

dynamics and regulation of nuclear speckles are not well understood, studies are shedding light on this phenomenon.

1.9   Nuclear stress granules

Nuclear stress granules (nSG) were originally described as sub-nuclear structures where HSF1 became concentrated following heat shock. HSF1 is a transcription factor and is the classical inducer of heat shock genes (Sarge et al., 1993). Exposure to elevated temperatures, heavy metals and amino acid analogues cause a rapid translocation of HSF1 to the nucleus, forming large, irregularly shaped bright staining granules (Cotto et al., 1997). HSF1 granules vary between 0.3 and 3 μm and appear as single globular granules or grape-like clusters of smaller globular structures (Sandqvist and Sistonen, 2004).
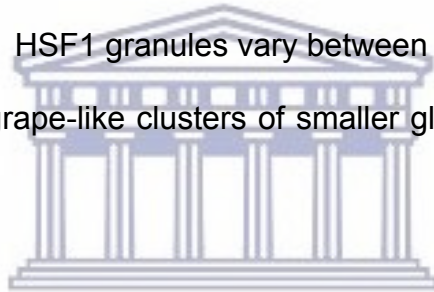
nSG are discrete bodies as they do not co-localize with other sub-nuclear bodies such as coiled bodies, SC35-containing speckles, kinetochores and PML bodies. HSF1 was the first component to be found in nSG but it has been proven that HSF2, which was previously considered refractory to stress stimuli, co-localises together with HSF1 in response to heat shock (Alastalo et al., 2003). HSF1 granules are remarkable structures that can be detected within 30 s of heat shock using live cell imaging (Jolly et al., 1999). Once the stress has passed, HSF1 granules gradually disappear.

1.9.1 SG formation

SG are phase dense entities that appear in the nucleus when cells encounter stressful conditions, including oxidative stress, exposure to heavy metals, thermal shock and UVC irradiation. SG are assembled in response to the stress-induced phosphorylation of the eukaryotic initiation factor (eIF)2α, the central trigger of the integrated stress response (ISR) (Kedersha et al., 2013). The key features of ISR are polysome disassembly, translational arrest and SG assembly (Kedersha et al., 2000). These key features enable the cell to reprogram its translational repertoire through a process known as mRNA triage.

Several environmental insults activate one or more stress-sensing serine/threonine kinases that phosphorylate serine residue 51 of (eIF)2α. Phosphorylation of (eIF)2α inhibits the formation of the $tRNA_i^{Met}$/GTP ternary complex that is required for translational initiation (Kedersha et al., 1999). In the absence of the ternary complex, formation of the 48S pre-initiation complex that normally assembles on the 5'-ends of capped mRNAs is disrupted, thereby producing a translationally stalled 48S complex that is unable to recruit the 60S ribosomal unit (Kedersha et al., 2002, Anderson and Kedersha, 2002).

The accumulation of stalled complexes is believed to result in the formation of SGs. It has also been reported that SG assembly could happen in the absence of the phosphorylation of (eIF)2α (Moutaoufik et al., 2014). Inhibition of translational rates by targeting the activity of (eIF)2α with either hippuristanol or pateamine is sufficient to

induce SG formation (Dang et al., 2006). Furthermore, it has been reported that over-expression of RNA-binding proteins (RBPs) such as SDC6 induce the formation of SG-like granules without translational repression (Kruger et al., 2013). Therefore, like nuclear speckles, the formation and decay of SGs is a matter which requires further investigation.
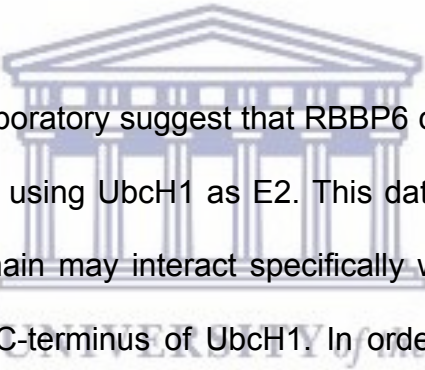
1.9.2 Function of SGs

SG formation has variable consequences for the cell. During stress, the accumulation of unfolded proteins can results in stalling of translation. This is followed by rapid sequestration of mRNA transcripts and their associated proteins into SGs (Buchan and Parker, 2009). This allows cells to direct their energy into translating mRNA that encode proteins that refold denatured proteins (Buchan and Parker, 2009). SGs are disassembled when the stress passes, releasing the mRNA transcripts so that translation can resume as normal (Waris et al., 2014).

This is supported by the study pioneered by Nover et al. (1989), which identified mRNA as a component of plant heat shock granules. Heat shocked granule mRNAs were found to encode constitutively expressed heat shock proteins but not newly synthesized heat shock proteins (Nover et al., 1989). Hence a proposition was made that plant heat shock granules served as storage repository for untranslated mRNAs (Nover et al., 1989). SGs have also been reported to prime T cells for rapid cytokine translation and secretion upon T cell receptor stimulation. The function of SG is not clearly understood but ongoing research is shedding light.

1.10 Aims and objectives of this study

Retinoblastoma Binding Protein 6 (RBBP6) is a multifunctional protein with a well-established role in mRNA processing. In this thesis we set out to investigate the role of RBBP6 in ubiquitination of YB-1, the cellular localisation of RBBP6 as well as its potential for auto-ubiquitination. Based on the structures of other E3 ubiquitin ligases such as Parkin, we hypothesized that the DWNN domain of RBBP6 may inhibit the ubiquitination activity of the RING finger domain by binding to it and occluding its active site. Hence we decided to investigate whether an interaction exists between the DWNN domain and the RING finger *in vitro.*

Unpublished data from our laboratory suggest that RBBP6 catalyses ubiquitination of Y-Box Binding Protein1 (YB-1), using UbcH1 as E2. This data led to the suggestion that the ubiquitin-like DWNN domain may interact specifically with the ubiquitin-associated (UBA) domain found at the C-terminus of UbcH1. In order to test this, UBA and the DWNN domain were expressed in bacteria and used in *vitro* assays to investigate a possible interaction. RBBP6 has been identified as a component of the human mRNA splicing machinery. A model has recently been proposed whereby the DWNN domains of isoforms 1 and 3 compete with each other for binding to CstF-64, a central component of the 3'-end processing complex. The question arises as to where in the cell this interaction takes place. Full-length RBBP6 has been reported to localise in the nucleus and more precisely in nuclear speckles, however very little is known of the localisation of isoform 3.

47

Unpublished data generated in our laboratory suggest that endogenous isoform 3 is predominantly cytoplasmic, but accumulates in nuclear speckle-like bodies following a number of stresses. One of the aims of this work was to investigate the cellular localisation of HA-tagged forms of isoforms 1 and 3 transfected into mammalian cells, using immunofluorescence microscopy. Of particular interest is the GG motif found at the C-terminus of the DWNN domain in both isoforms 1 and 3; a further aim was to investigate whether the GG motif played a role in the localisation of isoforms 1 and 3.

CHAPTER 2 : MATERIALS AND METHODS

Lists of reagents and buffers used can be found in Appendix I

Table 2.1: List of primary antibodies used for this thesis

Antibody	Species	Dilution for IHC	Dilution for immunoblot	Company	Catalog no.
α-HA	Mouse	1:100	1:1000	Santa Cruz	Sc-7392
α-FLAG	Mouse	1:200	1:2000	GenScript	A00187-100
α-SC35	Mouse	1:1000	NA	Abcam	Ab11826
α-HA	Goat	1:500	NA	Abcam	Ab9134
α-His	Mouse	NA	1:1000	GenScript	A00186S
α-DWNN	Mouse	NA	1:500	Bellstedt lab	N/A
α-Ring Finger	Rabbit	NA	1:1000	Bellstedt lab	N/A
α-zinc finger	Rabbit	NA	1:1000	Bellstedt lab	N/A
α-YB-1	Rabbit	NA	1:1000	Bellstedt lab	N/A

Table 2.2: List of secondary antibodies used for this thesis

Conjugate	Species	Target species	Dilution	Company	Catalog no.
Horseradish peroxidase	Goat	Mouse	1:1000	Santa Cruz	Sc-2005
Horseradish peroxidase	Donkey	Rabbit	1:3500	Abcam	Ab16284
AlexaFluor488	Donkey	Goat	1:1000	Jackson Immuno Research Laboratories	705-545-003
Cy3	Donkey	Mouse	1:1000	Jackson Immuno Research Laboratories	715-165-150

2.1 Description of non-commercial antibodies

A mouse mono-clonal antibody was raised against the DWNN domain, residues 1-81 of RBBP6, recombinantly-expressed in *Escherichia coli,* at the European Molecular Biology Laboratory, Monterotondo-Scalo, Italy. Rabbit polyclonal antibodies were raised against residues 1-81 of RBBP6 (α-DWNN), residues 248-335 of RBBP6 (α-RING), residues 80-197 of RBBP6 (α-zinc finger) and against full-length human YB-1, all recombinantly-expressed in *E. coli*, in the laboratory of Prof D. Bellstedt (Biochemistry Department, University of Stellenbosch, Stellenbosch, South Africa) using the naked bacteria method (Bellstedt et al., 1987).

2.2 Bacterial strains and genotype composition

E. coli strain BL21 Codon-Plus (DE3)-RIPL: F– *ompT hsdS*(rB– mB–) *dcm+* Tetr *gal* λ(DE3) *endA* Hte [*argU proL* Camr] [*argU ileY leuW* Strep/Specr] was used to express recombinant proteins. These cells contain extra copies of rare *E. coli* argU, ileY, LeuW and proL tRNA genes which corrects for codon bias, thereby dramatically improving expression sequences from other organisms.

E. coli strain XL10-Gold: endA1 glnV44 recA1 thi-1 gyrA96 relA1 lac Hte Δ(mcrA)183 Δ(mcrCB-hsdSMR-mrr)173 tet^{R}F'[proAB lacI^{q}ZΔM15 Tn10(Tet^R Amy Cm^R)] was used to produce plasmid DNA. Mutations in endA1 inactivate intracellular endonucleases that degrade plasmid DNA, and in recA1, eliminate homologous recombination, thereby reducing the chance of deletions and plasmid multimerisation which makes this stain suitable for high quality plasmid DNA production.

http://etd.uwc.ac.za/

2.3   Plasmid vectors

2.3.1   pGEX-6P-2

pGEX-6P-2 (see Figure 2.1) is a bacterial expression vector with a size of 4.9 Kb which expresses the target protein as a fusion to the C-terminus of Glutathione-S-transferase (GST) from *Schistosoma japonica*. GST aids in purification of recombinant proteins from *E. coli* native proteins and increases the solubility of the fusion protein. A recognition sequence for 3C protease from human rhinovirus located between GST and the MCC facilitates post-translation removal of GST from the fusion protein. The vector incorporates an IPTG-inducible *tac* promoter to drive high levels of expression. The vector confers ampicillin resistance to transformed bacterial cells.

2.3.2   pCMV-UWC

pCMV-UWC (see Figure 2.2) is a modified form of the pCMV-HA mammalian expression plasmid created by replacing the multiple cloning cassette (MCC) with that from pEGFP-C1. It was generated to facilitate sub-cloning of large inserts such as RBBP6 (5.4 kbp), which would have been difficult using PCR amplification. It was created by Genscript Inc. by insertion of the sequence: 5'-TCCGGACTCAGATCTCGAGCTCAAGCTTCGAATTCTGCAGTCGACGGTACCGCGG GCCCGGGA-3' between the sequences 5'-CCAGATTACGCTCTT-3' and 5'-GGGATCCAGACATGA-3' in pCMV-HA. It enables expression of the target gene in mammalian cells with an N-terminal HA epitope tag for immunodetection using anti-HA antibodies. The vector contains an ampicillin resistance gene for bacterial selection.

51

2.3.3 pcDNA3

pcDNA3 (see Figure 2.3) is a mammalian expression vector with a size of 5.4 Kb. The vector drives expression of mammalian proteins under a CMV promoter and T7 promoter for bacterial selection. In addition, pcDNA3 contains a neomycin gene that aids in selection of transformed mammalian cells using the antibiotic Geneticin® (G418).

2.4   Preparation of competent *E. coli* cells for transformation

Bacterial strains were streaked onto LB agar plates and allowed to grow for 18 hours. A single colony was picked and inoculated into TYM broth and allowed to grow overnight. The cell culture was then scaled up to 400 ml using fresh TYM broth. This was allowed to grow until an optical density OD600 was in the range 0.4-0.6 at 37 °C with shaking. Cells were rapidly chilled in ice water and the transferred into 500 ml polyproplylene tubes and centrifuged at 6000 g for 10 minutes at 4 °C. Supernatants were discarded and pellets were re-suspended in 100 ml of chilled Tfb1 and allowed to incubate on ice for 30 minutes. Cells were recovered by centrifugation at 6000 g for 8 minutes. Resultant pellets were gently re-suspended in 15 ml of Tfb2. 150 µl suspensions were aliquoted and immediately placed in a -80 °C freezer.

2.5   Bacterial transformations with plasmid DNA

Transformations were carried out using the bacterial strains described in Section 2.2. Generally, 50 µl of the competent *E. coli* cells were transformed with 25-50 ng of DNA. Firstly, the cells were allowed to thaw on ice and then allowed to incubate with DNA for

at least 15 minutes. Thereafter the cells were heat shocked at 42 °C for 90 seconds, followed by incubation on ice for 2 minutes. Pre-warmed LB was added and transformed cells were incubated with shaking at 37 °C for an hour and then plated onto LB agar plates with appropriate antibiotics.

2.6 Manipulation of plasmid DNA: cloning

2.6.1 PCR amplification of gene fragments

Gene fragments suitable for cloning were amplified by Polymerase Chain Reaction (PCR), incorporating restriction enzyme sites and stop codons, as appropriate. Generally, the PCR reaction consisted of 50 ng of template DNA, 50 ng of each primer, 1 U of Taq DNA polymerase and 200 µM of dNTPs in a total volume of 25 µl. Below is a table that shows all primer sequences used for the creation of various constructs for this project.
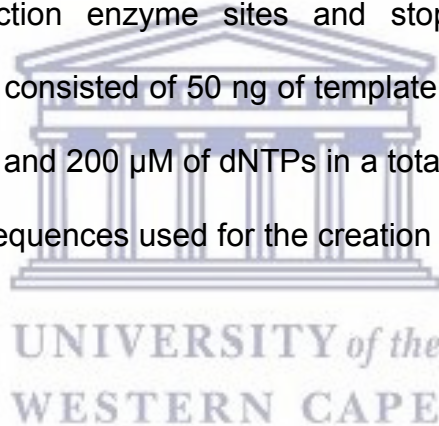
The PCR reaction was allowed to proceed under the following general parameters:

Initial denaturation 96 °C for 4 minutes

Denaturation 94 °C for 1 minute

Annealing 60 °C for 1 minute ⎫ 30 cycles

Elongation 72 °C for 2 minutes

Final elongation 72 °C for 10 minutes

A

B
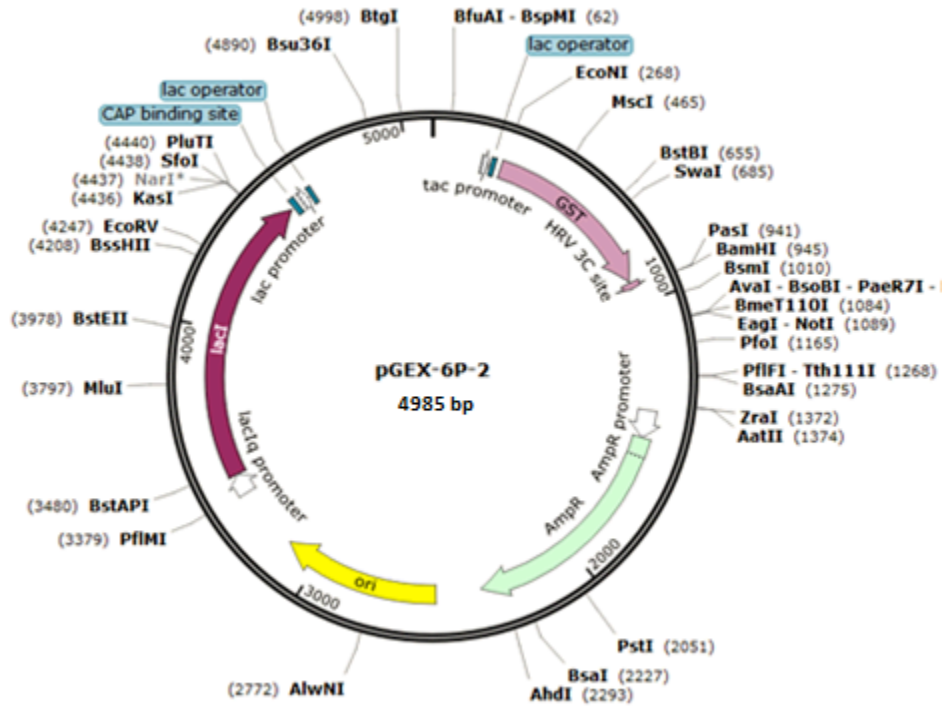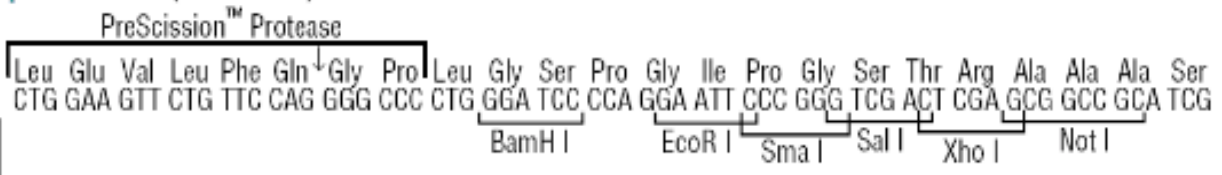
Figure 2.1: Restriction map of pGEX-6P-2 including the multiple cloning cassette.
(A) The pGEX-6P-2 vector is a bacterial expression vector that drives the expression of recombinant proteins under a *tac* promoter. (B) The MCC facilitates the cloning of target DNA and is followed by a 3C protease site, which facilitates cleavage with 3C protease.
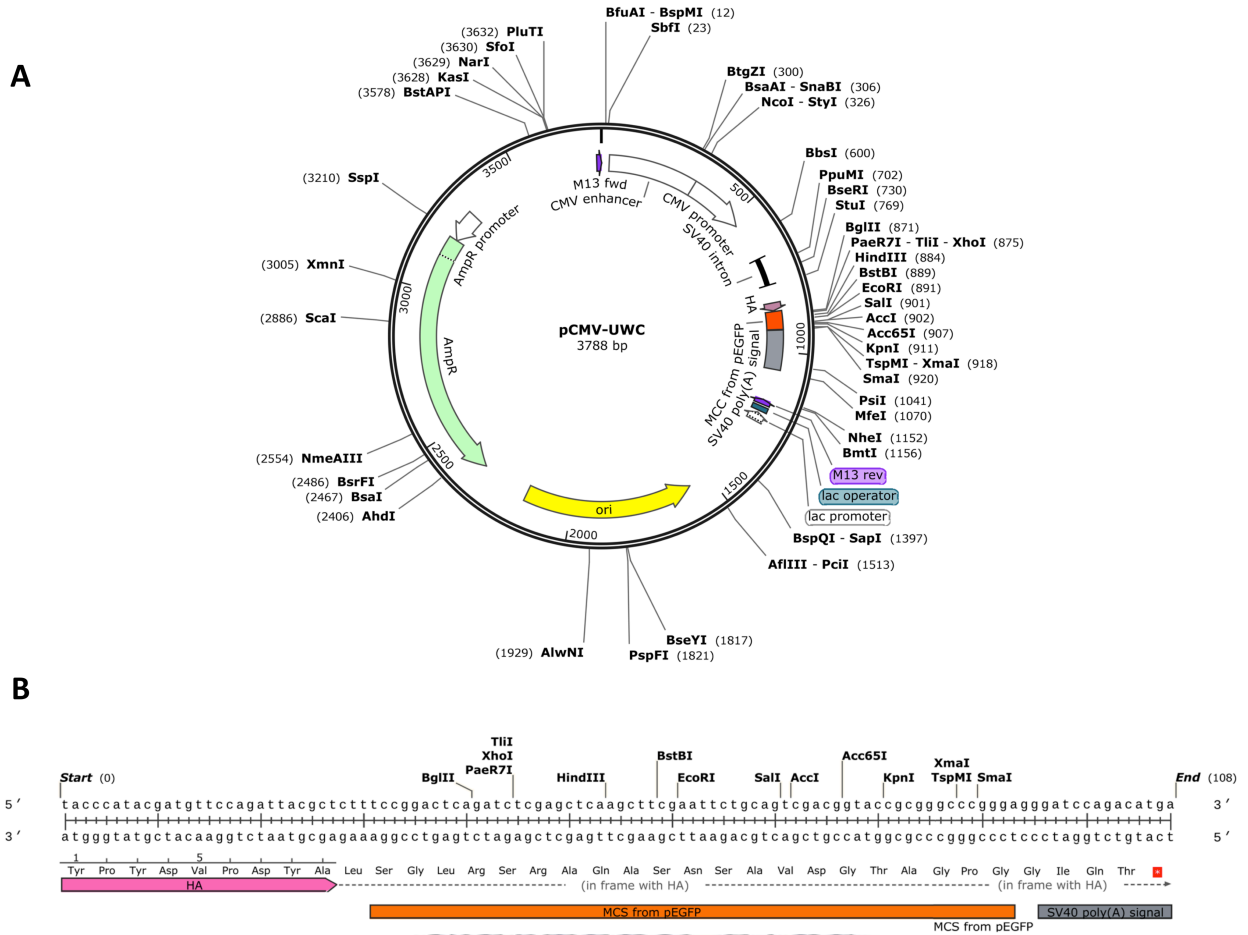
Figure 2.2: Restriction map of pCMV-UWC including the multiple cloning cassette.
(A) pCMV-UWC is a mammalian expression vector that expresses a protein under the control of the CMV promoter. (B) The MCS facilitates cloning of a target and the HA tag aids in immunodetection using western blots or immunofluorescence microscopy.
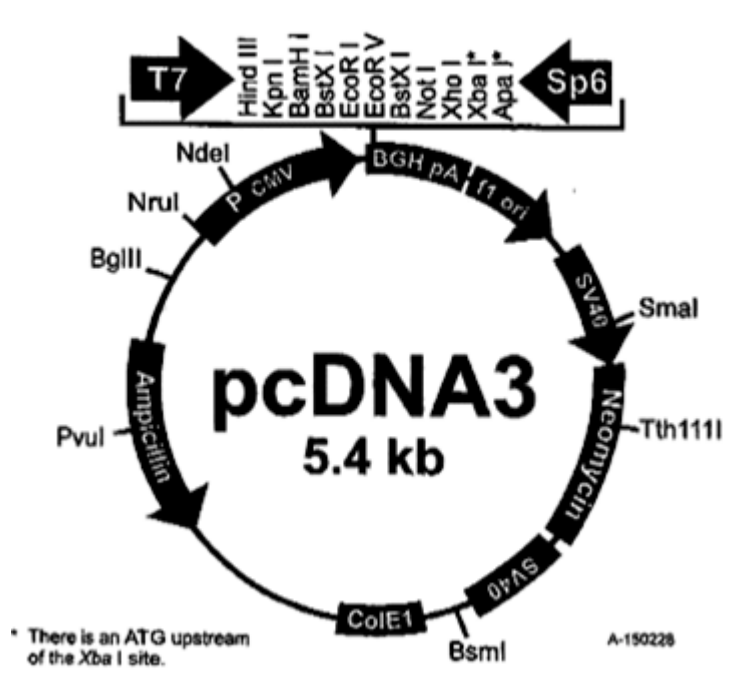
Figure 2.3: Restriction map of pcDNA3, including the multiple cloning cassette. The plasmid contains the CMV promoter for high-level constitutive expression in mammalian cells, as well as a T7 promoter for bacterial expression. It contains a neomycin antibiotic resistance gene for mammalian selection and an ampicillin resistance gene for bacterial selection.
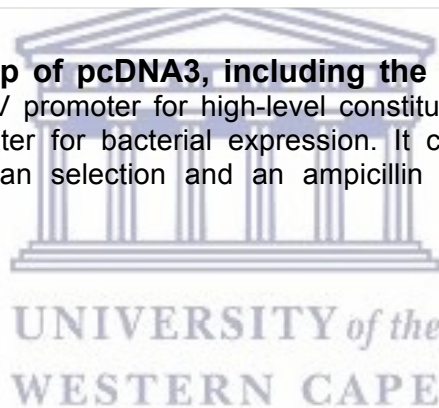
2.6.2 Restriction digestion of DNA

All enzymes were used according the manufacturer's instructions. A typical digestion reaction consisted of 1-5 µg of DNA which was incubated at 37 °C for an hour with no shaking. Digested DNA fragments were analyzed on a 1 % agarose gel and then gel purified using the Thermo Fisher Scientific GeneJet gel extraction kit, according to the manufacturer's instructions.

Table 2.3: Primers used for the amplification of various gene fragments and constructs. Complimentary regions are shown in black, restriction enzyme sites in green and stop codons in red. 6 Six G/C-rich bases were added to the 5'-end to increase the efficiency of cleavage of the amplicon by restriction enzymes.

Primer name	Primer sequence
pGEX-UBA-F	5'-GAG GCG GGA TCC AGT CCA GAA TAC ACC AAA AAA AT-3'
pGEX-UBA-R	5'-GAG GCG CTC GAG TTA TCA GTT ACT CAG AAG CAA TTC T-3'
pCMV-UWC-DWNN-PI-F	5'-GAG GCG CTC GAG CTT CCT GTG TGC ATT ATA AAT TTT-3'
pCMV-UWC-DWNN-PI-R	5'-GAG GCG GGT ACC TCA TTA AAT TCT TCT AAC AAT TAC A-3'
pcDNA3-DWNN13-F	5'-GAG GCG GGA TCC ATG TCC TGT TGT GCA TTA TAA ATT TTC C -3'
pcDNA3-DWNN13-R	5'-GAG GCG TCT AGA TCA TTA TAA AGG TAA AAG CAA TCT -3'

2.6.3 Ligation of DNA fragments

A general ligation reaction was set up to a final volume of 20 µl using 15-25 ng of vector and 12-30 ng of insert DNA depending on the ratio desired. Normally 1:5 and 1:7 insert DNA ratios were used. 1 Weiss unit of T4 DNA ligase (Thermo Fisher Scientific) was added. Ligation reactions were allowed to proceed overnight at 4 °C or at room temperature for 3 hours.

2.6.4 Verification of cloned sequences

Plasmid DNA was extracted from putative positive transformants subjected to double digestion using the same enzymes used in the cloning, in order to release the cloned insert. Sequences were verified by direct sequencing at Inqaba Biotec™ (Inqaba Biotechnical Industries, Hatfield, South Africa). The sequence of the expected plasmid

was constructed using SnapGene Viewer (GSL Biotech LLC, Chicago, IL, US; www.snapgene.com) and compared against the experimental sequence reads. Unknown sequences were aligned with the known sequence using the BLAST 2 alignment tool (http://blast.ncbi.nlm.nih.gov/Blast). Once verified, high quality, endotoxin-free plasmid DNA was extracted and stored at -20 °C.

2.6.5 Agarose gel electrophoresis

The sizes of DNA plasmids and fragments were assessed by electrophoresis using a 1 % agarose homemade gel made in 1X TAE buffer. GR Green for visualization at 280 nm was added to the gel to a final concentration of 0.5 µg/ml. DNA molecular weight markers (Thermo Fisher Scientific) were loaded alongside samples. Electrophoresis was carried out at 90 V for 100 minutes, unless otherwise stated. Gels were visualized and imaged using the transluminator connected to a DC 120 UV-camera.

2.6.6 Quantification of DNA

Purified DNA was quantified using Nanodrop (ND-1000 spectrophotometer, Biotechnologie GmbH) by measuring the absorbance at 280 nm.

2.7 Recombinant protein production and purification

2.7.1 Protein production

Expression constructs were transformed into *E. coli* BL21 Codon Plus as described in Section 2.5 and plated on LB agar containing the appropriate antibiotics. Colonies were picked and grown in 20-30 ml LB broth with appropriate antibiotics to create starter

58

cultures. Starter cultures were scaled up to a final volume of 1L with appropriate antibiotics and grown to an optical density OD_{600} of 0.4-0.6. Prior to induction, 200 µM $ZnSO_4$ was added to zinc-binding proteins to enable proper folding. Protein expression was carried out by adding varying concentrations of IPTG. Induction was allowed to proceed at 30 °C for 16 hours with shaking. Cells were harvested by centrifugation at 6000 xg for 15 minutes. Pellets were re-suspended in cell lysis buffer and stored at -20 °C.

2.7.2 Protein purification

2.7.2.1   Extraction of proteins

Pellets were allowed to thaw on ice and then sonicated for 5X 30-second pulses, with incubation on ice between pulses, using a MSE Soniprep 150 Plus ultrasonic Disintegrator (57 Kangley Bridge road, Lower Sydenham, London, UK). Sonicated pellets were centrifuged at 4300 rpm for 1 hour to obtain a clarified lysate.

2.7.2.2   Purification of fusion proteins from lysates

A glutathione agarose column (BIORAD) was prepared according to the manufacturer's instructions. The column was allowed to pack by gravity. Preparation proceeded by first allowing the beads to incubate in 8 M urea at 37 °C for 30 minutes. The column was allowed to flow and 5X column volumes of dH_2O was loaded onto the column and allowed to flow through. This was followed by the addition of 5X column volumes of cleansing buffer 1 and cleansing buffer 2 with dH_2O washes in between. Finally the column was equilibrated with 5X column volumes of 1X PBS. The clarified protein was

loaded onto the column and the flow through was collected. The column was washed with 3 column volumes of buffer before eluting. Proteins were eluted with 20 mM reduced glutathione. The final elution was carried out using 1 M NaCl. Columns were stored in 1 M NaCl with 0.2 % NaN$_3$.

2.7.2.3   Dialysis and removal of GST with 3C protease

Elution fractions containing GST fusion protein were pooled and transferred to a Snakeskin™ dialysis bag (3.5 kDa MWCO) and dialysed against 1X PBS with 1 mM DTT at 4 °C. After four hours 3C protease was added and cleavage was allowed to proceed overnight. After cleavage, GST was separated from the target protein using a glutathione agarose column.

2.7.3.4   Analysis of proteins using SDS-PAGE

Analysis of proteins was carried out using 12 % SDS-PAGE gels. TGX™ and TGX Stain-Free™ FastCast™ Gels were prepared according to the manufacturer's instructions (BioRad). Protein samples were prepared by adding an equal volume of 2X sample buffer and then boiling at 95 °C for 8 minutes. Samples were centrifuged for 10 minutes and the supernatant was loaded onto a prepared gel. Generally, 10-20 μl of each prepared protein sample was loaded and separated by electrophoresis using the BIORAD Mini Protean system at 40 mA or 200V for 25 to 30 minutes. Gels were stained with Coomassie staining solution for 30 minutes and destained water overnight. Gels for western blot analysis were immediately placed in transfer buffer following electrophoresis for further processing.

2.8 Extraction and immunoprecipitation of proteins from human lysates grown on mono-layer

Lysate was prepared by discarding the media from the flask and then washing the cells twice with 1X PBS. This was followed by the addition of extraction buffer (1 mM DTT, 0.5 Triton X-100 in 1X PBS) and incubation on ice for 5 minutes. The bottom of the flask was scraped using a scraper and the cells were transferred to a 15 ml Greiner tube and then sonicated 3 X with 15-second pulses with incubation on ice between the pulses. This was then followed by centrifugation at 3000x g for 30 minutes. The supernatant was removed and glycerol was added to a final concentration of 10 %. Lysate was stored at -80 °C. A general immunoprecipitation was carried out with 100 µg of lysate and with 1 µg of antibody. The reaction was allowed to proceed with shaking at 25 °C for an hour. After that 50 µl of Protein A/G PLUS agarose beads (sc-2003, Santa Cruz Biotechnology, Inc., CA, USA) were added and this was allowed to proceed for 2 hours with rolling at 4 °C. This was followed by three washes with 500 µl of 1X PBS at 12 000 rpm. The beads were re-suspended in 1X PBS with glycerol for a final concentration of 5 %.

2.9 *In vitro* ubiquitination assays

Ubiquitination assays were set up using recombinantly expressed and immunoprecipitated proteins. Generally, a ubiquitination assay consisted of buffer made up of 0.5 mM ZnSO4, 5 % glycerol, 5-10 mM Mg-ATP, 1 mM DTT or β-mercaptoethanol in 1X PBS. A general *in vitro* ubiquitination assay is shown on Table, 2.2. Reactions were carried out at 37 °C with shaking for 2-16 hours. After incubation, proteins were

61

precipitated with acetone and then re-suspended in 2X sample buffer. Samples were analyzed by immunoblotting.

Table 2.4: Reagents for in vitro ubiquitination assay

Reagent	Experiment
His-E1	400 nM
E2	2 mM
E3 (R3/ R2)	5 µg
HA-Ubiquitin	1 mM
YB1	10 µg
Mg-ATP	5 mM
Buffer	Added to a final volume of 150 µl

2.10 GST pull-down interaction assays

GST pull-down assays are used to investigate the physical interaction between two proteins. One protein (the "bait") is expressed as a fusion with GST tag, which is used to immobilize the protein on glutathione-conjugated agarose resin. A second protein (the "prey") is incubated with the bait and then subjected to repeated washing in order to wash away unbound proteins. Finally the resin and any attached proteins are loaded onto an SDS-PAGE gel and western blotted with antibodies targeting the prey protein in order to determine whether it was retained on the resin by an interaction with the bait protein.

GST-tagged bait protein was incubated with 20 % fresh agarose at room temperature with shaking. After 1 hour prey proteins were added and allowed to couple through incubation for a further 2 hours. The sample was centrifuged at 5000 rpm for 5 minutes

and the supernatant was discarded. To increase the stringency 0.5 M NaCl prepared in 1X PBS was added to the 2nd three washes and 5 % SDS prepared in water was added to the 3rd set of three washes. Excess supernatant was removed and beads were re-suspended in 35 µl of 2X sample buffer, boiled at 95 °C for 8 minutes and then subjected to SDS-PAGE. Western blotting was carried out as described in Section 2.11.

2.11 Immunoblotting

After running an SDS-PAGE gel, proteins were transferred onto the PVDF membrane by using transfer buffer (25 mM Tris, 0.2 M glycine, 20 % ethanol). After transfer, the membrane was blocked with 1 % casein in PBST (1X PBS with 0.1 % Tween® 20). This was followed with incubation with primary and then secondary antibodies. Unbound antibodies were washed off 3 times for 5 minutes with PBST. Visualisation was carried out by incubating the membrane with Clarity Western ECL substrate (BIORAD) and then imaging with the BioSpectrum® Imaging System, Chemi HR 410 UVP system.

2.12 Cell culture studies

2.12.1 Cells used in this study

A549 cells are human alveolar basal epithelial cells. They are squamous in nature and grow as adherent mono-layers *in vitro*. They function in the diffusion of substances across the alveoli and lungs.

63

2.12.2 Preparation of media

All cell culture reagents were purchased and prepared in a sterile manner to avoid contamination. A549 cells were cultured in Dulbecco's Modified Eagle Medium (DMEM) or DMEM F12 media, which was supplemented with 10 % Fetal bovine Serum (FBS) and 10 % penicillin-streptomycin (pen strep). Prepared media was aliquoted into 50 ml Greiner tubes and stored at 4 °C for not more than 2 months.

2.12.3 Growing of mammalian cells (seeding)

A549 cells were purchased from the American Type Culture Collection and cultured using their guidelines. Frozen stocks stored at -140 °C were allowed to thaw on ice. 5 ml of prepared media aliqoted into 15 ml Greiner tubes to which thawed cells were added. Re-suspended cell solution was mixed by gently inverting and centrifuging at 2200 rpm for 2 minutes. Supernatant was removed and cells were re-suspended in 5 ml of prepared media and grown in T-25 flasks or 12-well culture plates. Cells were incubated at 37 °C with 5 % CO_2. Media was changed every second day until the cells were confluent.

2.12.4 Trypsinization of cells

Cells were trypsinized or passaged once ~80 % confluency was reached. For trypsinization, media was discarded and cells were rinsed once with 5 ml 1X PBS. PBS was discarded and 2 ml of Trypsin-Versene (EDTA mixture) 1X was added. Trypsinization was allowed to proceed at 37 °C for 5 minutes. After 5 minutes, 2 ml of complete media was added to the trypsinized cells and they were collected by

64

centrifugation at 2200 rpm for 2 minutes. Cells were re-suspended in media and grown again. Cells were passaged not more than 10 times and then another stock of cells was started.

2.13   Seeding of cells for transfections

Trypsinization of cells was carried as described above. After re-suspension of cells in 3 ml complete media, a 10 μl aliquot of the suspension was transferred into an Eppendorf tube. 10 μl of trypan blue solution, 0.4 % was added to the suspension and gently mixed by pipetting up and down. 10 μl of the suspension was loaded onto Countess® Cell Counting Chamber Slides and the slide was inserted in Countess® Automated Cell Counter slide chamber and cells were counted. Generally 12-well culture plates were used for transfections. A day prior to transfection, $1X\ 10^5$ cells were seeded onto wells which had 12 mm diameter cover slips on them to achieve 60-80 % confluency on the day of transfection.
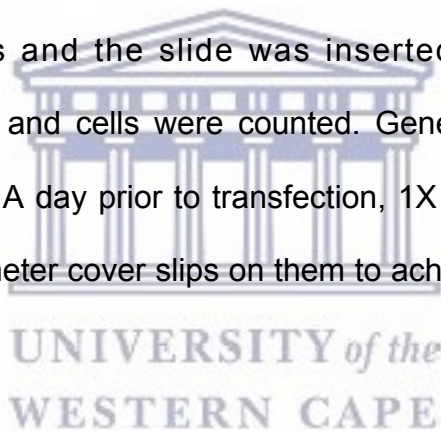
2.13.1 Preparation of DNA for transfection

 Constructs to be used were transformed into *E. coli* XLGOLD cells. Purification of DNA was carried out using Thermo Fisher Scientific GeneJet maxi prep kit. Purified DNA was stored at -20 °C.

2.13.2 Preparation of a DNA complex for transfection

On the day of transfection, all reagents were brought to room temperature. A general transfection protocol to transfect a single well is shown in Table 2.5. Cells were rinsed

65

once with 1X PBS and enough serum free media was added to cover the cover slip. Prepared DNA complex was allowed to incubate for 20 minutes and added to the well. After 4 hours, complete media was added to cells and allowed to grow overnight. Complexes were removed the following day in the morning and complete media was added. Cells were allowed to grow for 24-48 hours at which they were processed for immunofluorescence microscopy or western blotting.

Table 2.5: Reagents for a transfection assay for a 12-well plate

Reagent	Experiment	Control
DNA	200-350 ng	-
Transfection reagent	3.3 µl	3.3 µl
DMEM F12 serum free media	To a final volume of 52 µl	To a final volume of 52 µl

2.14   Stress induction experiments by heat shock

Generally stress experiments were carried out on transfected cells after 24 h. Flasks were placed in an incubator at 45 °C for 10 minutes. Cells were allowed to recover for 10-15 minutes in an incubator at 37 °C with 5 % CO_2.

2.15   Immunofluorescence staining protocol for fixed cells

Cells were fixed and stained after 24-48 hours as outlined in the following protocol. Cells were permeabilized with 500 µl of ice cold methanol for 5 minutes at -20 °C. Methanol was removed and cells were fixed with 500 µl of 4 % formaldehyde for 5 minutes at room temperature. Formaldehyde was removed and cells were rinsed three times with centrifugation for 5 minutes in PBST. Cells were blocked with 1 % BSA for 30

minutes. Generally primary antibody was diluted in 1% BSA and was added and incubated overnight at 4 °C. After incubation, cells were washed three times ten minute intervals with PBST and secondary antibody diluted in 1 % BSA was added and incubated for 1 hour. After incubation cells were washed three times ten minutes intervals in PBST to remove unbound secondary antibody. The nucleus was stained with Hoechst 33342 reagent diluted to a working concentration of 2 µg/ml. Prepared Hoechst 33342 reagent was added onto the well and allowed to incubate for 3-5 minutes and then removed. Cells were washed three times five minute intervals with PBST to remove excess Hoechst reagent. Cover slips were mounted onto slides using Mowiol and allowed to dry overnight. Cells were imaged using a Zeiss Axioplan 2 imaging microscope system.

2.16 Protein extraction from transfected cells for immunoblotting

Lysate was prepared by discarding the media from the flask and then washing the cells twice with 1X PBS. This was followed by the addition of RIPA buffer (50mM Tris, pH 7.4, 150 mM NaCl, 0.1 % SDS, 0.5 % sodium deoxycholate, 1 % Triton X 100) A cell scraper was used to scrape cells from the bottom of the well plate. Cells were aspirated through a pipette 20 times to form a homogenous solution. This was followed by an ice for 5 minutes and then centrifugation at 14 000 xg for 15 minutes to separate cell debris. Supernatant was transferred on a fresh Eppendorf tube and stored at -80 °C.

CHAPTER 3 : INVESTIGATION OF INTERACTIONS BETWEEN THE UBIQUITIN ASSOCIATED (UBA) DOMAIN OF UBCH1 AND N-TERMINAL DOMAINS OF RETINOBLASTOMA BINDING PROTEIN 6 (RBBP6)

3.1   Introduction

Retinoblastoma Binding Protein 6 (RBBP6) has been reported to play a number of diverse roles within the cell. Of these the most well established is its role in mRNA processing: RBBP6 forms part of the 3'-end processing complex in both humans and yeast, promoting the selection of weaker, more proximal polyadenylation sites which increase expression of many proteins associated with proliferation and tumourigenesis (Di Giammartino and Manley, 2014, Lee and Moore, 2014).

Isoform 3, which consists of little more than the N-terminal ubiquitin-like domain of the full-length protein, is expressed off an alternative promoter and appears to be able to modify the function of the full-length protein by competing with the DWNN domain on the full-length protein, for binding to CstF-64, the 64-kDa subunit of the Cleavage Stimulation Factor.

In addition to this role in mRNA processing, RBBP6 has what appears to be an unrelated role as an E3 ubiquitin ligase, modifying the stabilities of important proteins by ubiquitinating them. In 2007 Li et al. (2007) showed that RBBP6 assists MDM2 to ubiquitinate p53 during development, and that knock out of RBBP6 leads to overexpression of p53 and consequent apoptosis and embryonic lethality. Our own

laboratory has shown that RBBP6 is able to ubiquitinate Y-Box Binding Protein 1 (YB-1) both *in vivo* and *in vitro*, in the latter case without the need for YB-1 is a potent oncogene as well as playing an important role in mRNA processing. It is also able to ubiquitinate and suppresses zBTN38, which plays a role in regulation of the DNA damage response (Miotto et al., 2014).

In an *in vitro* ubiquitination study conducted in our laboratory, the R3 fragment of RBBP6 (residues 1-335) was found have E3 ubiquitin ligase activity against Y-Box Binding Protein 1 (YB-1), using UbcH1 as the ubiquitin conjugating enzyme, or E2. Evidence suggested that the ubiquitination catalyzed by R3 and UbcH1 was poly-ubiquitination, since it produced high molecular weight forms of YB-1 stretching up to the top of the SDS-PAGE gel. However this effect was not observed when R2, a shorter fragment of RBBP6 excluding the DWNN domain, was used as the E3 ligase. Moreover, ubiquitination with different E2 enzymes such as UbcH5a, UbcH5b and UbcH5c yielded what appeared to be multiple mono-ubiquitination as compared to UbcH1.

The E2-like domain of UbcH1 is expected to bind to the RING finger of the E3, in this case R3, in order to effect transfer of the ubiquitin from its catalytic cysteine to the substrate, which in this case is YB-1. In addition to the conserved E2-like domain, UbcH1 also contains an ubiquitin associated domain (UBA) at its C-terminus, which is absent in UbcH5a, UbcH5b and UbcH5c. Since the DWNN domain of R3 has an ubiquitin-like structure, we hypothesized that the UBA of UbcH1 might facilitate the primary interaction by binding to the DWNN domain. If so, this may explain why R2,

69

which lacks the DWNN domain, did not ubiquitinate YB-1 as efficiently as R3. Hence we set out to investigate a possible interaction between the UBA domain of UbcH1 and the DWNN domain of RBBP6. At the same time we investigated whether the UBA interacted with the other two domains making up the R3 fragment of RBBP6.

Ubiquitination is a well known post-translational modification that signals proteins for destruction (Chung et al., 2001). Auto-ubiquitination is the process by which an E3 enzyme catalyses the addition of ubiquitin chains onto itself (Amemiya et al., 2008). Other E3 ligases like Parkin are known to inhibit their own ubiquitination. Since RBBP6 is reported to function as an E3 ligase in the ubiquitination of YB-1.

This chapter documents the cloning of the UBA of UbcH1 and heterologous expression of the UBA domain of UbcH1 as a GST-fusion protein, as well as expression of various domains from R3. Precipitation of GST-UBA was carried out using glutathione agarose and detection of co-precipitated proteins was carried out using antibodies targeting the respective domains of R3. This chapter also documents investigation of the auto-ubiquitination potential of RBBP6.

3.2   Recombinant expression of UBA

3.2.1 Generation of a pGEX-6P2-UBA expression construct

Primers pGEX-UBA-F and pGEX-UBA-R were designed to amplify the ubiquitin-associated domain of UbcH1, as shown in Table 2.3. The primers incorporated BamHI and XhoI restriction sites for cloning into the same sites in the MCC of pGEX-6P2. A

stop codon was included immediately before the XhoI site in the reverse primer. Figure 3.1 (A) shows successful amplification of UBA at the expected size of 132 bp. The PCR product was purified using the GeneJet gel purification kit, digested with BamHI and XhoI and cloned into pGEX-6P2 following digestion with the same enzymes.

Plasmid DNA from positive transformants was isolated and subjected to double digestion with the BamHI and XhoI. Figure 3.2 (B) shows the successful release of a fragment corresponding to the size of UBA in lanes 2, 4, 6, 8 and 12. The DNA sequence was confirmed by direct sequencing, as shown in Appendix II.

3.2.2 Small scale production of GST-UBA

pGEX-6P-2-UBA was transformed into *E. coli* BL21 Codon Plus cells and protein expression and purification carried out as described in Section 2.7. Expression was carried out at 30 °C and 25 °C, in each case at a range of ITPG concentrations between 0.1 and 1 mM, as shown. In each case total lysate (left lane) and clarified lysate (right lane) are shown side by side so that the solubility of the fusion protein can be assessed. An uninduced culture, to which no IPTG was added but was otherwise treated identically to the other samples, was included in lane 1. Between 0.1 mM and 1 mM IPTG there was a clear induction of a band at approximately 30 kDa, which is consistent with the expected size of 31.5 kDa, but no further increase in expression was observed with increasing concentrations of IPTG.

71
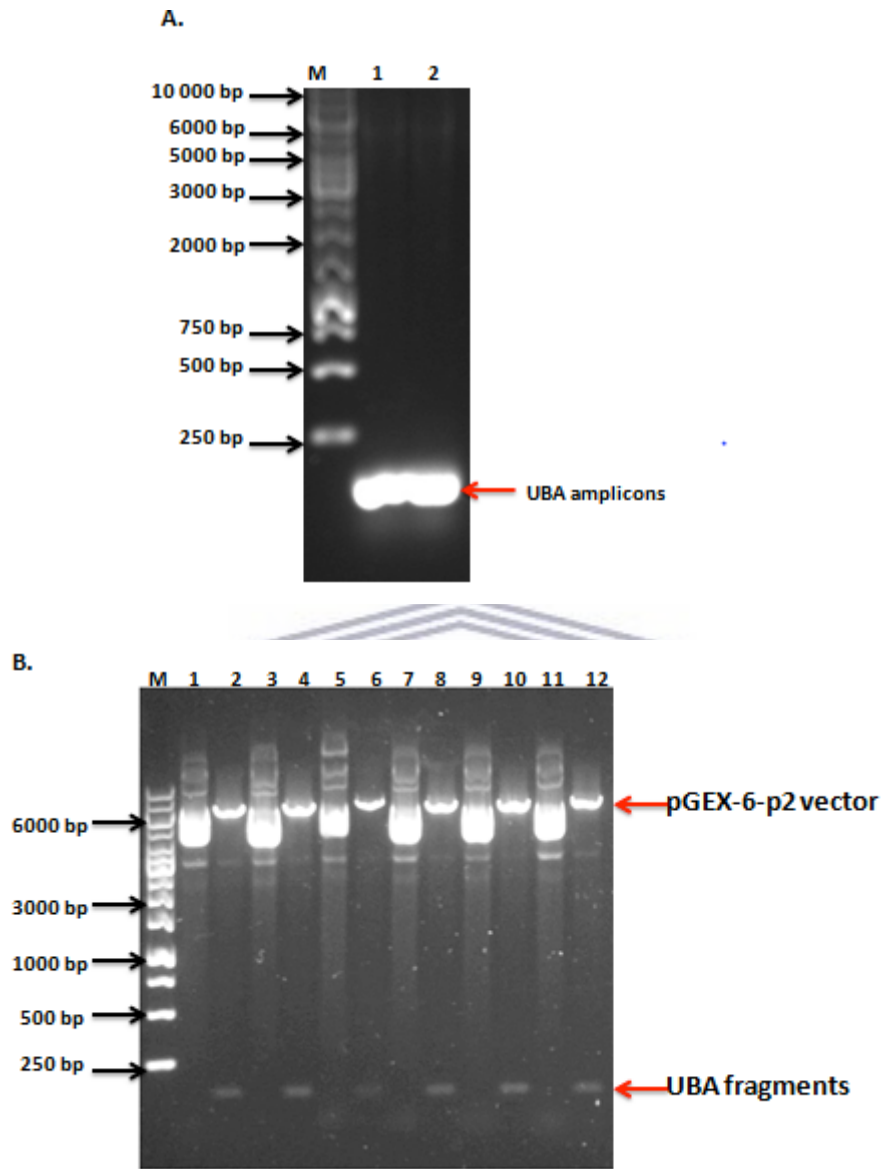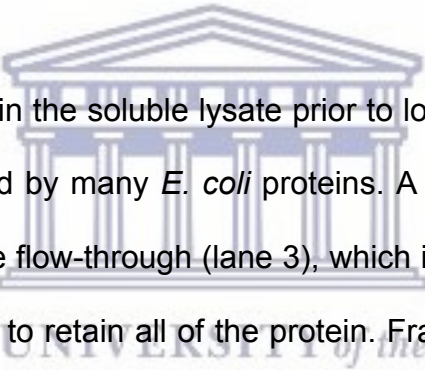
Figure 3.1: Cloning of UBA fragment into pGEX-6P2 (A) The UBA fragment was amplified from pGEX-6P2-UbcH1. Lanes 1 and 2 confirm the amplification of UBA with a size ~132 base pairs. The amplicon was double digested and cloned into pGEX-6P2. (B) An agarose gel confirming the presence of UBA after cloning. Lanes 1, 3, 5, 7, 9 and 11 show undigested plasmid DNA. Lanes 2, 4, 6, 8 and 12 show the presence of UBA after double digestion.

Since the expression appeared better at 25 °C, conditions of 0.1 mM IPTG at 25 °C were adopted for subsequent large-scale expressions.

3.2.3 Large-scale protein production of GST-UBA

Large-scale protein production of GST-UBA was carried out at 25 °C and 0.1 mM IPTG, as described in Section 2.7.1. Following lysis the fusion protein was separated from *E. coli* proteins using glutathione affinity chromatography, as described in Section 2.7.2. Lane 6 of Figure 3.3 shows successful elution of a band corresponding to GST-UBA, with an approximate MW of 31.5 kDa.

The same band was present in the soluble lysate prior to loading onto the column (lane 2), where it was accompanied by many *E. coli* proteins. A band consistent with that of GST-UBA can be seen on the flow-through (lane 3), which indicates that the capacity of the column was not sufficient to retain all of the protein. Fractions containing GST-UBA were pooled and dialised against dialysis buffer as described in Section 2.7.2.3. Samples containing GST-UBA were pooled together and glycerol was added to a final concentration of 10 % and stored at -20 °C.

3.3 Recombinant expression of the DWNN domain, RING finger and zinc knuckle proteins

pGEX constructs for the RING finger, zinc knuckle and DWNN13 from RBBP6 were already available in our laboratory (Lutya, 2002, Kappo, 2009).
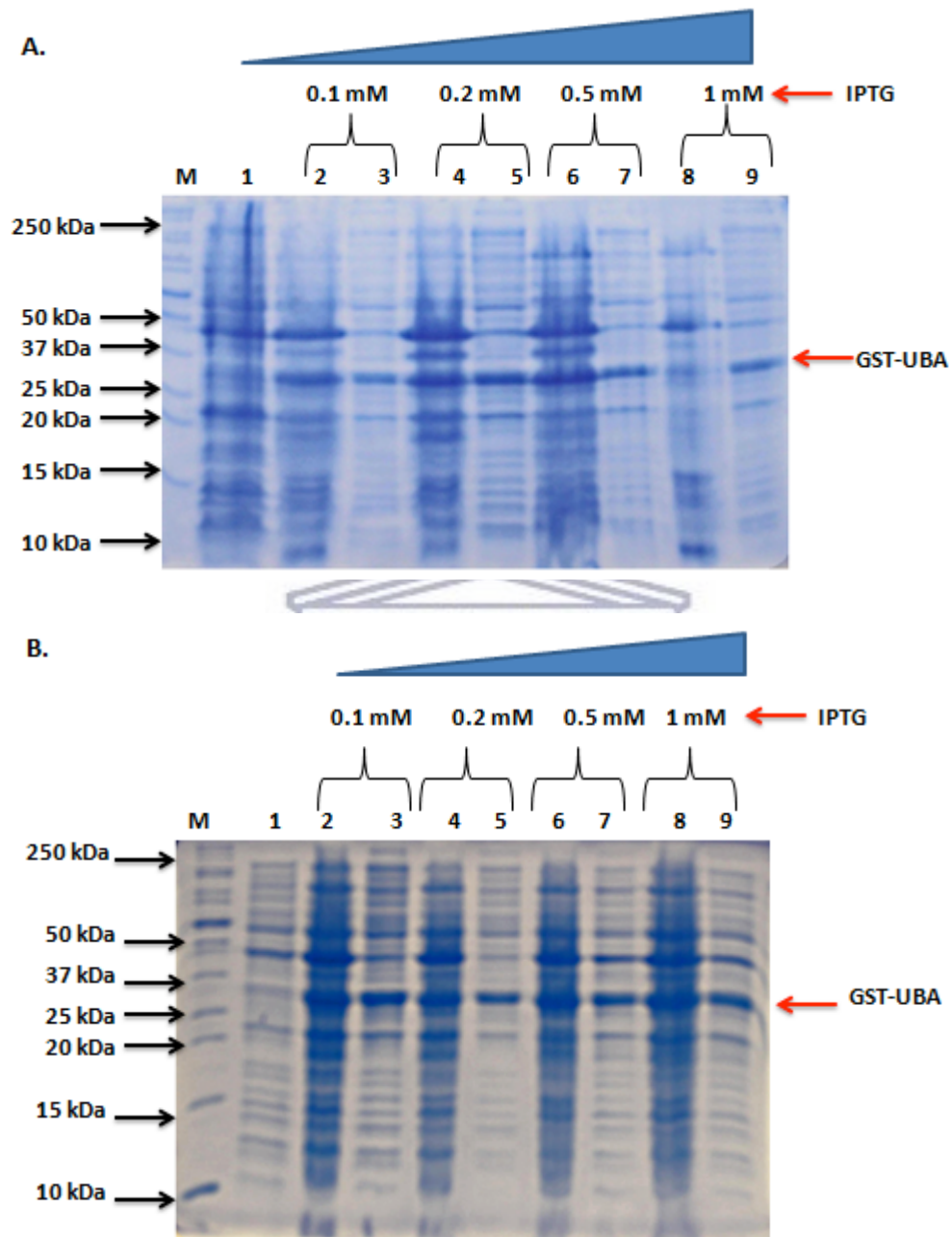
Figure 3.2: SDS-PAGE analyses of small scale test expressions of GST-UBA. Expression was carried out at 30 °C (A) and 25 °C (B), at a range of ITPG concentrations, as shown. In each case, re-suspended pellet and clarified lysate are shown side by side. A band consistent to that GST-UBA can be seen on both conditions and in the pellet as well as clarified lysate.
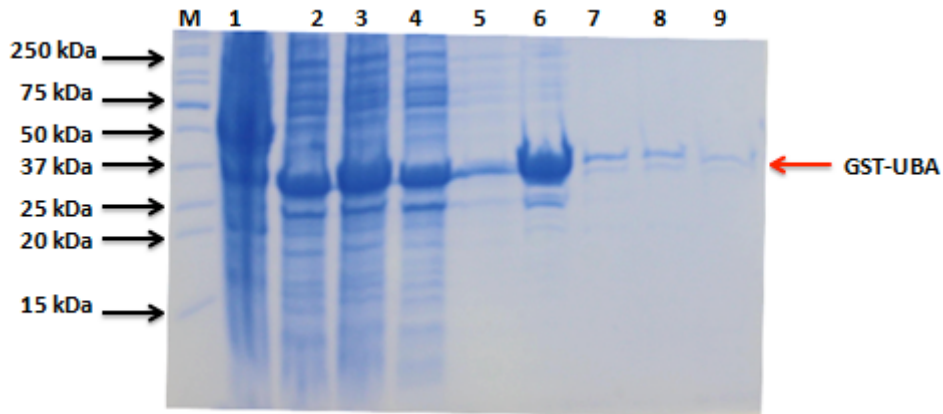
Figure 3.3: SDS-PAGE analysis of large scale UBA protein production. Lane 1 shows the insoluble pellet and lane 2 shows the lysate before loading onto the column. Lane 3 shows flow through and lanes 4 and 5 show column washes 1 and 3. Lanes 6-9 show elution fractions.

DWNN13 is identical to isoform 3, which contains the DWNN domain followed by a 37-residue unstructured C-terminal tail. The name DWNN13 has been adopted in our laboratory because its molecular mass is approximately 13 kD. Expression was carried out in *E. coli* BL21 Codon Plus cells and was induced with 0.5 mM ITPG at 30 °C. In the case of the RING finger and zinc knuckle 100 µM $ZnSO_4$ was added to provide the sufficient zinc ions for incorporation into these zinc-binding proteins.

Figure 3.4 (A) shows the purification of GST-DWNN13. Lanes 6-9 show elution of a prominent band of approximately 40 kDa, which is consistent with the expected size of GST-DWNN13 (26 kDa for GST and 13 kDa for isoform 3). Comparison of lanes 2 and 3 shows that most of the GST-fusion protein was successfully retained by the glutathione agarose column. Eluted fractions were pooled, dialised against cleavage buffer to remove free glutathione and cleaved with 3C protease, as described in Section

2.7.2.3. The sample was then returned to the glutathione agarose column to remove the cleaved GST, as shown in Figure 3.4(B). DWNN13, which was not retained by the column, can be seen in the flow through (lane 2) as a band at less than 20 kDa. Most of the GST and uncleaved GST-DWNN13 was retained by the column, although faint bands can still be seen at 26 kDa and 40 kDa respectively. The band at approximately 45 kDa corresponds to GST-3C protease. GST and uncleaved fusion protein retained by the column were eluted in lanes 6-9.

Samples containing DWNN13 were pooled together and glycerol was added to a final concentration of 10 % and stored at -20 °C. Purification of the RING finger of RBBP6 is shown in Figure 3.5. GST-RING was expressed and purified (data not shown) and dialised against cleavage buffer as previously described in Section 2.7.2.3. Lane 1 of Figure 3.5 shows RING finger following cleavage with 3C, showing successful separation into a band of around 9 kDa (RING) and one of 26 kDa (GST).

GST was efficiently retained by the column and subsequently eluted following addition of reduced glutathione (lanes 7-9), with the RING being found in the flow through (lanes 2-4). Fractions containing RING were pooled and subjected to an extra round of gluthathione agarose purification to remove all residual GST. Glycerol was added to a final concentration of 10 % and the samples were stored at -20 °C. Purification of the zinc knuckle is shown in Figure 3.6. GST-zinc knuckle was efficiently retained by the column and eluted following addition of glutathione, appearing as a band of approximated 40 kDa in lanes 6-9 of panel (A).

76
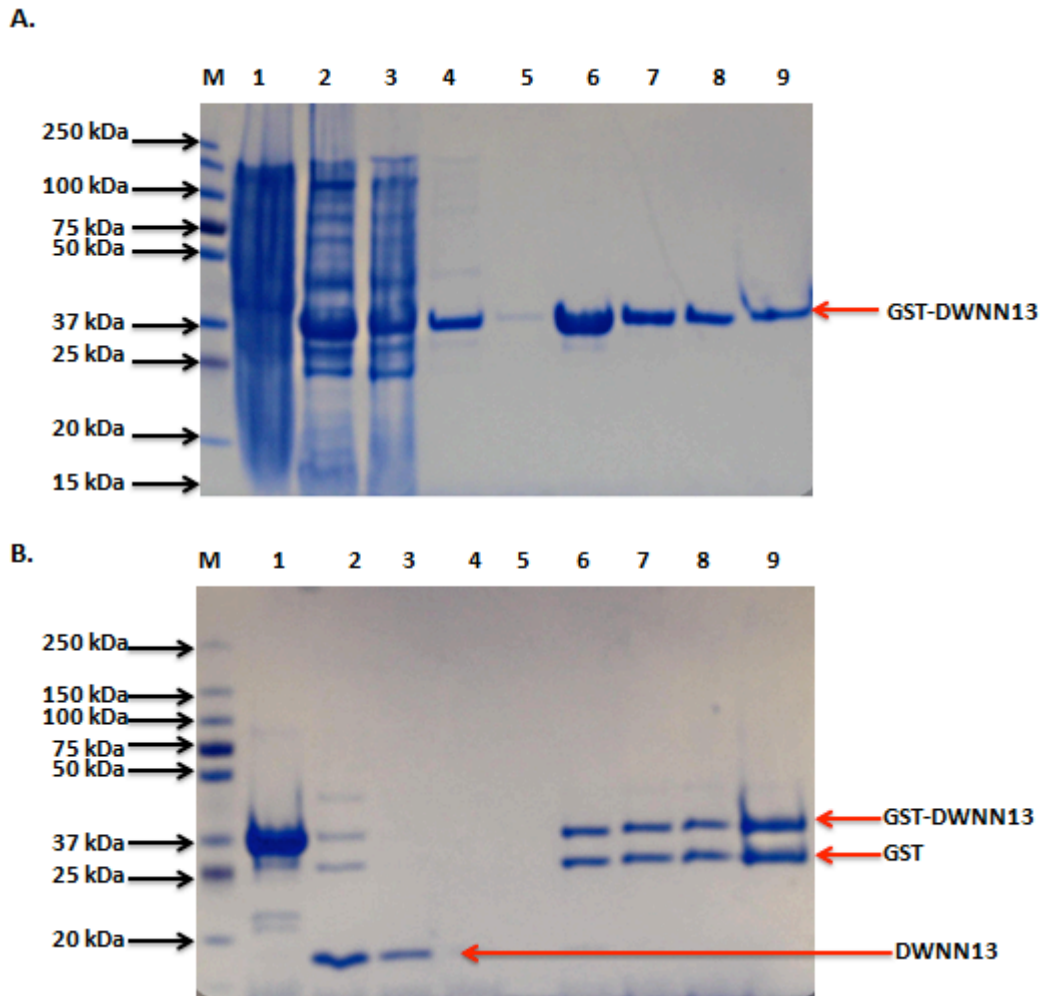
Figure 3.4: Purification of DWNN13. (A) Lane M shows the molecular weight marker, Lane 1 is the insoluble protein, Lane 2 is the soluble protein and Lane 3 is the flow through. Lanes 4-5 show column washes 1 and 3 and lanes 6-9 show the fraction eluted from the glutathione agarose column. (B) Purification of DWNN after cleavage with 3C protease. Lane M is the marker, Lane 1 is the uncleaved protein and lane 2 is the flow through after cleavage with 3C. Lanes 3-5 are column washes and lanes 6-9 are eluted fusion protein and GST retained on the glutathione agarose column.
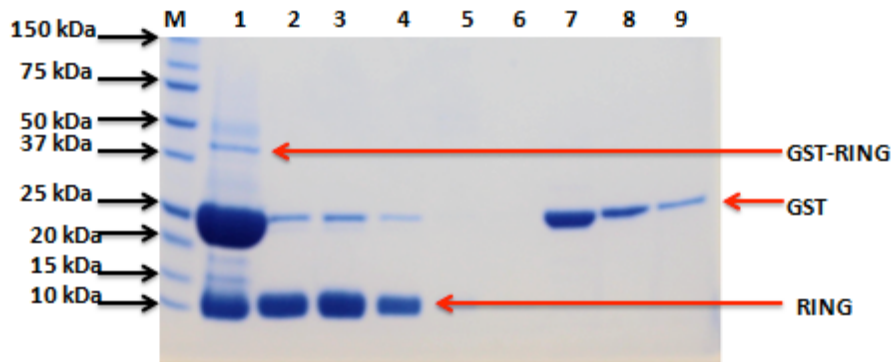
Figure 3.5: Purification of RING finger. Lane M is the marker; Lane 1 is the cleaved protein showing bands at 26 kDa, corresponding to GST, and 11 kDa corresponding to the RING. Lane 2 is the flow through after cleavage with 3C and lane 3-6 are column washes; these contain mainly RING although residual amounts of GST are still present. Lanes 7-9 contain exclusively GST eluted from the column by the addition of reduced glutathione.

This is consistent with the expected mass of 39.6 kDa (26 kDa for GST and 12.8 kDa for the zinc knuckle). Cleavage with 3C protease yielded a band of around 26 kDa, corresponding to GST, and a band around 12 kDa corresponding to the zinc finger, as shown in lane 1 of panel (B). Unfortunately the majority of the sample was lost; however the amount that remained was sufficient for interaction studies.

The cleaved sample was returned to the glutathione agarose column and the majority of the GST was removed (lanes 8-9) with the zinc finger and some residual GST remaining in the flow through. Samples containing the zinc finger were returned to the glutathione agarose column, after which the zinc finger sample was free of GST-fusion and of free GST.
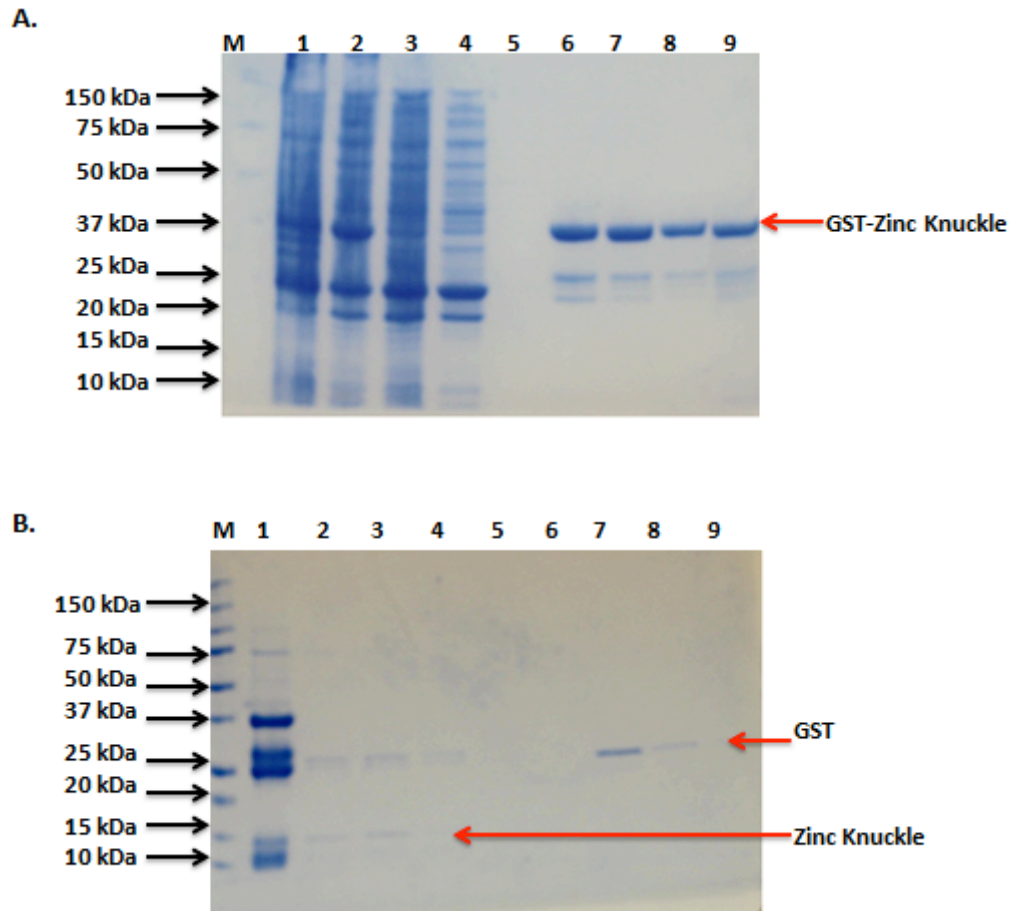
Figure 3.6: Purification and cleavage of zinc knuckle domain. (A) Lane M shows the molecular weight marker, Lane 1 is the insoluble protein, Lane 2 is the soluble protein and Lane 3 is the flow through. Lanes 4-5 show column washes 1 and 3 and lanes 6-9 show the fraction eluted from the glutathione agarose column. (B) Purification of zinc knuckle after cleavage with 3C protease. Lane M is the marker, Lane 1 is the uncleaved protein and lane 2 is the flow through after cleavage lane 3-5 are column washes and lanes 6-9 are eluted fusion protein.

79

3.4 R3 catalyses the poly-ubiquitination of YB-1 using UbcH1

Before embarking on investigation of a direct interaction between the UBA of UbcH1 and RBBP6, we decided to repeat the *in vitro* ubiquitination assay showing that R3 was able to ubiquitinate YB-1 with UbcH1 as E2. The assay was first performed by Dr Andrew Faro in our laboratory (A. Faro and DJR Pugh, unpublished data).
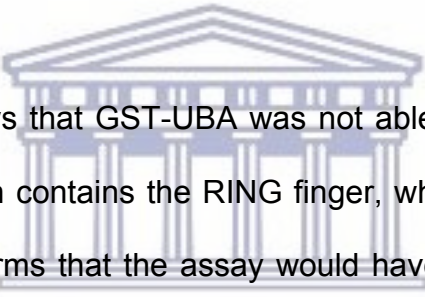
An *in vitro* ubiquitination assay was set up as described in Section 2.9. To serve as substrate, endogenous YB-1 was immunoprecipitated from A549 cell lysate, as described in Section 2.8. To serve as E3, bacterially expressed samples of the R3 and R2 fragments of RBBP6 were kindly donated by Dr Andrew Faro and Mr Mihlali Mlaza, co-workers in our laboratory. Bacterially expressed UbcH1 was donated by Ms Lauren Jooste, also a coworker in our laboratory. Immunodetection of YB-1 was carried out using a polyclonal antibody raised against the whole of YB-1 (Bellstedt laboratory, see Section 2.1 for details). YB-1 can be seen as a 50 kDa band in all lanes of Figure 3.7.

When used as an E3 ligase in conjunction with E2 UbcH1, R3 was able to catalyze poly-ubiquitination of YB-1 evidenced by a smear of higher molecular weight isoforms stretching up to the top of the gel (lane 4). R2, in contrast, was not (lane 3). This finding supports our hypothesis that R2 was unable to ubiquitinate YB-1 due the absence of the DWNN domain. It further suggested that the UBA domain of UbcH1 may interact directly with the DWNN domain, since it is known to interact with other ubiquitin-like domains. We decided to test this hypothesis by investigating whether an interaction could be

80

detected *in vitro* between the UBA domain and the different domains of RBBP6 making up R3.

3.5 The DWNN domain and RING finger of RBBP6 do not interact with the UBA of UbcH1

GST pull-down assays were carried using the GST-UBA as the "bait" and DWNN13 (isoform 3) or the RING finger as the "prey", as described in Section 2.10. Detection was carried by western blot using antibodies raised against the DWNN and RING finger domain, as described in Section 2.11.

Panel (A) of Figure 3.8 shows that GST-UBA was not able to co-precipitate the RING finger (lane 6). Lane 8, which contains the RING finger, which had not been subjected to pull down with GST, confirms that the assay would have been able to detect RING finger had it been present. Panel (B), similarly, shows that GST-UBA was not able to co-precipitate DWNN13 (lane 6), even though DWNN13 would have been detected by the antibody had it been present (lane 8).

3.6 The zinc knuckle interacts with the UBA of UbcH1

On the other hand Figure 3.9 shows that there is a definite interaction between the UBA and the zinc knuckle. GST-UBA was able to co-precipitate the zinc knuckle (lane 6), producing a clear band at the same MW as the zinc finger in lane 8, which was not subjected to GST pull-down

81
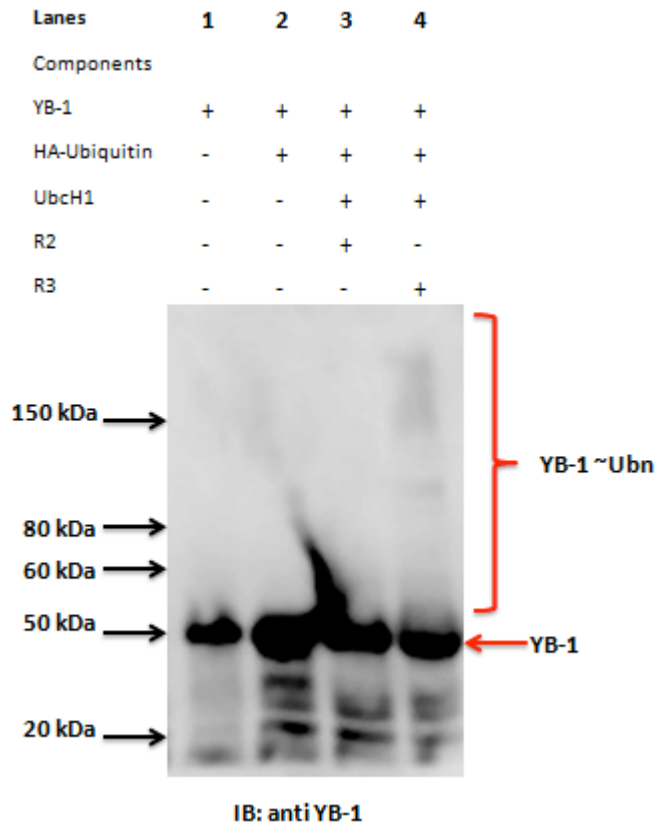
Figure 3.7: R3 catalyses the ubiquitination of YB-1 using UbcH1. YB-1 immunoprecipitated from A549 cell lysate migrates at the expected size of 50 kDa (lane 1). Detection was carried out using a rabbit polyclonal antibody raised against YB-1 and a donkey anti-rabbit secondary antibody conjugated to HRP. The high molecular weight smear above 150 kDa in lane 4 is evidence of poly-ubiquitination when R3 is used as E3, which is absent when R2 is used as E3 (lane 3).

A.

Lanes	1	2	3	4	5	6	7	8
GST-UBA	-	+	-	-	-	+	-	-
RBBP6-RING	-	-	+	+	-	+	-	+
GST	+	-	+	-	-	-	-	-

10 kDa → [blot] ← RBBP6-RING

IB: anti-RBBP6 RING

B.

Lanes	1	2	3	4	5	6	7	8
GST-UBA	-	+	-	-	-	+	-	-
DWNN	-	-	+	+	-	+	-	+
GST	+	-	+	-	-	-	-	-

13 kDa → [blot] ← DWNN

IB: anti-DWNN
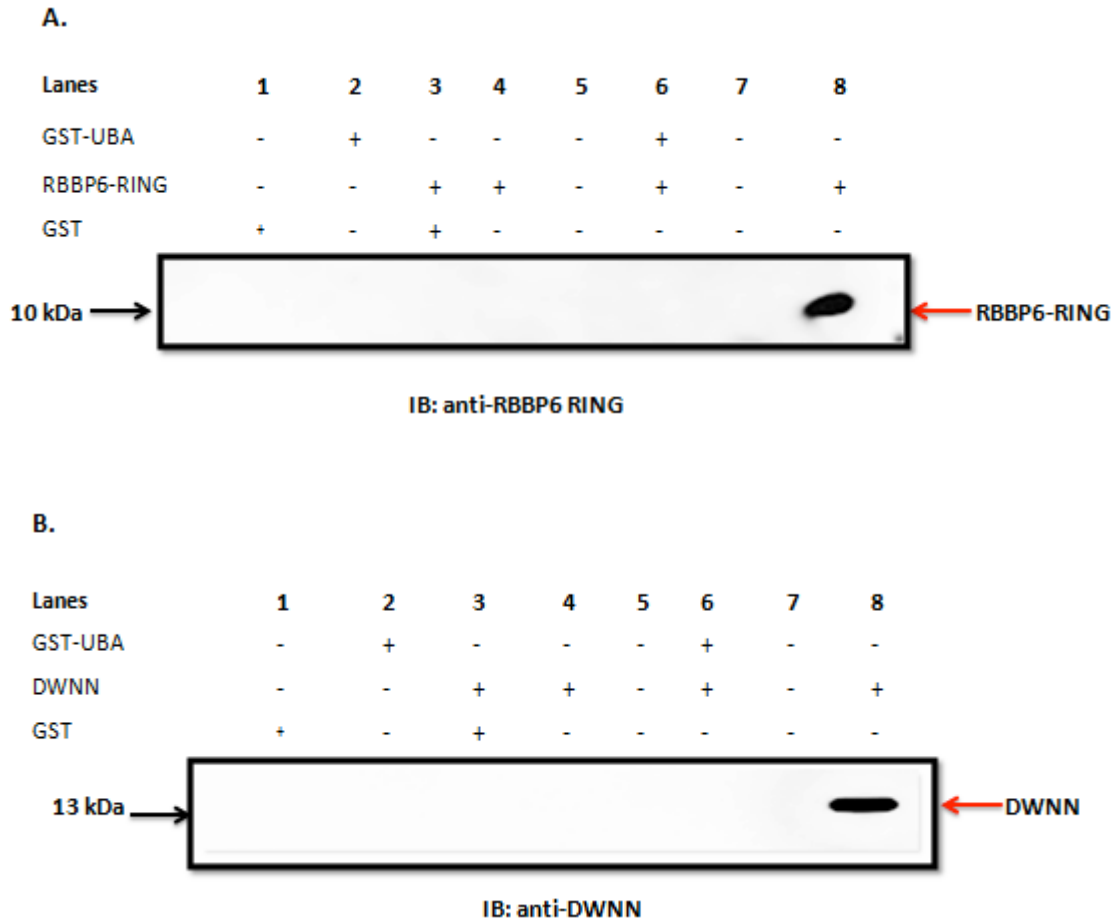
Figure 3.8: The UBA is unable to precipitate the RING finger and DWNN domain of RBBP6. (A) Co-precipitated RING finger is not present in lane 6, despite the presence of GST-UBA and glutathione-agarose resin. The RING finger in lane 8 was loaded directly onto the gel without being subjected to washes. It shows where the RING finger is expected to appear on the western blot and confirms that the RING finger would be detected if it were present. (B) Co-precipitated DWNN is not present in lane 6, despite the presence of GST-UBA and glutathione-agarose resin. The DWNN domain in lane 8 was loaded directly onto the gel without being subjected to washes. It shows where the DWNN domain is expected to appear on the western blot and confirms that the DWNN finger would be detected if it were present.

Lanes	1	2	3	4	5	6	7	8
GST-UBA	-	+	-	-	-	+	-	-
Zinc Finger	-	-	+	+	-	+	-	+
GST	+	-	+	-	-	-	-	-

10 kDa → ← Zinc Finger

IB: anti-Zinc Finger
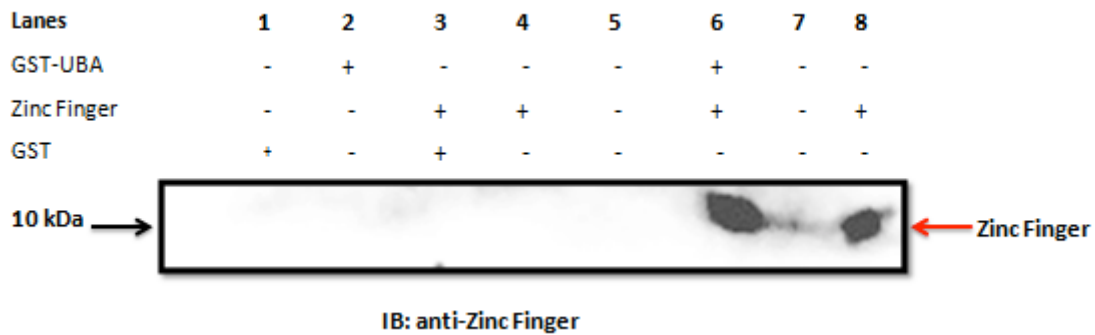
Figure 3.9: The UBA is able to co-precipitate the zinc knuckle domain of RBBP6. GST-UBA was able to co-precipitate the zinc knuckle (lane 6) whereas GST alone was not able (lane 3). The zinc knuckle was also not precipitated when bait was omitted altogether (lane 4). The zinc knuckle in lane 8 was loaded directly onto the gel without being subjected to washes. It confirms that the precipitated protein in lane 6 is in fact the zinc finger and that it is recognized by the anti-zinc knuckle antibody.

GST alone was not able to co-precipitate the zinc knuckle (lane 3), and nor was the glutathione agarose alone (lane 4), from which we conclude that the UBA alone is responsible for the co-precipitation of the zinc finger. Since the UBA interacts with the zinc knuckle, then it should also interact with the R2 and the R3 fragments of RBBP6, since they both contain the zinc knuckle. However Figure 3.10 shows that R2 is not co-precipitated with GST-UBA (lane 6), although lane 8 (R2, not subjected to pull-down) confirms that R2 would have been detected had it been present.

The lack of an interaction between R2 and the UBA is surprising, given the apparently strong interaction between the zinc knuckle and the UBA shown in Figure 3.9. It is possible that the presence of the RING finger suppresses binding of the UBA to the zinc finger.

Lanes	1	2	3	4	5	6	7	8
GST-UBA	-	+	-	-	-	+	-	-
His-R2	-	-	+	+	-	+	-	+
GST	+	-	+	-	-	-	-	-

25 kDa → [R2 band visible in lane 8] ← R2

IB: anti-HIS
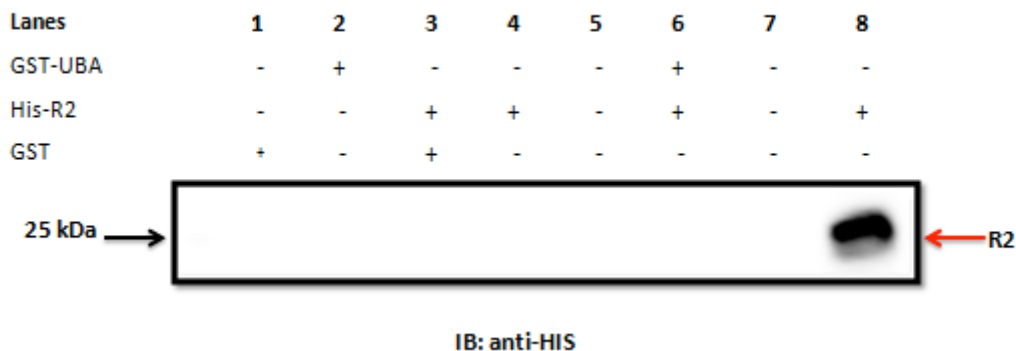
Figure 3.10: UBA is unable to co-precipitate R2. Co-precipitated R2 is not present in lane 6, despite the presence of GST-UBA and glutathione-agarose resin. The R2 band in Lane 8 was loaded directly onto the gel without being subjected to washes. It shows where R2 is expected to appear on the western blot and confirms that R2 would be detected if it were present.

Alternatively, since the zinc knuckle spans residues 80-197 of RBBP6, whereas R2 spans residues 143-335, it is possible that the interaction site with UBA lies within residues 80-142, which is not present in R2. But, whatever the reason, the lack of interaction of the UBA with R2 may explain the lack of ubiquitination of YB-1 by R2 and UbcH1. If so then, since R3 is able to ubiquitinate YB-1 with the help of UbcH1, R3 would be expected to interact with UBA. This possibility was not investigated in this work but warrants further investigation.

3.7   Investigation of the auto-inhibition of RBBP6

Although the structures of the ubiquitin-like DWNN domain, the zinc knuckle and the RING finger from human RBBP6 have been separately determined (PDB 2C7H, 2YSA and 3ZTG respectively), the overall spatial arrangement of the three domains making up the N-terminus of RBBP6 is yet to be determined. Nevertheless sequence analysis predicts that the DWNN domain is joined to the zinc knuckle and RING finger by a long

85

flexible linker that may allow it to loop around and contact the RING finger domain in a manner similar to that of the protein Parkin. Parkin is an E3 ubiquitin ligase that plays an important role in the etiology of Parkinson's Disease (Valente et al., 2004, Chaugule et al., 2011). It has an ubiquitin-like domain at its N-terminus that has been shown to regulate the auto-ubiquitination activity of Parkin by binding to, and blocking access to, the RING finger domain which is responsible for ubiquitination activity (Chaugule et al., 2011).

Since the DWNN and RING finger domains of RBBP6 were already at hand, we decided to use a GST pull-down asay to test whether the DWNN domain interacts with the RING finger domain of RBBP6 *in vitro*. GST-RING was used as the bait and the DWNN domain (following removal of the GST tag) as the prey, with detection of the DWNN domain being carried out using a mono-clonal antibody raised against a sample of the DWNN domain expressed in bacteria.
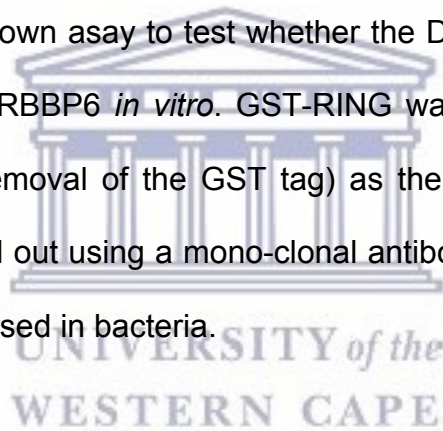
Figure 3.11 shows that no interaction was observed between the DWNN domain and GST-RING (lane 6), although the mono-clonal antibody would have been able to detect co-precipitated DWNN had it been present (lane 8). As previously, the DWNN domain in lane 8 was loaded directly onto the gel without being subject to any precipitation. The above assay was conducted several times with increasing concentrations of DWNN (1 µM, 5 µM and 10 µM) while the RING was kept constant at 1 µM , but in no case was any interaction observed.

Lanes	1	2	3	4	5	6	7	8
GST-RING	-	+	-	-	-	+	-	-
DWNN	-	-	+	+	-	+	-	+
GST	+	-	+	-	-	-	-	-

13 kDa →   ← DWNN

IB: anti-DWNN

Figure 3.11: The RING finger of RBBP6 is unable to co-precipitate the DWNN domain. Co-precipitated DWNN is not present in lane 6, despite the presence of GST-RING and glutathione-agarose resin. DWNN in Lane 8 was loaded directly onto the gel without being subjected to washes. It shows where DWNN is expected to appear on the western blot and confirms that the RING finger would be detected if it were present.

87

CHAPTER 4 : INVESTIGATION OF THE ROLE OF THE GLY-GLY MOTIF AND THE C-TERMINAL TAIL IN THE LOCALISATION OF RBBP6-ISOFORM 3

4.1   Introduction

Isoform 3 of RBBP6 consists of the DWNN domain found in all other isoforms of RBBP6, followed by a 37-residue C-terminal tail (residues 82-118) of which the last 17 are not found in any of the other isoforms. The DWNN domain adopts a structure similar to that of ubiquitin, raising the question of whether it may become attached to other proteins in the manner of ubiquitin and other ubiquitin-like modifiers.

This possibility is supported by the fact that the DWNN domain contains a Gly-Gly motif at precisely the same position as that found in ubiquitin (Pugh et al., 2006), where it functions as the conjugation point. Furthermore, unpublished data from our laboratory suggests that isoform 3 of RBBP6 translocates rapidly to nuclear speckles following a number of cell stresses, including heat shock and UV-induced damage (AV Szmyd-Potapczyk and DJR Pugh, unpublished data).

The other isoforms do not appear to be induced by stress, but are constitutively localized in speckles. A possible explanation for this behavior is that isoform 3 becomes covalently attached to another, so-far unidentified, protein that translocates to nuclear speckles following stress. If so, then removing the Gly-Gly motif from isoform 3 may abolish the localisation to nuclear speckles as well as abolishing the effect of stress on the localisation of isoform 3. In this study we set out to investigate the role of the Gly-

Gly motif in the heat stress response of isoform 3. Two approaches were adopted: the first involved mutating the Gly-Gly motif to Ala-Ala (AA), while leaving the rest of isoform 3, including the C-terminal tail, unchanged. This construct was named DWNN13-AA, in contrast to DWNN13, which is an alternative name for isoform 3 of RBBP6.

The second approach involved truncation of isoform 3 immediately before the Gly-Gly, thereby removing the unique tail as well as the Gly-Gly. Since this construct terminated with the residues Proline-Isoleucine (PI) it was named DWNN-PI. DWNN13-AA and DWNN-PI, along with DWNN13 (isoform 3), were transfected into A549 cells and their subcellular localisations investigated using immunofluorescence microscopy, in both resting and heat shocked cells. Visualization was carried out using antibodies targeting either the HA tag or FLAG immunotags incorporated into the constructs.

The first section of this chapter describes the generation of the mammalian expression constructs used in the study. Results of the localisation study are presented in the second half of the chapter.

4.2   Generation of constructs for mammalian cell transfections

4.2.1   Generation of a pcDNA3-FLAG-DWNN13 construct

A DNA construct expressing isoform 3 with an N-terminal HA-tag (pCMV-UWC-DWNN13) had been generated by Ms Andronica Ramaila before this project was initiated. The pcDNA3-FLAG-DWNN13 construct was generated as part of this work to express FLAG-tagged DWNN13 in mammalian cells. The pcDNA3 vector was chosen

89

since it encodes a neomycin resistance gene, which gave us the option to select for stable transformants using the antibiotic G418. pcDNA3-FLAG-p53, containing the p53 gene cloned between the BamHI and XbaI sites of pcDNA3, was a gift from Thomas Roberts (Addgene plasmid #10838). p53 was excised with BamHI and XbaI and the linearised vector was recovered.

Full-length DWNN was amplified from an existing construct, pmEGFP-DWNN13, using primers (pcDNA3-DWNN13-F and -R) shown in Table 2.3. Primers were designed to incorporate BamHI and XbaI restriction sites respectively for cloning into the same sites in the pcDNA3 vector. Two stop codons (TAA TGA, shown in red) were added to ensure truncation of the protein immediately after the end of DWNN13.

Successful amplification of DWNN13, which has an expected size of 360 bp, can be seen in (Figure 4.1(A)). The amplicon was digested with BamHI and XbaI and purified using the GeneJet gel purification kit (Thermo Fisher Scientific, Waltham MA, USA). Digestion of the pcDNA3-p53 construct with BamHI and XbaI, to release the p53 fragment (~1300 bp) can be seen in Fig 4.1 (B). The linearized vector, with a size of ~5500 bp, was cut out of the gel and purified using the GeneJet gel purification kit. The DWNN13 fragment was cloned into the pcDNA3 vector, as described in Section 2.6. Putative positive transformants were screened using colony PCR, which showed that all colonies contained the DWNN13 insert (Figure 4.1(C)).

90
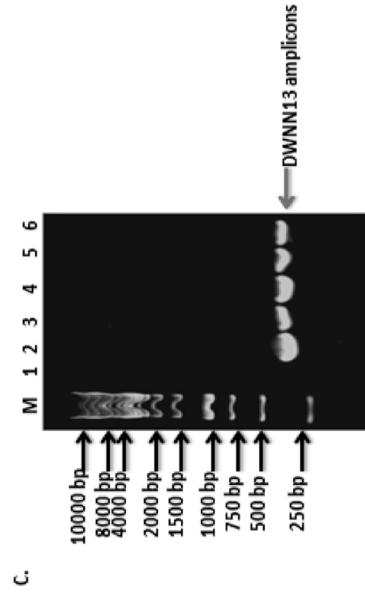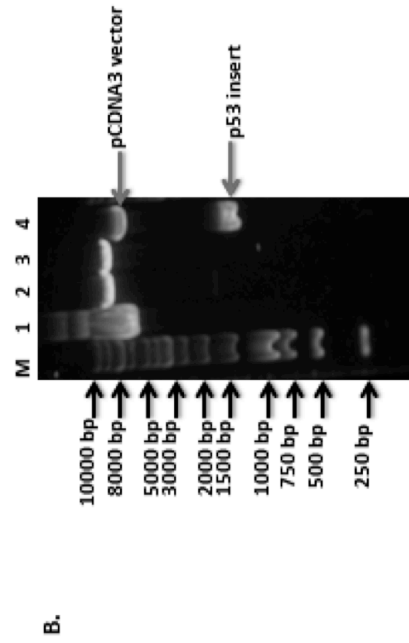
Figure 4.1 Generation of the pcDNA3-DWNN13 construct. (A) Lanes 2-4 show amplification of DWNN13, running at the expected size of 360 bp. The negative (no DNA) control is in lane 1. (B) Lane 4 shows double digestion of pcDNA3 with BamHI and XbaI, releasing two bands corresponding to the pcDNA3 vector and the p53 insert. Lanes 2 and 3 shows single digests with BamHI and XbaI respectively. Lane 1 shows undigested plasmid DNA. (C) Confirmation of the cloning of DWNN13 into pcDNA3 using PCR-colony assay. The negative (no DNA) control is in lane 1.

91

The sequence of the cloned insert was verified by direct sequencing and found to be exactly correct. The DNA sequence of the construct can be found in Appendix II.

4.2.2 Generation of the pCMV-UWC-DWNN-PI construct

The pCMV-UWC-DWNN-PI construct was generated to express HA-tagged DWNN-PI in mammalian cells. The pCMV-UWC vector was generated by Genscript Inc., by replacing the multiple cloning cassette (MCC) of pCMV-HA with that from pGFP-C1, as described in Section 2.3.2. Primers DWNN-PI-F and DWNN-PI-R (Table 2.3) were designed to amplify residues 1-77 from an existing construct, pmEGFP-DWNN13, incorporating XhoI and KpnI restriction sites for insertion into the same sites in pCMV-UWC.

Stop codons (TAA TGA, shown in red) were incorporated immediately before the KpnI site. Since the last base of the XhoI site was not in frame with the HA-tag, two additional bases (CT, shown in yellow) were added before the start of DWNN-PI to bring it back into frame with the HA-tag in the pCMV-UWC vector. The initial Met of DWNN-PI was not included in the construct to avoid any chance of incorrect initiation of translation.

An amplicon consistent with the expected size of DWNN-PI (260 bp) can be seen in lanes 1-6 of Figure 4.2(A). The fragment was digested with XhoI and KpnI, and cloned into pCMV-UWC, which had been linearised with the same enzymes.

92
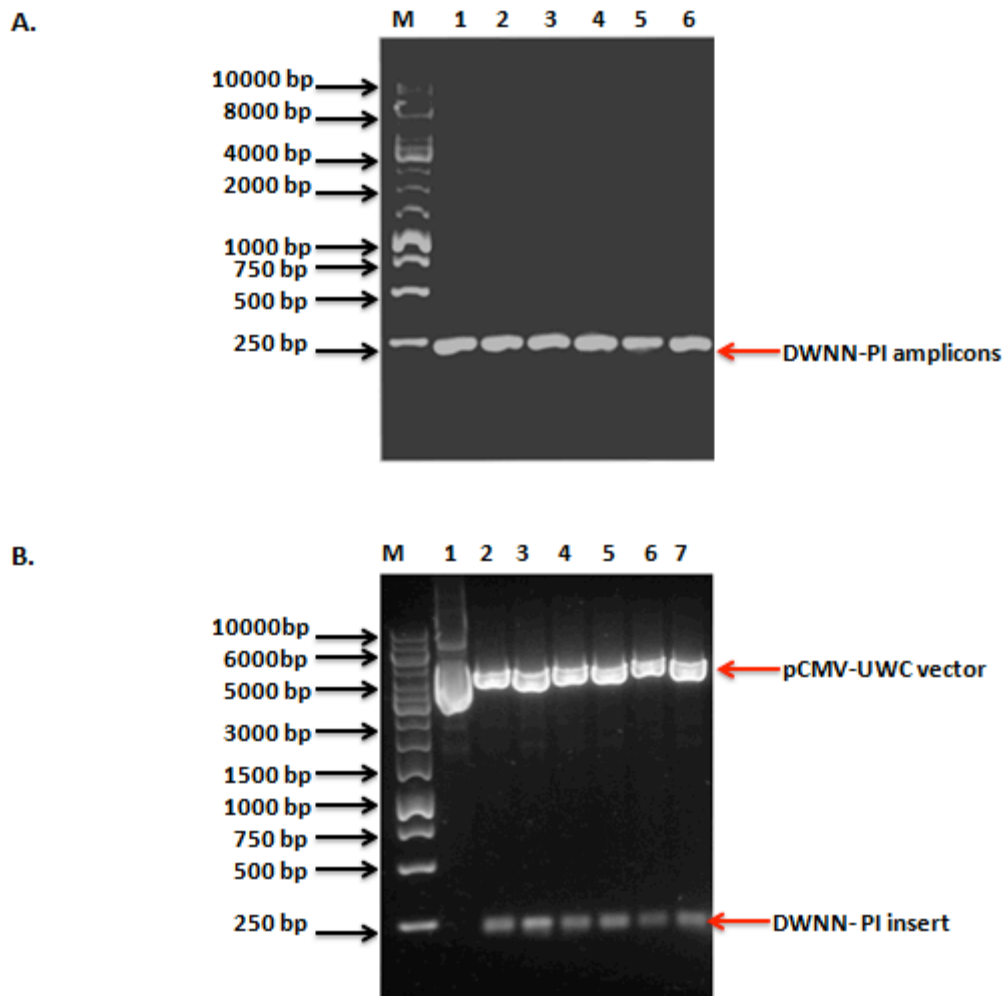
Figure 4.2: Generation of a pCMV-UWC-DWNN-PI construct. (A) The band in lanes 1-6 is consistent with the size of DWNN-PI (260 bp). (B) Screening of putative colonies after ligation shows that colonies on lanes 2-7 contain the desired DWNN-PI fragment cloned into pCMV-UWC. Lane 1 contains undigested DNA from colony 1.

93

Putative positive colonies were screened by double digestion to release the cloned fragment; release of a presumptive DWNN-PI fragment migrating at approximately 250 bp can be seen in lanes 2-7 of panel (B). The sequence of the cloned insert was verified by direct sequencing and found to be exactly correct, as shown in Appendix II.

4.2.3 Generation of the pCMV-UWC-DWNN-AA construct

The pCMV-UWC-DWNN13-AA construct was generated to express HA-tagged DWNN13-AA, which is identical to DWNN13 (isoform 3), with the exception that the Gly-Gly motif has been replaced by Ala-Ala. A DNA sequence coding for the G78A-G79A mutant of DWNN13, flanked by XhoI and KpnI restriction sites, was synthesized by GenScript USA Inc. (Piscataway NJ, USA) and supplied in a pUC57 vector. The insert was excised from pUC57 using XhoI and KpnI (Figure 4.3) and inserted into pCMV-UWC, following linearization with the same enzymes (data not shown). DNA was extracted from putative positive transformants and the sequence verified by direct sequencing, as shown in Appendix II.

4.3   Removal of the Gly-Gly motif affects the cellular localisation of isoform 3

Before embarking on immunofluorescence studies, the antibodies were validated to ensure that the detected signal was only due to transfected DNA and not auto-fluorescence or non-specific antibody binding. To test this, un-transfected cells were stained with primary and secondary antibody to show that no signal was present. (Figure 4.4 (A and B)).

94
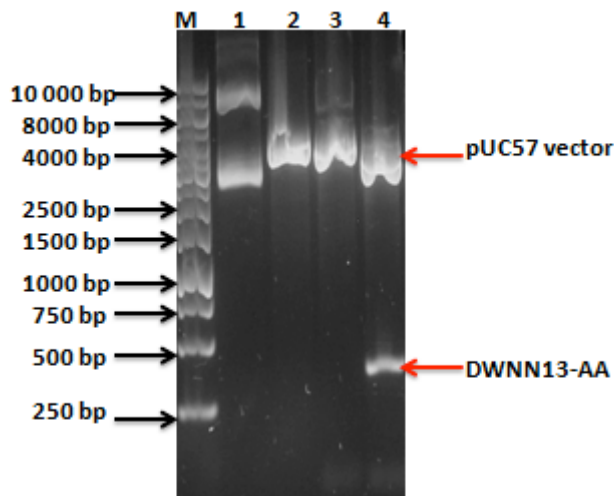
Figure 4.3: Generation of a pCMV-UWC-DWNN13-AA construct. Lane 1 shows undigested plasmid DNA. Lane's 2-3 show singly digested plasmid DNA with XhoI and KpnI respectively. Lane 4 shows the release of DWNN13-AA fragment of ~371 bp.

A secondary antibody control (omitting the primary antibody) was also performed to ensure that detected signal was from transfected cells rather than background and unspecific antibody binding (Figure 4.4 (C and D)). In all instances, the controls showed that the antibodies were specific and could confidently be used for immunofluorescence studies. Various modifications of DWNN13 (RBBP6 isoform 3), tagged with HA, were transfected into A549 cells and their localisation investigated using immunofluorescence microscopy, detecting with anti-HA antibodies.

Unlike full-length RBBP6 (isoform 1), which localises exclusively in nuclear speckles (AV Szmyd-Potapczuk, M Mlaza and DJR Pugh, unpublished data), HA-DWNN13 (isoform 3) is predominantly cytoplasmic (Figure 4.5 (A)), with a lower density in the nucleus.

95
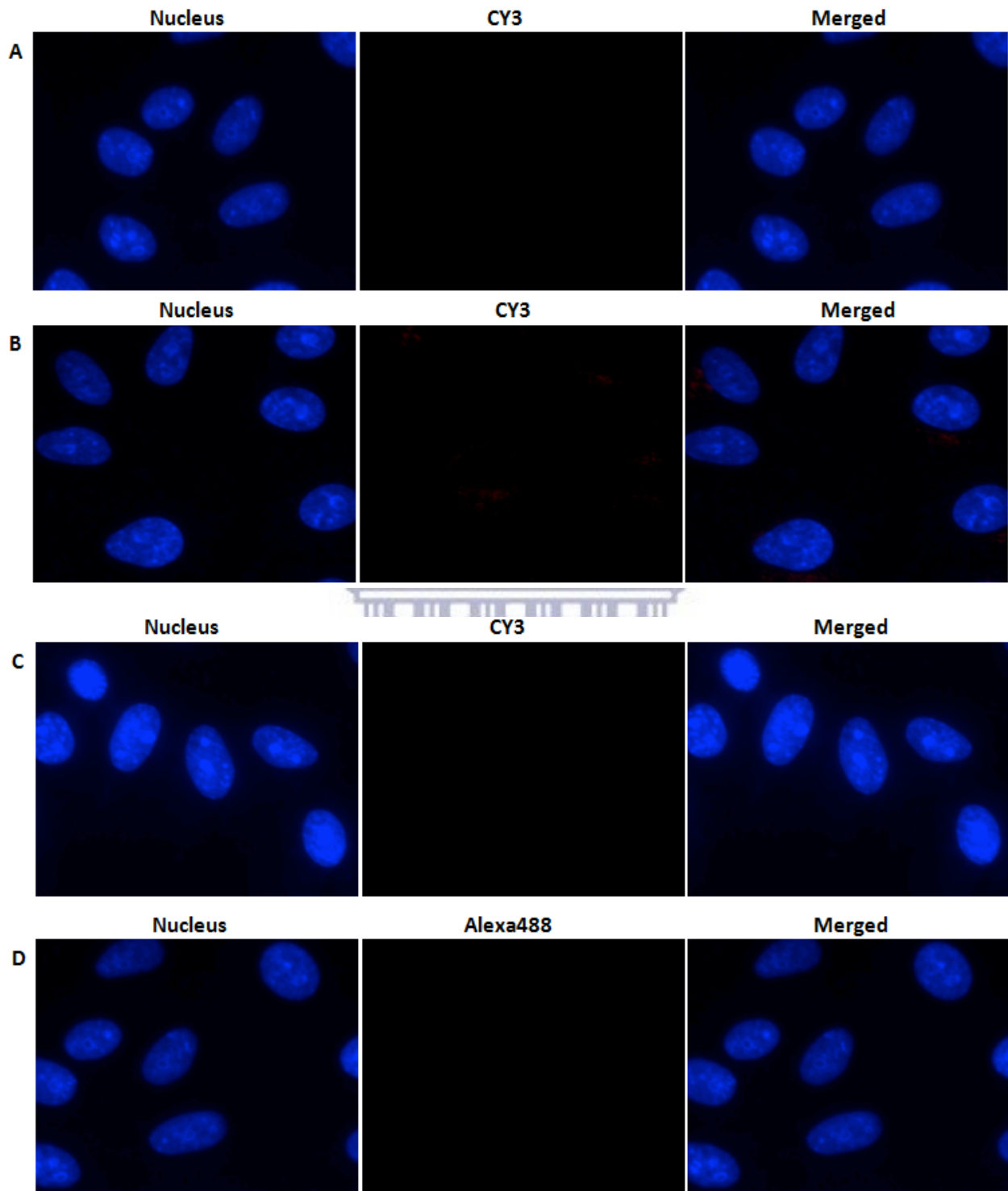
Figure 4.4: Immunofluorescence controls. (A) Un-transfected cells without staining, (B) Un-transfected cells stained with anti-HA and CY3, (C) Un-transfected cells stained with a secondary antibody CY3 and (D) Un-transfected cells stained with Alexa488 secondary antibody. The DNA stain Hoechst 33342 was used to visualize the nucleus. Cells were observed using a fluorescence microscope equipped with a 100x objective lens.

96
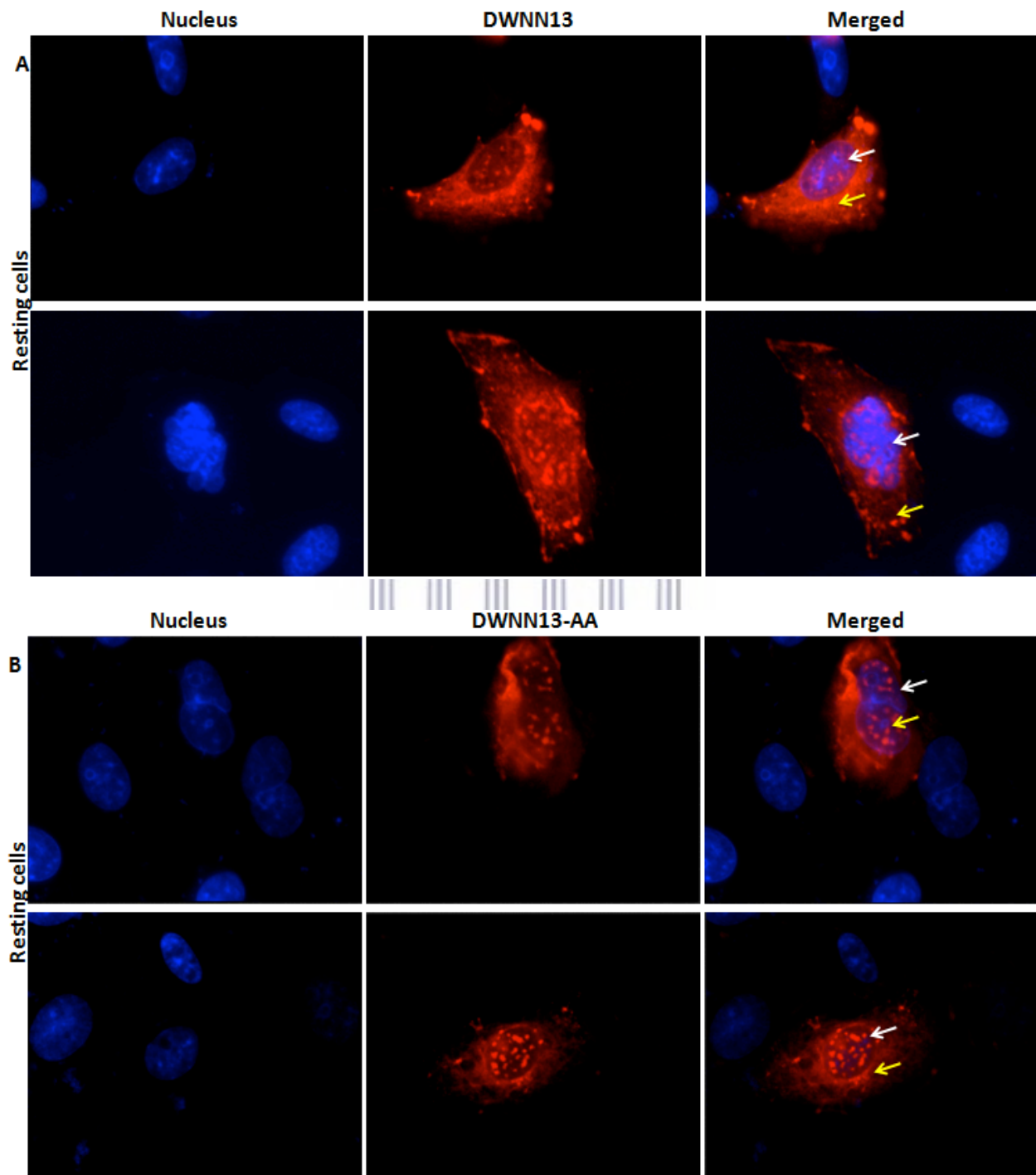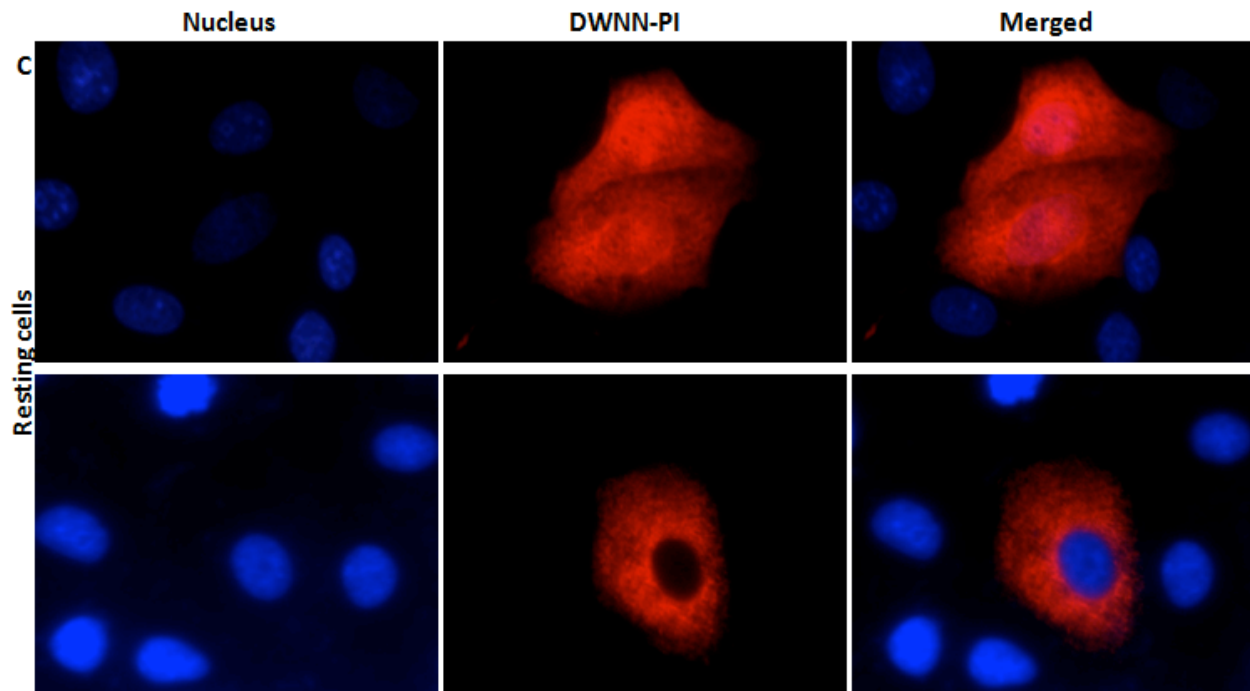
Figure 4.5: Removal of the Gly-Gly motif affects the cellular localisation of DWNN13. (A and B). DWNN13 and DWNN13-AA have a predominantly cytoplasmic localisation and speckle-like localisation in the nucleus. (C) DWNN-PI has variable phenotypes ranging from even distribution (Top panel) and completely cytoplasmic localisation with no evidence of speckling in the nucleus. A549 cells were transfected for 24 hours and immunostained with anti-HA and secondary antibody labeled with CY3 (red). Cells in Panel B were immunostained with Alexa488 secondary antibody. The DNA stain Hoechst 33342 was used to visualize the nucleus. Cells were observed using a fluorescence microscope equipped with a 100x objective lens. The yellow arrow is pointing to speckle-like structures and the white arrow is pointing to the cytoplasm.

In addition, a number of prominent punctate structures, similar to nuclear speckles, can be seen in the nucleus. Surprisingly, replacement of the di-glycine motif with Ala-Ala did not affect the overall cellular distribution of DWNN13 (Figure 4.5 (B)). This is surprising because, if DWNN13 were being localized to the punctate bodies as a result of conjugation involving the Gly-Gly motif, then removal of the motif might have been expected to lead to abolition of the "speckles". This suggests that DWNN13 does not become covalently attached to other proteins through the Gly-Gly motif.

98

As an alternative to replacing the Gly-Gly motif with Ala-Ala, DWNN13 was truncated immediately before the Gly-Gly, ending with Proline-Isoleucine (PI), yielding a construct named HA-DWNN-PI. The results are very different, as can be seen in (Figure 4.5 (C and D)). The transfected cells fall into two distinct groups: approximately 86 % (panel C) show equal smooth densities of signal in the nucleus and the cytoplasm, with no evidence of speckle-like bodies in the nucleus. Approximately 14 % (panel D) show complete absence of signal in the nucleus.

While the clear differences in phenotype exhibited by DWNN-PI may be due to the absence of the Gly-Gly motif, it is also possible that the determinant of the change may reside elsewhere in the C-terminal tail region, in residues 80-118. In order to distinguish between the role of the tail and the role of the Gly-Gly motif, it would have been useful to investigate the localisation of a construct terminating immediately after the Gly-Gly motif. Although the intention was to generate this construct, dubbed DWNN-GG, difficulties were experienced in cloning it and due to time constraints it could not be included in this study. The construct has subsequently been made by a co-worker and shown to have a localisation similar to that of DWNN-PI. This result supports the conclusion that the GG motif does not play a role in the localisation of isoform 3, and that the real determinant lies elsewhere in the C-terminal tail.

4.4   Isoform 3 colocalises with SC35

SC35 is a speckle-resident splicing factor that is commonly used a marker of nuclear speckles. Indeed nuclear speckles are sometimes referred to in the literature as "SC35-

99

bodies" (Spector and Lamond, 2011). RBBP6 has previously been reported to localize to nuclear speckles (Simons et al, 1997), but the punctate bodies in which it is found have never been conclusively shown to be nuclear speckles. We therefore set out to show that HA-DWNN13 and HA-DWNN13-AA co-localise with SC35 before and after heat stress, by performing a dual immunofluorescence investigation using antibodies targeting endogenous SC35 as well as antibodies targeting the HA tag. (Figure 4.6 (A)) confirms that the anti-SC35 antibody detects punctate bodies entirely within the nucleus, as expected.

Panels B and C show dual staining of A549 cells transiently transfected with HA-DWNN13, before and after heat stress respectively. The localisation of HA-DWNN13 in resting cells, shown in green in panel B, left column, is consistent with that shown earlier, being mostly cytoplasmic with evidence of speckle-like bodies in the nucleus but with no significant evidence of heat stress induction. SC35 is shown in red (middle column). When the red and green images are superimposed the speckle-like bodies change from red to yellow/orange in both stressed and unstressed cells, showing that the bodies to which HA-DWNN13 localises superimpose very well on nuclear speckles. We conclude that HA-DWNN13 does indeed localize to nuclear speckles.

Dual staining of DWNN13-AA with SC35 in unstressed cells was not successful and so the results could not be included. However successful dual staining following stress can be seen in Figure 4.6, panel D. Here, too, it is clear from the yellow colour of the merged slides that HA-DWNN13-AA localizes to the same speckles as SC35. HA-

DWNN-PI exhibits the same phenotypes in heat shocked cells as in unstressed cells, and no evidence of any response to heat stress can be seen in (Figure 4.7 (E)).

4.5   Western blot analysis of DWNN13 constructs

Because the size of the detected protein is not apparent, immunofluorescence microscopy carries the risk of unintended proteins being detected due to binding of the primary antibody to more than one target (Buchwalow et al., 2011).

The risk is higher with gene-specific primary antibodies, which are often not fully tested to ensure that they only detect the desired protein. Fortunately the risk is significantly reduced when detecting exogenous proteins carrying immunotags such as HA and FLAG, since antibodies raised against them have typically been thoroughly tested in many laboratories and found to be specific for the respective tags (Johnson, 2014). It is nevertheless desirable to confirm that the protein being detected has the expected molecular weight, both to confirm that the correct protein is being detected and also to confirm that is being expressed at the expected molecular weight, without being subject to truncation or other post-translational processing. With this motivation in mind we set out to detect the various HA-tagged constructs in cell lysates by western blot, detecting with anti-HA antibodies. Despite repeated attempts we were completely unsuccessful.

This is surprising as we have routinely visualized these proteins using immunofluorescence microscopy, which means that they are recognized by anti-HA antibodies within the context of the cell.

101
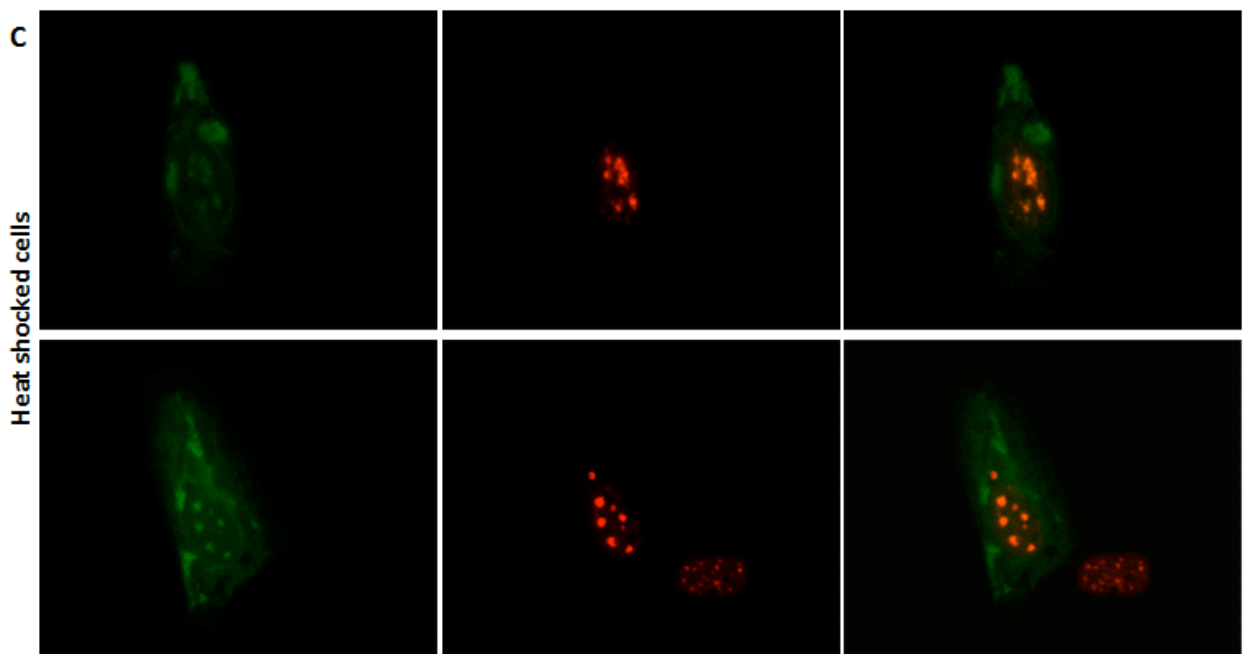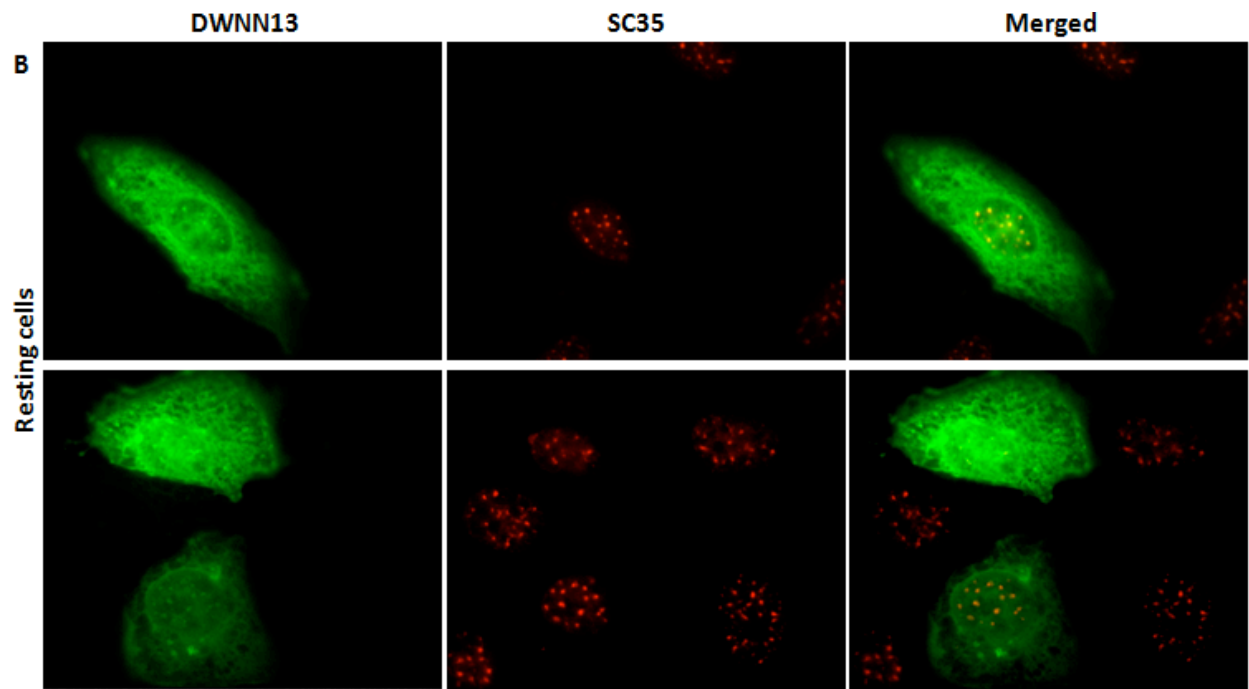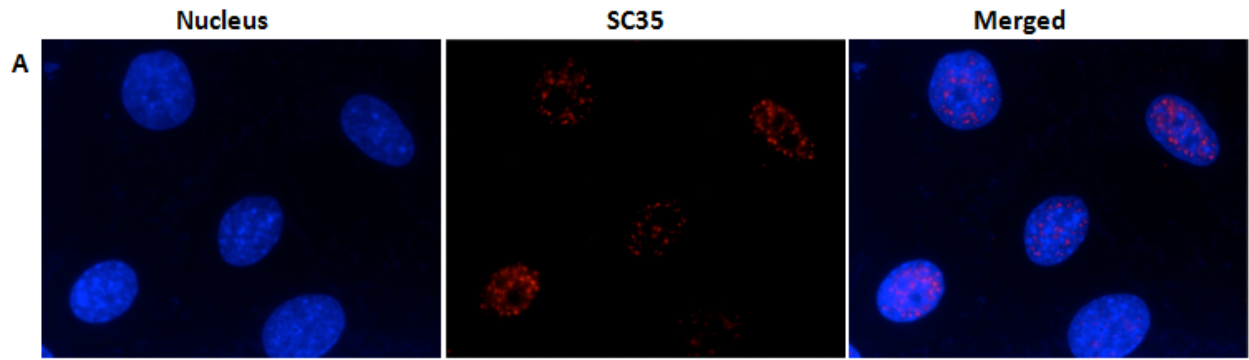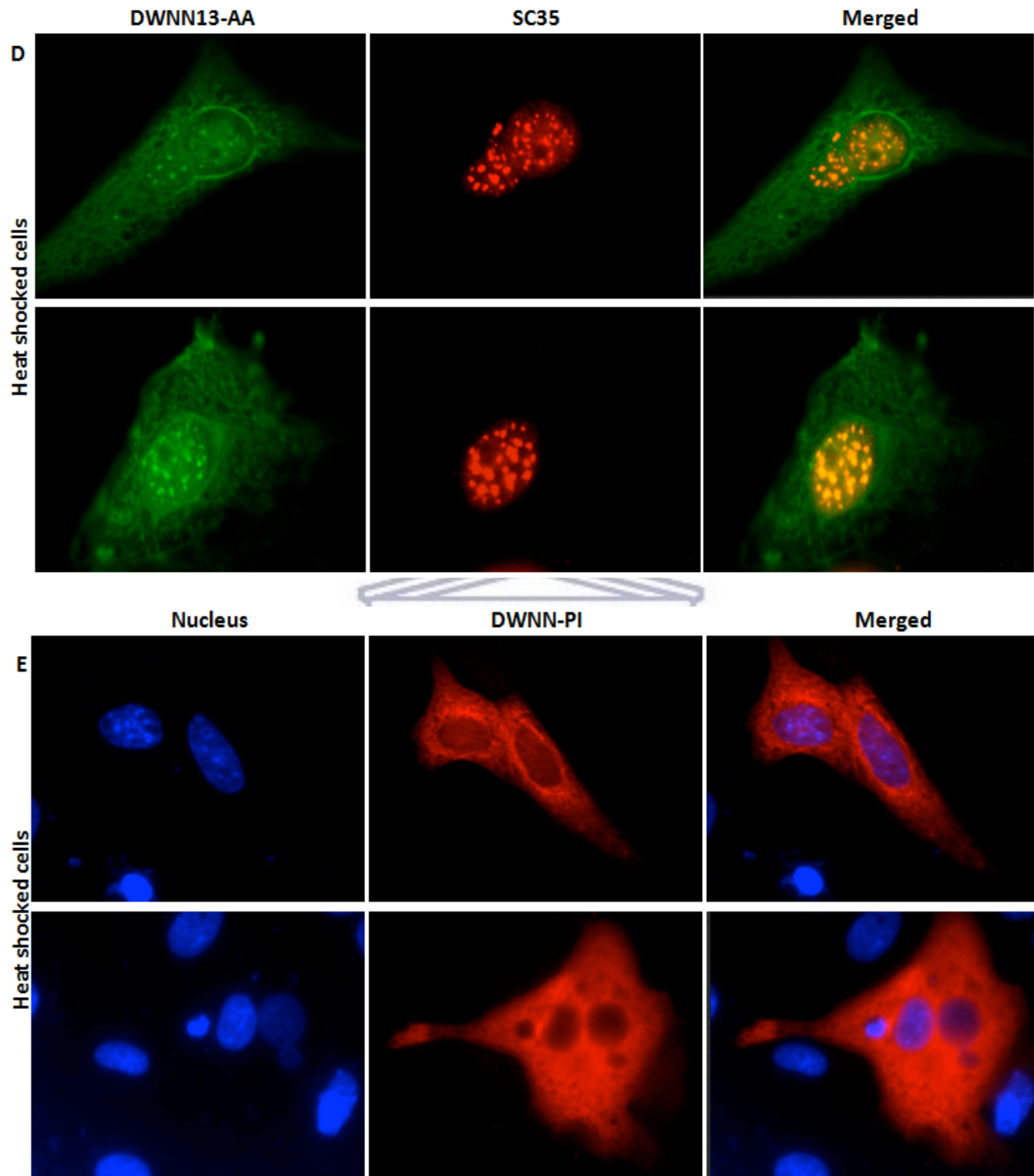
Figure 4.6: DWNN13 and DWNN13-AA colocalise with SC35 in nuclear speckles. (A) Localisation of endogenous SC35. A549 cells were grown to a confluency of ~70 % and immunostained with anti-SC35 and secondary antibody labeled with CY3 (red). DNA was stained with Hoechst 33342 A549. Cells were transfected with DWNN13 for 24h and subjected to heat shocking at 45 °C for 10 minutes. (B) Co-localisation of DWNN13 with SC35 before stress. (C) Co-localisation of DWNN13 with SC35 after heat stress. Endogenous SC35 was stained with anti-SC35 and exogenous DWNN13 was stained with anti-HA. Secondary antibody

103

labeled with Alexa488 was used to visualize DWNN13 and a secondary antibody labeled with CY3 was used to visualize SC35. (D) A549 cells were transfected with DWNN13-AA for 24h and subjected to heat shocking at 45 °C for 10 minutes. (E) Localisation of DWNN-PI after heat stress. Cells were transfected with DWNN13 for 24h and subjected to heat shocking at 45 °C for 10 minutes. Endogenous SC35 was stained with anti-SC35 and exogenous DWNN13-AA was stained with anti-HA. Secondary antibody labeled with Alexa 488 was used to visualize DWNN13-AA and a secondary antibody labeled with CY3 was used to visualize SC35 Cells were visualized using an immunoflourescence microscope equipped with a 100x objective lens.

However co-workers in our laboratory have reported similar difficulties detecting bacterially-expressed HA-DWNN13 and HA-DWNN-PI by western blot, using anti-HA antibodies. No difficulty was encountered detecting the same bacterially-expressed proteins using antibodies raised against the DWNN domain itself, confirming that there are no issues with the stability of the proteins nor with their propensity to migrate through SDS-PAGE gels; however, it does provide evidence that these proteins may be difficult to detect using anti-HA antibodies in mammalian cell lysates, for reasons that are not understood.
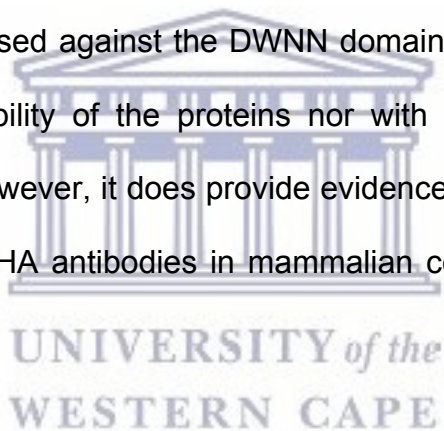
To investigate whether this problem could be specific to the HA-tag, we transiently transfected A549 cells with the pcDNA3-DWNN13 construct generated in Section 4.2.1 and western blotted the resulting cell lysate with anti-FLAG antibodies (see Table 2.1 for details). The results are shown in (Figure 4.7). A band migrating at a size consistent with 13 kDa is present in transfected cells (lane 4) but not in identical un-transfected cells (lane 2) or in cells treated only with transfection reagent (lane 3). The above result confirms that FLAG-DWNN13 is present in mammalian cell lysates, as a protein of the expected molecular weight. It is the first evidence that has been produced in our

laboratory that exogenous DWNN13 can be detected in mammalian cell lysates. It suggests that future work involving exogenous RBBP6 constructs may require existing HA tags to be replaced with FLAG tags.

The faint smear in lane 4 extending above DWNN13 and up to the top of the gel is intriguing. It may provide the first evidence that DWNN13 is involved in higher molecular weight complexes. Furthermore, their resistance to disruption by the denaturing conditions in SDS-PAGE would suggest that they are covalent interactions, possibly consistent with covalent attachment to other proteins in a process such as DWNNylation. However caution should be exercised in deducing that the interaction must be covalent, because experience of SDS-PAGE suggests that strong interactions are also surprisingly resistant to disruption.
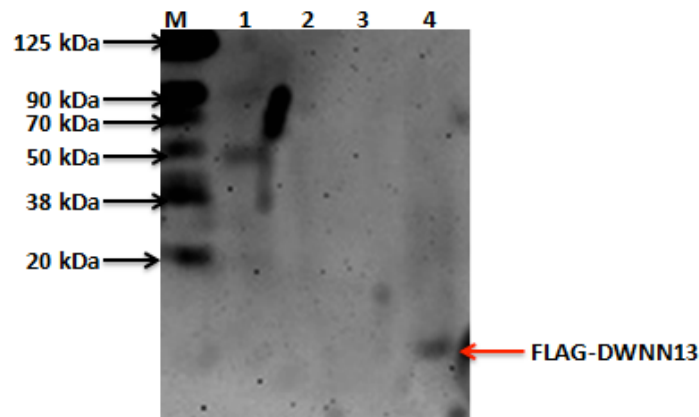
Figure 4.7: Immunoblotting of cells transfected with FLAG-DWNN13. A549 cells were transfected with FLAG-DWNN13 for 24 hours before lysis. A faint band consistent with 13 kDa is apparent in lane 4, which are derived from cells transfected with FLAG-DWNN13, but not in lane 2, which are un-transfected, nor in lane 3 which are treated with transfection reagent only. Western Blotting was carried out using an anti-FLAG antibody.

CHAPTER 5 : DISCUSSION, CONCLUSIONS AND FUTURE PROSPECTS

5.1 Investigation of interactions between the ubiquitin associated (UBA) domain of UbcH1 and N-terminal domains of Retinoblastoma Binding Protein 6 (RBBP6)

Previous studies have shown that the R3 fragment of RBBP6 (DWNN, zinc and RING) was able to catalyse poly-ubiquitnation of YB-1 using the E2 UbcH1, whereas R2 (zinc and RING) was not, suggesting that an interaction may exist between the UBA domain of UbcH1 and the DWNN domain of RBBP6. The UBA domain of UbcH1 has been reported to bind to ubiquitin and thereby enhance the production of poly-ubiquitin chains.
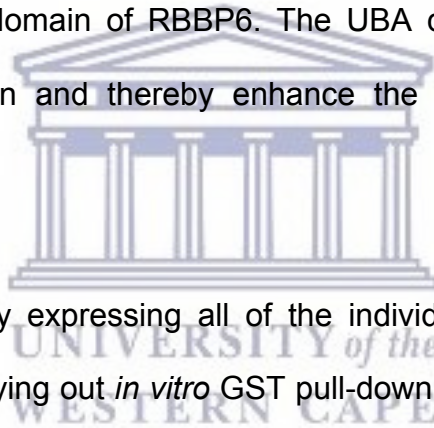
We tested this possibility by expressing all of the individual domains, and the UBA domain, in bacteria and carrying out *in vitro* GST pull-down assays. Our results indicate that there is no interaction between the UBA and the DWNN domain (Figure 3.8 (B)), nor between the UBA and the RING finger domain (Figure 3.8 (A)), but that a robust interaction exists between the UBA and the zinc knuckle (Figure 3.9).

Surprisingly a similar interaction was not observed between UBA and the R2 fragment of RBBP6 (Figure 3.10), despite the fact that R2 includes the zinc finger. The assay was repeated a number of times, but no evidence of an interaction was observed. While it is surprising, it is nevertheless consistent with ubiquitination studies carried out in our laboratory showing that R2 does not poyubiquitinate YB-1 as efectively as the R3

106

fragment. It suggests that the presence of the RING finger blocks the UBA binding site on the zinc knuckle (i.e. in R2), and that this is aleviated when the DWNN domain is present (i.e. in R3). To test this hypothesis it would have been useful to investigate whether R3 is more effectively precipitated by GST-UBA than R2. Unfortunately R3 was found to be too unstable after removal fo the GST tag. An attempt was made to clone an HA-tagged form of UBA so that GST-R3 could be used as the bait, but it had to be abanded due to lack of time.

The interaction between the UBA and the zinc finger is not a new phenomenon. Zinc fingers are well known for their function in gene transcription, translation, cytoskeleton organization, mRNA trafficking and protein folding. They are also known for their ability for binding ubiquitin and, more specifically, K-63 linked poly-ubiquitin chains. Ubiquitin binding zinc fingers, denoted UBZ, include Np14, A20, RAD18, WRNIP1, FAAP20 and SLX4 (Toma et al., 2015).
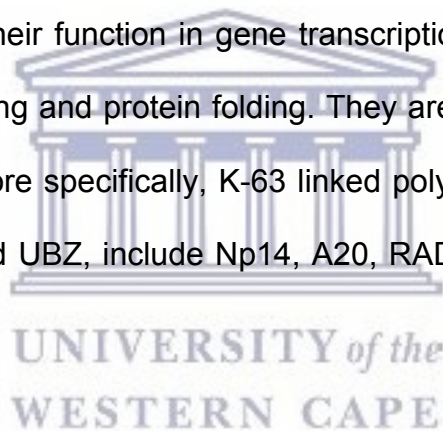
The above results suggest that the spatial arrangement of the three domains making up the N-terminus of RBBP6 has an imact on their function. Determination of the structure of the R3 fragment of RBBP6 may therefore provide important insights into the function of RBBP6. In the meantime, we have tested whether the DWNN domain is able to contact the RING finger domain and inhibit its auto-ubiquitination activity in a similar manner to that of Parkin. However, pull-down assays found no significant interaction between the DWNN domain and the RING finger (Figure 3.11).

107

5.2 Investigation of the role of the Gly-Gly motif and the C-terminal tail in the localisation of RBBP6-isoform 3

The second question investigated was whether the Gly-Gly motif found at the C-terminus of the DWNN domain has an effect on the cellular localisation of isoform 3. Consistent with investigations using endogenous protein, our results show that isoform 3 is predominantly cytoplasmic, but with unmistakable evidence of speckle-like bodies within the nucleus (Figure 4.5 (A)). Co-staining with anti-SC35 antibodies confirmed that the speckle-like bodies were indeed nuclear speckles (Figure 4.6 (B)).

However, our data did not allow us to decide whether the accumulation of isoform 3 in nuclear speckles increases following cell stress, as had been reported in the case of endogenous isoform 3 (AV Szmyd-Potapczyk and DJR Pugh, unpublished data). Replacement of the Gly-Gly motif with Ala-Ala (HA-DWNN13-AA) did not significantly affect the localisation of isoform 3 (Figure 4.5 (B)) and (Figure 4.6(D)). This would appear to rule out the possibility that the Gly-Gly motif plays a role in the covalent attachment of isoform 3 to other proteins, in a process analogous to ubiquitination.

Truncation of isoform 3 immediately before the Gly-Gly motif (HA-DWNN-PI) did produce a very different localisation, the protein being found both in the nucleus and the cytoplasm in most cells, although in some cells it was completely excluded from the nucleus. In neither case was there any evidence of nuclear speckles (Figure 4.5 (C)) and (Figure 4.6 (E)). Our data do not allow us to decide whether the above effect is due to the absence of the Gly-Gly motif or something elsewhere in the C-terminal tail.

108

Attempts were made to express a fragment of isoform 3 terminating immediately after the Gly-Gly motif but time did not allow it to be completed. However a co-worker has since expressed the same construct and found that its localisation is very similar to that of HA-DWNN-PI (i.e both nuclear and cytoplasmic), but with no evidence of nuclear speckling. This implies that the DWNN domain itself is not responsible for accumulation in nuclear speckles. It also implies that something in the C-terminal tail of isoform 3 (residues 80-118) must be responsible both for causing it to be exported from the nucleus, as well as causing it to accumulate in nuclear speckles.

The localisation of the speckle-targeting motif to the 37 residues making up the C-terminal tail of isoform 3 is intriguing. Searches of the literature show that there is no one motif responsible for targeting to nuclear speckles (Eilbracht and Schmidt-Zachmann, 2001). The most frequently identified motif is the SR domain, which has been shown to be necessary for targeting a number of splicing factors to nuclear speckles (Cáceres et al., 1997). However a number of other motifs, including a histidine-rich motif, have been reported (Salichs et al., 2009).

5.3   Conclusions and future prospects

In this study we set out to investigate the interaction between the ubiquitin-associated domain (UBA) of the ubiquitin-conjugating enzyme UbcH1 and the N-terminal domains of RBBP6. Our major finding was that an interaction exists between the UBA and the zinc knuckle domain of RBBP6. This work therefore lays the groundwork for future studies investigating the structure of the complex. Such a study will identify amino acid

residues directly involved in the interaction, which can be mutated with the aim of blocking the interaction. Such mutants can then be used in *in vitro* studies to assess the importance of RBBP6 as a negative regulator of YB-1. Since YB-1 is a highly oncogenic protein, these studies may lead to the development of strategies and therapeutics able to suppress YB-1 and alleviate cancer.

The second major focus of this work was investigating the role potentially played by the Gly-Gly motif in the cellular co-localisation of RBBP6 isoforms. The major finding was that the Gly-Gly motif does not appear to influence the localisation of isoform 3, hence ruling out the possibility that the DWNN domain functions as an ubiquitin-like modifier. Nevertheless we have shown that the C-terminal tail (residues 80 – 118) does influence the localisation of isoform 3; without it isoform 3 is both nuclear and cytoplasmic, with no evidence of speckling, whereas with it isoform 3 is predominantly cytoplasmic, with clear evidence of accumulation in nuclear speckles.
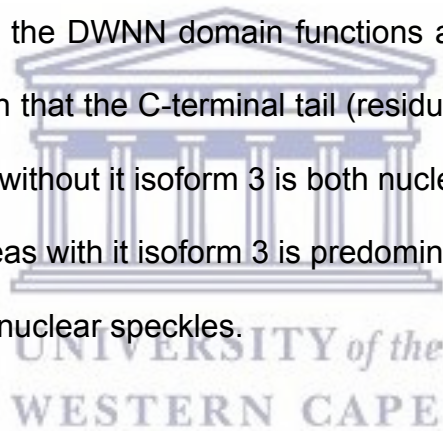
Future work will focus on making further truncations of the C-terminal tail in order to further localize the motif responsible for exporting isoform 3 out of the nucleus, and for causing it to accumulate in nuclear speckles. Co-workers in the laboratory, building on the results reported here using the HA-DWNN-PI construct, have shown that removal or unfolding of the DWNN domain leads to total exclusion of RBBP6 from the nucleus. Future work will include attempts to generate single amino acid mutants which achieve the same nuclear exclusion with minimal change to the rest of the protein. In the context of the model proposed by Di Giammartino and co-workers—that isoform 3 regulates the

polyadenylation activity of isoform 1—mutants of RBBP6 that are excluded from the nucleus or accumulate in nuclear speckles will prove very useful in demonstrating the importance of the role of RBBP6 in regulation of gene expression through modulation of 3'-polyadenylation.

.

BIBLIOGRAPHY

ABRAHAM, R. T. 2001. Cell cycle checkpoint signaling through the ATM and ATR kinases. *Genes & development,* 15**,** 2177-2196.

ÅKERFELT, M., MORIMOTO, R. I. & SISTONEN, L. 2010. Heat shock factors: integrators of cell stress, development and lifespan. *Nature Reviews Molecular Cell Biology,* 11**,** 545-555.

ALASTALO, T., HELLESUO, M., SANDQVIST, A., HIETAKANGAS, V., KALLIO, M. & SISTONEN, L. 2003. Formation of nuclear stress granules involves HSF2 and coincides with the nucleolar localization of Hsp70. *Journal of cell science,* 116**,** 3557-3570.

ALMEIDA, K. H. & SOBOL, R. W. 2007. A unified view of base excision repair: lesion-dependent protein complexes regulated by post-translational modification. *DNA repair,* 6**,** 695-711.

AMEMIYA, Y., AZMI, P. & SETH, A. 2008. Autoubiquitination of BCA2 RING E3 ligase regulates its own stability and affects cell migration. *Molecular Cancer Research,* 6**,** 1385-1396.

ANDERSON, P. & KEDERSHA, N. 2002. Stressful initiations. *Journal of Cell Science,* 115**,** 3227-3234.

ASAKUNO, K., KOHNO, K., UCHIUMI, T., KUBO, T., SATO, S., ISONO, M. & KUWANO, M. 1994. Involvement of a DNA binding protein, MDR-NF1/YB-1, in human MDR1 gene expression by actinomycin D. *Biochemical and biophysical research communications,* 199**,** 1428-1435.

112

BAKTHISARAN, R., TANGIRALA, R. & RAO, M. 2015. Small heat shock proteins: Role in cellular functions and pathology. *Biochim Biophys Acta,* 1854**,** 291-319.

BARTEK, J. & LUKAS, J. 2003. Chk1 and Chk2 kinases in checkpoint control and cancer. *Cancer cell,* 3**,** 421-429.

BASAKI, Y., TAGUCHI, K., IZUMI, H., MURAKAMI, Y., KUBO, T., HOSOI, F., WATARI, K., NAKANO, K., KAWAGUCHI , H., OHNO, S., KOHNO, K., ONO, M. & KUWANO, M. 2010. Y-box binding protein-1 (YB-1) promotes cell cycle progression through CDC6-dependent pathway in human cancer cells. *European Journal of Cancer,* 46**,** 954-965.

BELLSTEDT, D., HUMAN, P., ROWLAND, G. & VAN DER MERWE, K. 1987. Acid-treated, naked bacteria as immune carriers for protein antigens. *Journal of immunological methods,* 98**,** 249-255.

BENJAMIN, I. J. & MCMILLAN, D. R. 1998. Stress (heat shock) proteins molecular chaperones in cardiovascular Biology and disease. *Circ Res,* 83**,** 117-132.

BENJAMIN, I. J., SHELTON, J., GARRY, D. J. & RICHARDSON, J. A. 1997. Temporospatial expression of the small HSP/αB-crystallin in cardiac and skeletal muscle during mouse development. *Developmental dynamics,* 208**,** 75-84.

BETTENCOURT, B. R., HOGAN, C. C., NIMALI, M. & DROHAN, B. W. 2008. Inducible and constitutive heat shock gene expression responds to modification of Hsp70 copy number in Drosophila melanogaster but does not compensate for loss of thermotolerance in Hsp70 null flies. *BMC biology,* 6**,** 5.

BOGYO, M., SHIN, S., MCMASTER, J. S. & PLOEGH, H. L. 1998. Substrate binding and sequence preference of the proteasome revealed by active-site-directed affinity probes. *Chemistry & Biology,* 5**,** 307-320.

BOZAYKUT, P., OZER, N. K. & KARADEMIR, B. 2014. Regulation of protein turnover by heat shock proteins. *Free Radic Biol Med,* 77**,** 195-209.

BRAITHWAITE, A. W., DEL SAL, G. & LU, X. 2006. Some p53-binding proteins that can function as arbiters of life and death. *Cell Death Differ,* 13**,** 984-993.

BUCHAN, J. R. & PARKER, R. 2009. Eukaryotic stress granules: the ins and outs of translation. *Molecular cell,* 36**,** 932-941.

BUCHWALOW, I., SAMOILOVA, V., BOECKER, W. & TIEMANN, M. 2011. Non-specific binding of antibodies in immunohistochemistry: fallacies and facts. *Scientific reports,* 1**,** 28.

BURROUGHS, A. M., JAFFEE, M., IYER, L. M. & ARAVIND, L. 2008. Anatomy of the E2 ligase fold: implications for enzymology and evolution of ubiquitin/Ub-like protein conjugation. *Journal of structural biology,* 162**,** 205-218.

CABISCOL, E., BELLı´, G., TAMARIT, J., ECHAVE, P., HERRERO, E. & ROS, J. 2002. Mitochondrial Hsp60, resistance to oxidative stress, and the labile iron pool are closely connected in saccharomyces cerevisiae. *The Journal Of Biological Chemistry,* 277**,** 44531-44538.

CÁCERES, J. F., MISTELI, T., SCREATON, G. R., SPECTOR, D. L. & KRAINER, A. R. 1997. Role of the modular domains of SR proteins in subnuclear localization and alternative splicing specificity. *The Journal of cell biology,* 138**,** 225-238.

CAPPELLO, F., DAVID, S., RAPPA, F., BUCCHIERI, F., MARASÀ, L., BARTOLOTTA, T. E., FARINA, F. & ZUMMO, G. 2005. The expression of HSP60 and HSP10 in large bowel carcinomas with lymph node metastase. *Bmc Cancer,* 5**,** 139.

CASTLE, P. E., ASHFAQ, R., ANSARI, F. & MULLER, C. Y. 2005. Immunohistochemical evaluation of heat shock proteins in normal and preinvasive lesions of the cervix. *Cancer letters,* 229**,** 245-252.

CATES, J., GRAHAM, G. C., OMATTAGE, N., PAVESICH, E., SETLIFF, I., SHAW, J., SMITH, C. L. & LIPAN, O. 2011. Sensing the heat stress by Mammalian cells. *BMC Biophys,* 4**,** 16.

CAUSTON, H. C., REN, B., KOH, S. S., HARBISON, C. T., KANIN, E., JENNINGS, E. G., LEE, T. I., TRUE, H. L., LANDER, E. S. & YOUNG, R. A. 2001. Remodeling of yeast genome expression in response to environmental changes. *Molecular biology of the cell,* 12**,** 323-337.

CHANDRA, D., CHOY, G. & TANG, D. G. 2007. Cytosolic accumulation of Hsp60 during apoptosis with or without apparent mitochondrial release evidence that its pro-apoptotic or pro-survival functions involve differential interactions with caspase-3. *Journal of Biological Chemistry,* 282**,** 31289-31301.

CHANG, Y. G., SONG, A. X., GAO, Y. G., SHI, Y. H., LIN, X. J., CAO, X. T., LIN, D. H. & HU, H. Y. 2006. Solution structure of the ubiquitin-associated domain of human BMSC-UbP and its complex with ubiquitin. *Protein Sci,* 15**,** 1248-1259.

CHAUGULE, V. K., BURCHELL, L., BARBER, K. R., SIDHU, A., LESLIE, S. J., SHAW, G. S. & WALDEN, H. 2011. Autoregulation of Parkin activity through its ubiquitin-like domain. *The EMBO journal,* 30**,** 2853-2867.

115

CHEN, J., TANG, H., WU, Z., ZHOU, C., JIANG, T., XUE, Y., HUANG, G., YAN, D. & PENG, Z. 2013. Overexpression of RBBP6, alone or combined with mutant tp53, is predictive of poor prognosis in colon cancer. *The Journal of cell biology,* 8**,** 1-9.

CHEN, M. & MANLEY, J. L. 2009. Mechanisms of alternative splicing regulation: insights from molecular and genomics approaches. *Nature reviews Molecular cell biology,* 10**,** 741-754.

CHEN, Z. & PICKART, C. M. 1990. A 25-kilodalton ubiquitin carrier protein (E2) catalyzes multi-ubiquitin chain synthesis via lysine 48 of ubiquitin. *J. Biol. Chem,* 265**,** 21835–21842.

CHIBI, M., MEYER, M., SKEPU, A., REES, D. J., MOOLMAN-SMOOK, J. C. & PUGH, D. J. R. 2008. RBBP6 interacts with multifunctional protein YB-1 through its RING finger domain, leading to ubiquitination and proteosomal degradation of YB-1. *J Mol Biol,* 384**,** 908-916.

CHOWDARY, T. K., RAMAN, B., RAMAKRISHNA, T. & RAO, C. M. 2004. Mammalian Hsp22 is a heat-inducible small heat-shock protein with chaperone-like activity. *Biochemical Journal,* 381**,** 379-387.

CHUNG, K. K. K., DAWSON, V. L. & DAWSON, T. M. 2001. The role of the ubiquitin-proteasomal pathway in Parkinson's disease and other neurodegenerative disorders. *Trends in neurosciences,* 24**,** 7-14.

CIOCCA, D. R. & CALDERWOOD, S. K. 2005. Heat shock proteins in cancer: diagnostic, prognostic, predictive, and treatment implications. *Cell stress & chaperones,* 10**,** 86-103.

CLEAVER, J. E., LAM, E. T. & REVET, I. 2009. Disorders of nucleotide excision repair: the genetic and molecular basis of heterogeneity. *Nature Reviews Genetics,* 10**,** 756-768.

CORDIER, F., GRUBISHA, O., TRAINCARD, F., VÉRON, M., DELEPIERRE, M. & AGOU, F. 2009. The zinc finger of NEMO is a functional ubiquitin-binding domain. *Journal of Biological Chemistry,* 284**,** 2902-2907.

CORNFORD, P. A., DODSON, A. R., PARSONS, K. F., DESMOND, A. D., WOOLFENDEN, A., FORDHAM, M., NEOPTOLEMOS, J. P., KE, Y. & FOSTER, C. S. 2000. Heat shock protein expression independently predicts clinical outcome in prostate cancer. *Cancer research,* 60**,** 7099-7105.

COTTO, J., FOX, S. & MORIMOTO, R. I. 1997. HSF1 granules: a novel stress-induced nuclear compartment of human cells. *Journal of cell science,* 110**,** 2925-2934.

CYR, D. M., HÖHFELD, J. & PATTERSON, C. 2002. Protein quality control: U-box-containing E3 ubiquitin ligases join the fold. *Trends in biochemical sciences,* 27**,** 368-375.

DANG, Y., KEDERSHA, N., LOW, W. K., ROMO, D., GOROSPE, M., KAUFMAN, R., ANDERSON, P. & LIU, J. O. 2006. Eukaryotic inititian factor 2α-independent pathway of stress granule induction by the natural product pateamine A. *Journal of Biological Chemistry,* 281**,** 32870-32878.

DE BONT, R. & VAN LAREBEKE, N. 2004. Endogenous DNA damage in humans: a review of quantitative data. *Mutagenesis,* 19**,** 169-185.

DESHAIES, R. J. & JOAZEIRO, C. A. 2009. RING domain E3 ubiquitin ligases. *Annu Rev Biochem,* 78**,** 399-434.

117

DEXHEIMER, T. S. 2013. DNA repair pathways and mechanisms. *DNA repair of cancer stem cells.* Springer.

DEZWAAN, D. C. & FREEMAN, B. C. 2008. HSP90: the Rosetta stone for cellular protein dynamics? *Cell Cycle,* 7**,** 1006–1012.

DI GIAMMARTINO, D. C., LI, W., OGAMI, K., YASHINSKIE, J. J., HOQUE, M., TIAN, B. & MANLEY, J. L. 2014. RBBP6 isoforms regulate the human polyadenylation machinery and modulate expression of mRNAs with AU-rich 3' UTRs. *Genes Dev,* 28**,** 2248-2260.

DI GIAMMARTINO, D. C. & MANLEY, J. L. 2014. New links between mRNA polyadenylation and diverse nuclear pathways. *Mol Cells,* 37**,** 644-649.

DIKIC, I. & ROBERTSON, M. 2012. Ubiquitin ligases and beyond. *BMC Biol,* 10**,** 22.

DUBIŃSKA-MAGIERA, M., JABŁOŃSKA, J., SACZKO, J., KULBACKA, J., JAGLA, T. & DACZEWSKA, M. 2014. Contribution of small heat shock proteins to muscle development and function. *FEBS letters,* 588**,** 517-530.

DUNDR, M. & MISTELI, T. 2010. Biogenesis of nuclear bodies. *Cold Spring Harb Perspect Biol,* 2**,** 1-15.

DYE, B. T. & SCHULMAN, B. A. 2007. Structural mechanisms underlying posttranslational modification by ubiquitin-like proteins. *Annu. Rev. Biophys. Biomol. Struct.,* 36**,** 131-150.

EILBRACHT, J. & SCHMIDT-ZACHMANN, M. S. 2001. Identification of a sequence element directing a protein to nuclear speckles. *Proc Natl Acad Sci U S A,* 98**,** 3849-3854.

ELISEEVA, I. A., KIM, E. R., GURYANOV, S. G., OVCHINNIKOV, L. P. & LYABIN, B. N. 2011. Y-Box- Binding Protein 1 (YB-1) and Its Functions. *Biochemistry,* 76**,** 1402-1433.

ELKON, R., UGALDE, A. P. & AGAMI, R. 2013. Alternative cleavage and polyadenylation: extent, regulation and function. *Nat. Rev. Genet,* 14**,** 496-506.

FULDA, S., GORMAN, A. M., HORI, O. & SAMALI, A. 2010. Cellular stress responses: cell survival and cell death. *Int J Cell Biol,* 2010**,** 1-25.

GAMSJAEGER, R., LIEW, C. K., LOUGHLIN, F. E., CROSSLEY, M. & MACKAY, J. P. 2007. Sticky fingers: zinc-fingers as protein-recognition motifs. *Trends in biochemical sciences,* 32**,** 63-70.

GIGLIA-MARI, G., ZOTTER, A. & VERMEULEN, W. 2011. DNA damage response. *Cold Spring Harbor perspectives in biology,* 3, a000745.

GIMÉNEZ-BONAFÉ, P., FEDORUK, M. N., WHITMORE, T. G., AKBARI, M., RALPH, J. L., ETTINGER, S., GLEAVE, M. E. & NELSON, C. C. 2004. YB-1 is upregulated during prostate cancer tumor progression and increases P-glycoprotein activity. *Prostate,* 3**,** 337-349.

GONDA, R. L., GARLENA, R. A. & STRONACH, B. 2012. Drosophila heat shock response requires the JNK pathway and phosphorylation of mixed lineage kinase at a conserved serine-proline motif. *PloS one,* 7**,** e42369.

GRUBER, B. M., KRZYSZTOŃ-RUSSJAN, J., BUBKO, I. & ANUSZEWSKA, E. L. 2010. Possible role of HSP60 in synergistic action of anthracyclines and sulindac in HeLa cells. *Acta Pol Pharm Drug Res,* 67**,** 620-624.

HAAS, A. L. & ROSE, I. A. 1982. The mechanism of ubiquitin activating enzyme. A kinetic and equilibrium analysis. *Journal of Biological Chemistry,* 257**,** 10329-10337.

HALDEMAN, M. T., XIA, G., KASPEREK, E. M. & PICKART, C. M. 1997. Structure and function of ubiquitin conjugating enzyme E2-25K: the tail is a core-dependent activity element. *Biochemistry,* 36**,** 10526-10537.

HARTL, F. U. & HAYER-HARTL, M. 2002. Molecular chaperones in the cytosol: from nascent chain to folded protein. *Science,* 295**,** 1852–1858.

HASLBECK, M. & VIERLING, E. 2015. A first line of stress defense: small heat shock proteins and their function in protein homeostasis. *J Mol Biol,* 427**,** 1537-1548.

HAZKANI-COVO, E., LEVANON, E. Y., ROTMAN, G., GRAUR, D. & NOVIK, A. 2004. Evolution of multicellularity in Metazoa: comparative analysis of the subcellular localization of proteins in Saccharomyces, Drosophila and Caenorhabditis. *Cell Biol Int,* 28**,** 171-178.

HERRMANN, J., LERMAN, L. O. & LERMAN, A. 2007. Ubiquitin and ubiquitin-like proteins in protein regulation. *Circulation research,* 100**,** 1276-1291.

HOEIJMAKERS, J. H. 1993. Nucleotide excision repair II: from yeast to mammals. *Trends in Genetics,* 9**,** 211-217.

HOLLSTEIN, M., SIDRANSKY, D., VOGELSTEIN, B. & HARRIS, C. C. 1991. p53 mutations in human cancers. *Science,* 253**,** 49-54.

HSU, P. L. & HSU, S. M. 1998. Abundance of heat proteins (hsp89, hsp60, and hsp27) in malignant Hodgkin's disease. *Cancer Res,* 98**,** 5507–5513.

HUANG, P., MA, X., ZHAO, Y. & MIAO, L. 2013a. The C. elegans Homolog of RBBP6 (RBPL-1) regulates fertility through controlling cell proliferation in the germline and nutrient synthesis in the intestine. *PLoS One,* 8**,** 58736.

IZUMI, H., IMAMURA, T., NAGATANI, G., ISE, T., MURAKAMI, T., URAMOTO, H., TORIGOE, T., ISHIGUCHI, H., YOSHIDA, Y., NOMOTO, M. & OKAMOTO, T. 2001. Y boxbinding protein-1 binds preferentially to single-stranded nucleic acids and exhibits 3`–5` exonuclease activity. *Nucleic Acids Res,* 29**,** 1200–1207.

JÄÄTTELÄ, M. 1999. Heat shock proteins as cellular lifeguards. *Annals of medicine,* 31**,** 261-271.

JACKSON, S. E. 2013. Hsp90: structure and function. *Top Curr Chem,* 328**,** 155-240.

JACOBS, A. L. & SCHÄR, P. 2012. DNA glycosylases: in DNA repair and beyond. *Chromosoma,* 121**,** 1-20.

JEE, H. 2016. Size dependent classification of heat shock proteins: a mini-review. *J Exerc Rehabil,* 12**,** 255-259.

JIANG, J., BALLINGER, C. A., WU, Y., DAI, Q., CYR, D. M. & HOHFELD, J. 2001. CHIP is a U-box-dependent E3 ubiquitin ligase: identification of Hsc70 as a target for ubiquitylation. *J Biol Chem,* 276**,** 42938-42944.

JIN, J., LI, X., GYGI, S. P. & HARPER, J. W. 2007. Dual E1 activation systems for ubiquitin differentially regulate E2 enzyme charging. *Nature,* 447**,** 1135-1138.

JOHNSON, M. 2014. *HA Hemagglutinin Tag Antibody and FAQs* [Online]. Synatom Research, Princeton, New Jersey, United States: Labome. Available: https://www.labome.com/method/HA-Hemagglutinin-Tag-Antibody-and-FAQs.html [Accessed 18/12/2017]

JOLLY, C. & MORIMOTO, R. I. 2000. Role of the heat shock response and molecular chaperones in oncogenesis and cell death. *Journal of the National Cancer Institute,* 92**,** 1564-1572.

JOLLY, C., USSON, Y. & MORIMOTO, I. R. 1999. Rapid and reversible relocalization of heat shock factor 1 within seconds to nuclear stress granules. *Proceedings of the National Academy of Sciences,* 96**,** 6769-6774.

JUN, S. 2010. DNA chemical damage and its detected. *International Journal of Chemistry,* 2**,** 261-265.

KALCHMAN, M. A., GRAHAM, R. K., XIA, G., KOIDE, H. B., HODGSON, J. G., GRAHAM, K. C., GOLDBERG, Y. P., GIETZ, R. D., PICKART, C. M. & HAYDEN, M. R. 1996. Huntingtin is ubiquitinated and interacts with a specific ubiquitin-conjugating enzyme. *Journal of Biological Chemistry,* 271**,** 19385-19394.

KAMPINGA, H. H. & CRAIG, E. A. 2010. The HSP70 chaperone machinery: J proteins as drivers of functional specificity. *Nat. Rev.,* 11**,** 579-592.

KAMPINGA, H. H., HAGEMAN, J., VOS, M. J., KUBOTA, H., TANGUAY, R. M., BRUFORD, E. A., CHEETHAM, M. E., CHEN, B. & HIGHTOWER, L. E. 2009. Guidelines for the nomenclature of the human heat shock proteins. *Cell Stress Chaperones,* 14**,** 105-111.

KAPPO, M. A. 2009. *Solution structure of the RING finger domain from the human splicing-associated protein RBBP6 using heteronuclear Nuclear Magnetic Resonance (NMR) Spectroscopy.* PhD Biotechnology, University of the Western Cape.

KAPPO, M. A., AB, E., HASSEM, F., ATKINSON, R. A., FARO, A., MULEYA, V., MULAUDZI, T., POOLE, J. O., MCKENZIE, J. M., CHIBI, M., MOOLMAN-SMOOK, J. C., REES, D. J. & PUGH, D. J. 2012. Solution structure of RING finger-like domain of retinoblastoma-binding protein-6 (RBBP6) suggests it functions as a U-box. *J Biol Chem,* 287**,** 7146-7158.

KAUFMANN, S. H. E. 1990. Heat shock proteins and the immune response. *Immunology today,* 11**,** 129-136.

KEDERSHA, N., CHEN, S., GILKS, N., LI, W., MILLER, I., STAHL, J. & ANDERSON, P. 2002. Evidence that ternary complex (eIF2-GTP-tRNAMet)-deficient preinitiation complexes are core constituents of mammalian stress granules. *Mol. Biol. Cell,* 13**,** 195-210.

KEDERSHA, N., CHO, M. R., LI, W., YACONO, P. W., CHEN, S., GILKS, N., GOLAN, D. E. & P., A. 2000. Dynamic shuttling of TIA-1 accompanies the recruitment of mRNA to mammalian stress granules. *J. Cell Biol,* 151**,** 1257–1268.

KEDERSHA, N., IVANOV, P. & ANDERSON, P. 2013. Stress granules and cell signaling: more than just a passing phase? *Trends Biochem Sci,* 38**,** 494-506.

KEDERSHA, N. L., GUPTA, M., LI, W., MILLER, I. & ANDERSON, P. 1999. RNA-binding proteins TIA-1 and TIAR link the phosphorylation of eIF-2α to the assembly of mammalian stress granules. *J Cell Biol,* 147**,** 1431–1442.

KERSCHER, O., FELBERBAUM, R. & HOCHSTRASSER, M. 2006. Modification of proteins by ubiquitin and ubiquitin-like proteins. *Annu. Rev. Cell Dev. Biol.,* 22**,** 159-180.

KIM, Y. D., LEE, J. Y., OH, K. M., ARAKI, M., ARAKI, K., YAMAMURA, K. & JUN, C. D. 2011. NSrp70 is a novel nuclear speckle-related protein that modulates alternative pre-mRNA splicing in vivo. *Nucleic Acids Res,* 39**,** 4300-4314.

KIM, Y. E., HIPP, M. S., BRACHER, A., HAYER-HARTL, M. & HARTL, F. U. 2013. Molecular chaperone functions in protein folding and proteostasis. *Annu Rev Biochem,* 82**,** 323-355.

KOHNO, K., IZUMI, H., UCHIUMI, T., ASHIZUKA, M. & KUWANO, M. 2003. The pleiotropic functions of the Y-box-binding protein, YB-1. *Bioessays,* 25**,** 691–698.

KOIKE, K., UCHIUMI, T., OHGA, T., TOH, S., WADA, M., KOHNO, K. & KUWANO, M. 1997. Nuclear translocation of the Y-box binding protein by ultraviolet irradiation. *FEBS Lett,* 417**,** 390–394.

KREGEL, K. C. 2002. Disaggregating chaperones: an unfolding story. *Current Protein and Peptide Science,* 10**,** 432–446.

KRIEHUBER, T., RATTEI, T., WEINMAIER, T., BEPPERLING, A., HASLBECK, M. & BUCHNER, J. 2010. Independent evolution of the core domain and its flanking sequences in small heat shock proteins. *FASEB J,* 24**,** 3633-3642.

KRISHNA, S. S., MAJUMDAR, I. & GRISHIN, N. V. 2003. Structural classification of zinc fingers SURVEY AND SUMMARY. *Nucleic acids research,* 31**,** 532-550.

KROKAN, H. E., DRABLØS, F. & SLUPPHAUG, G. 2002. Uracil in DNA-occurrence, consequences and repair. *Oncogene,* 21**,** 8935.

KRUGER, T., HOFWEBER, M. & KRAMER, S. 2013. SCD6 induces ribonucleoprotein granule formation in trypanosomes in a translation-independent manner, regulated by its Lsm and RGG domains. *Mol Biol Cell,* 24**,** 2098–2111.

KUMAR, S., YOSHIDA, Y. & NODA, M. 1993. Cloning of a cDNA which encodes a novel ubiquitin-like protein. *Biochemical and biophysical research communications,* 195**,** 393-399.

LAMOND, A. I. & SLEEMAN, J. E. 2003. Nuclear substructure and dynamics. *Current Biology,* 13**,** R825-R828.

LAMOND, A. I. & SPECTOR, D. L. 2003. Nuclear speckles: a model for nuclear organelles. *Nat Rev Mol Cell Biol,* 4**,** 605–612.

LAW, J. H., LI, Y., TO, K., WANG, M., ASTANEHE, A., LAMBIE, K., JONES, S. J. M., GLEAVE, M. E., EAVES, C. J. & DUNN, S. E. 2010. Molecular decoy to the Y-Box binding protein-1 suppresses the growth of breast and prostate cancer cells whilst sparing normal cell viability. *PLoS One,* 5**,** 1-11.

LEBRET, T., WATSON, R. W. G., MOLINIÉ, V., O'NEILL, A., GABRIEL, C., FITZPATRICK, J. M. & BOTTO, H. 2003. Heat shock proteins HSP27, HSP60, HSP70, and HSP90. *Cancer,* 98**,** 970-977.

LECKER, S. H., GOLDBERG, A. L. & MITCH, W. E. 2006. Protein degradation by the ubiquitin–proteasome pathway in normal and disease states. *Journal of the American Society of Nephrology,* 17**,** 1807-1819.

LEE, C., DHILLON, J., WANG, M. Y. C., GAO, Y., HU, K., PARK, E., ASTANEHE, E., HUNG, M., EIREW, P., EAVES, C. J. & DUNN, S. E. 2008. Targeting YB-1 in HER-2 overexpressing breast cancer cells induces apoptosis via the mTOR/STAT3 pathway and suppresses tumor growth in mice. *Cancer Res,* 68**,** 8661-8666.

LEE, S. D. & MOORE, C. L. 2014. Efficient mRNA polyadenylation requires a ubiquitin-like domain, a zinc knuckle, and a RING finger domain, all contained in the Mpe1 protein. *Mol Cell Biol,* 34**,** 3955-3967.

LI, L., DENG, B., XING, G., TENG, Y., TIAN, C., CHENG, X., YIN, X., YANG, J., GAO, X., ZHU, Y., SUN, Q., ZHANG, L., YANG, X. & HE, F. 2007. PACT is a negative regulator of p53 and essential for cell growth and embryonic development. *Proc Natl Acad Sci USA,* 104**,** 7951-7956.

LINDQUIST, S. 1986. The heat-shock response. *Annual review of biochemistry,* 55**,** 1151-1191.

LINDQUIST, S. & CRAIG, E. A. 1988. The heat-shock proteins. *Annual Review of Genetics,* 22**,** 631–677.

LUTYA, P. T. 2002. *Expression and purification of the novel protein domain DWNN.* MSc Biotechnology, University of the Western Cape.

MAO, Y. S., ZHANG, B. & SPECTOR, D. L. 2011. Biogenesis and function of nuclear bodies. *Trends in Genetics,* 27**,** 295-306.

MATHER, A., RAKGOTHO, M. & NTWASA, M. 2005. SNAMA, a novel protein with a DWNN domain and a RING finger-like motif: a possible role in apoptosis. *Biochim Biophys Acta,* 1727**,** 169-76.

MATSUMOTO, K. & WOLFFE, A. P. 1998. Gene regulation by Y-box proteins: coupling control of transcription and translation. *Trends Cell Biol,* 8**,** 318–323.

MATTHEWS, J. M., KOWALSKI, K., LIEW, C. K., SHARPE, B. K., FOX, A. H., CROSSLEY, M. & MACKAY, J. P. 2000. A class of zinc fingers involved in protein–protein interactions. *The FEBS Journal,* 267**,** 1030-1038.

126

MBITA, Z., MEYER, M., SKEPU, A., HOSIE, M., REES, J. & DLAMINI, Z. 2012. De-regulation of the RBBP6 isoform 3/DWNN in human cancers. *Mol Cell Biochem,* 362**,** 249-262.

MCMILLAN, D. R., XIAO, X., SHAO, L., GRAVES, K. & BENJAMIN, I. J. 1998. Targeted disruption of heat shock transcription factor 1 abolishes thermotolerance and protection against heat-inducible apoptosis. *J. Biol. Chem,* 273**,** 7523–7528.

MELCAK, I., CERMANOVA, S., JIRSOVA, K., KOBERNA, K., MALINSKY, J. & RASKA, I. 2000. Nuclear pre-mRNA compartmentalization: Trafficking of released transcripts to splicing factor reservoirs. *Mol Biol Cell,* 11**,** 497–510.

METZGER, M. B., HRISTOVA, V. A. & WEISSMAN, A. M. 2012. HECT and RING finger families of E3 ubiquitin ligases at a glance. *J Cell Sci,* 125**,** 531-537.

METZGER, M. B., PRUNEDA, J. N., KLEVIT, R. E. & WEISSMAN, A. M. 2014. RING-type E3 ligases: Master manipulators of E2 ubiquitin-conjugating enzymes and ubiquitination. *Biochimica et Biophysica Acta,* 1843**,** 47–60.

MIDDLETON, A. J. & DAY, C. L. 2015. The molecular basis of lysine 48 ubiquitin chain synthesis by Ube2K. *Scientific reports,* 5**,** 16793.

MINTZ, P. J., PATTERSON, S. D., NEUWALD, A. F., SPAHR, C. S. & SPECTOR, D. L. 1999. Purification and biochemical characterization of interchromatin granule clusters. *The EMBO Journal,* 18**,** 4308-4320.

MIOTTO, B., CHIBI, M., XIE, P., KOUNDRIOUKOFF, S., MOOLMAN-SMOOK, H., PUGH, D., DEBATISSE, M., HE, F., ZHANG, L. & DEFOSSEZ, P. A. 2014. The RBBP6/ZBTB38/MCM10 axis regulates DNA replication and common fragile site stability. *Cell Rep,* 7**,** 575-587.

127

MISTELI, T. & SPECTOR, D. L. 1999. RNA polymerase II targets pre-mRNA splicing factors to transcription sites in vivo. *Molecular cell,* 3**,** 697-705.

MOLFETTA, R., GASPARRINI, F., SANTONI, A. & PAOLINI, R. 2010. Ubiquitination and endocytosis of the high affinity receptor for IgE. *Molecular immunology,* 47**,** 2427-2434.

MORIMOTO, R. I. 1998. Regulation of the heat shock transcriptional response: cross talk between a family of heat shock factors, molecular chaperones, and negative regulators. *Genes & development,* 12**,** 3788-3796.

MORIMOTO, R. I. & SANTORO, M. G. 1998. Stress-inducible responses and heat shock proteins: new pharmacologic targets for cytoprotection. *Nat Biotechnol,* 16**,** 833-838.

MORISAKI, T., YASHIRO, M., KAKEHASHI, A., INAGAKI, A., KINOSHITA, H., FUKUOKA, T., KASASHIMA, H., MASUDA, G., SAKURAI, K., KUBO, N., MUGURUMA, K., OHIRA, M., WANIBUCHI, H. & HIRAKAWA, K. 2014. Comparative proteomics analysis of gastric cancer stem cells. *PLoS One,* 9**,** e110736.

MÖRKING, P. A., DALLAGIOVANNA, B. M., FOTI, L., GARAT, B., PICCHI, G. F., UMAKI, A. C., PROBST, C. M., KRIEGER, M. A., GOLDENBERG, S. & FRAGOSO, S. P. 2004. TcZFP1: a CCCH zinc finger protein of Trypanosoma cruzi that binds poly-C oligoribonucleotides in vitro. *Biochemical and biophysical research communications,* 319**,** 169-177.

MOSSER, D. D. & MORIMOTO, R. I. 2004. Molecular chaperones and the stress of oncogenesis. *Oncogene,* 23**,** 2907-2918.

MOUTAOUFIK, M. T., EL FATIMY, R., NASSOUR, H., GAREAU, C., LANG, J., TANGUAY, R. M., MAZROUI, R. & KHANDJIAN, E. W. 2014. UVC-induced stress granules in mammalian cells. *PLoS One,* 9**,** e112742.

NATHAN, D. F., VOS, M. H. & LINDQUIST, S. 1997. In vivo functions of the Saccharomyces cerevisiae Hsp90 chaperone. *Proceedings of the National Academy of Sciences,* 94**,** 12949-12956.

NEVINS, J. R. & DARNELL, J. E. 1978. Steps in the processing of Ad2 mRNA: Poly(A)$^+$ nuclear sequences are conserved and poly(A) addition precedes splicing. *Cell,* 15**,** 1477-1493.

NOVER, L., SCHARF, K. & NEUMANN, D. 1989. Cytoplasmic heat shock granules are formed from precursor particles and are associated with a specific set of mRNAs. *Mol. Cell. Biol,* 9**,** 1298-1308.

OHGA, T., UCHIUMI, T., MAKINO, Y., KOIKE, K., WADA, M., KUWANO, M. & KOHNO, K. 1998. Direct involvement of the Y-box binding protein YB-1 in genotoxic stress-induced activation of the human multidrug resistance 1 gene. *Journal of Biological Chemistry,* 273**,** 5997-6000.

OKAMOTO, T., IZUMI, H., IMAMURA, T., TAKANO, H., ISE, T., UCHIUMI, T., KUWANO, M. & K., K. 2000. Direct interaction of p53 with the Y-box binding protein, YB-1: a mechanism for regulation of human gene expression. *Oncogene,* 19**,** 6194–6202.

PAN, M., LI, K., LIN, S. & HUNG, W. 2016. Connecting the dots: from DNA damage and repair to aging. *International journal of molecular sciences,* 17**,** 685.

129

PARK-SARGE, O. & SARGE, K. D. 2005. Detection of sumoylated proteins. *Methods in molecular Biology* 301**,** 329.

PARK, C. J. & SEO, Y. S. 2015. Heat Shock Proteins: A Review of the Molecular Chaperones for Plant Immunity. *Plant Pathol J,* 31**,** 323-333.

PARSELL, D. A. & LINDQUIST, S. 1994. Heat Shock Proteins and Stress Tolerance. *Cold Spring Harbor Monograph Archive,* 26**,** 457-494.

PHAIR, R. D. & MISTELI, T. 2000. High mobility of proteins in the mammalian cell nucleus. *Nature,* 404**,** 604.

PICKART, C. M. 2001. Mechanisms underlying ubiquitination. *Annual review of biochemistry,* 70**,** 503-533.

POCKLEY, G. A. 2001. *Regulation of transcription of heat shock protein genes by heat shock factor* [Online]. Available:

http://journals.cambridge.org/fulltext_content/ERM/ERM3_23/S1462399401003556sup002.htm [Accessed 11/11/2016]

PUGH, D. J., AB, E., FARO, A., LUTYA, P. T., HOFFMANN, E. & REES, D. J. 2006. DWNN, a novel ubiquitin-like domain, implicates RBBP6 in mRNA processing and ubiquitin-like pathways. *BMC Struct Biol,* 6**,** 1-8.

QIU, X. B., SHAO, Y. M., MIAO, S. & WANG, L. 2006. The diversity of the DnaJ/Hsp40 family, the crucial partners for Hsp70 chaperones. *Cellular and Molecular Life Sciences CMLS,* 63**,** 2560-2570.

REDDY, A. S. N., DAY, I. S., GÖHRING, J. & BARTA, A. 2012. Localization and dynamics of nuclear speckles in plants. *Plant physiology,* 158**,** 67-77.

130

RICHARDSON, A., LANDRY, S. J. & GEORGOPOULOS, C. 1998. The ins and outs of a molecular chaperone machine. *Trends in biochemical sciences,* 23**,** 138-143.

RICHTER, K., HASLBECK, M. & BUCHNER, J. 2010. The heat shock response: life on the verge of death. *Molecular cell,* 40**,** 253-266.

SAIJO, M., SAKAI , Y., KISHINO, T., NIKAWA , N., MATSUURA, Y., MORINO, K., TAMAI, K. & TAYA, Y. 1995. Molecular cloning of a human protein that binds to the retinoblastoma protein and chromosomal mapping. *Genomics,* 27**,** 511–519.

SAKAI, Y., SAIJO, M., COELHO, K., KISHINO, T., NIIKAWA, N. & TAYA, Y. 1995. cDNA sequence and chromosomal localization of a novel human protein, RBQ-1 (RBBP6), that binds to the Retinoblastoma gene product. *Genomics,* 30**,** 98-101.

SALICHS, E., LEDD, A., MULARONI, L., ALBA, M. M. & DE LA LUNA, S. 2009. Genome-wide analysis of histidine repeats reveals their role in the localization of human proteins to the nuclear speckles compartment. *PLoS Genetics* 5**,** 1-18.

SANDQVIST, A. & SISTONEN, L. 2004. Nuclear stress granules. *The Journal of cell biology,* 164**,** 15-17.

SANFORD, J. R., GRAY, N. K., BECKMANN, K. & CÁCERES, J. F. 2004. A novel role for shuttling SR proteins in mRNA translation. *Genes & development,* 18**,** 755-768.

SARGE, K. D., MURPHY, S. P. & MORIMOTO, R. I. 1993. Activation of heat shock gene transcription by heat shock factor 1 involves oligomerization, acquisition of DNA-binding activity, and nuclear localization and can occur in the absence of stress. *Molecular and cellular biology,* 13**,** 1392-1407.

SATYAL, S. H., CHEN, D., FOX, S. G., KRAMER, J. M. & MORIMOTO, R. I. 1998. Negative regulation of the heat shock transcriptional response by HSBP1. *Genes & development,* 12**,** 1962-1974.

SCHEUFLER, C., BRINKER, A., BOURENKOV, G., PEGORARO, S., MORODER, L., BARTUNIK, H., HARTL, F. U. & MOAREFI, I. 2000. Structure of TPR domain–peptide complexes: critical elements in the assembly of the Hsp70–Hsp90 multichaperone machine. *Cell,* 101**,** 199-210.

SHAMOVSKY, I. & NUDLER, E. 2008. New insights into the mechanism of heat shock response activation. *Cellular and Molecular Life Sciences,* 65**,** 855–861.

SHENG, Y., HONG, J. H., DOHERTY, R., SRIKUMAR, T., SHLOUSH, J., AVVAKUMOV, G. V., WALKER, J. R., XUE, S., NECULAI, D. & WAN, J. W. 2012. A human ubiquitin conjugating enzyme (E2)-HECT E3 ligase structure-function screen. *Molecular & Cellular Proteomics,* 11**,** 329-341.

SHIBAHARA, K., SUGIO, K., OSAKI, T., SHIBAHARA, K., SUGIO, K. & OSAKI, T. 2001. Nuclear expression of the Y-Box binding protein, YB-1, as a novel marker of disease progression in non-small cell lung cancer nuclear expression of the Y-Box binding protein, YB-1, as a novel marker of disease progression in non-small cell lung cancer. *Clinical cancer research,* 7**,** 3151–3155.

SILVEIRA, C. G. T., KRAMPE, J., RUHLAND, B., DIEDRICH, K., HORNUNG, D. & AGIC, A. 2011. Cold-shock domain family member YB-1 expression in endometrium and endometriosis. *Human Reproduction,* 0**,** 1-10.

SIMONS, A., MELAMED-BESSUDO, C., WOLKOWICZ, R., SPERLING, J., SPERLING, R., EISENBACH, L. & ROTTER, V. 1997. PACT: cloning and characterization of a cellular p53 binding protein that interacts with Rb. *Oncogene,* 14**,** 145-155.

SOROKIN, A. V., SELYUTINA, A. A., SKABKIN, M. A., GURYANOV, S. G., NAZIMOV, I. V., RICHARD, C., TH'NG, J., YAU, J., SORENSEN, P. H. B. & OVCHINNIKOV, L. P. 2005. Proteasome-mediated cleavage of the Y-box-binding protein 1 is linked to DNA-damage stress response. *The EMBO journal,* 24**,** 3602-3612.

SPECTOR, D. L. & LAMOND, A. I. 2011. Nuclear speckles. *Cold Spring Harb Perspect Biol,* 3**,** 1-12.

SRI KRISHNA, S., MAJUMDAR, I. & GRISHIN, N. V. 2003. Structural classification of zinc fingers. *Nucleic acids research,* 31**,** 532-550.

STEGMULLER, J. & BONNI, A. 2010. Destroy to create: E3 ubiquitin ligases in neurogenesis. *F1000 Biol Rep,* 2**,** 38.

SUGASAWA, K., NG, J. M., MASUTANI, C., IWAI, S., VAN DER SPEK, P. J., EKER, A. P., HANAOKA, F., BOOTSMA, D. & HOEIJMAKERS, J. H. 1998. Xeroderma pigmentosum group C protein complex is the initiator of global genome nucleotide excision repair. *Molecular cell,* 2**,** 223-232.

SUTHERLAND, B. W., KUCAB, J., WU, J., LEE, C., CHEANG, M. C., YORIDA, E., TURBIN, D., DEDHAR, S., NELSON, C., POLLAK, M., LEIGHTON, G. H., MILLER, K., BADVE, S., HUNTSMAN, D., BLAKE-GILKS, C., CHEN, M., PALLEN, C. J. & DUNN, S. 2005. Akt phosphorylates the Y-box binding protein 1 at Ser102 located in the cold shock domain and affects the anchorage-independent growth of breast cancer cells. *Oncogene,* 24**,** 4281–4292.

TAVARIA, M., GABRIELE, T., KOLA, I. & ANDERSON, R. L. 1996. A hitchhiker's guide to human Hsp7O family. *Cell Stress Chaperones,* 1**,** 23-28.

TENNO, T., FUJIWARA, K., TOCHIO, H., IWAI, K., MORITA, E. H., HAYASHI, H., MURATA, S., HIROAKI, H., SATO, M. & TANAKA, K. 2004. Structural basis for distinct roles of Lys63-and Lys48-linked poly-ubiquitin chains. *Genes to Cells,* 9**,** 865-875.

THIRY, M. 1995. The interchromatin granules. *Histol Histopathol,* 10**,** 1035–1045.

TIWARI, S., THAKUR, R. & SHANKAR, J. 2015. Role of Heat-Shock Proteins in Cellular Function and in the Biology of Fungi. *Biotechnology Research International,* 2015**,** 1-11.

TO, K., FOTOVATI, A., REIPAS, K. M., LAW, J. H., HU, K., ASTANEHE, A., DAVIES, A. H., LEE, L., STRATFORD, A. L., RAOUF, A., JOHNSON, P., BERQUIN, I. M., ROYER, H., CONNIE, J. & DUNN, S. E. 2011. YB-1 induces expression of CD44 and CD49f leading to enhanced self-renewal, mammosphere growth, and drug resistance. *NIH Public Access,* 70**,** 2840-2851.

TOMA, A., TAKAHASHI, T. S., SATO, Y., YAMAGATA, A., GOTO-ITO, S., NAKADA, S., FUKUTO, A., HORIKOSHI, Y., TASHIRO, S. & FUKAI, S. 2015. Structural basis for ubiquitin recognition by ubiquitin-binding zinc finger of FAAP20. *PloS one,* 10**,** e0120887.

TORNALETTI, S. & HANAWALT, P. C. 1999. Effect of DNA lesions on transcription elongation. *Biochimie,* 81**,** 139-146.

TRIPATHI, V., SONG, D. Y., ZONG, X., SHEVTSOV, S. P., HEARN, S., FU, X., DUNDR, M. & PRASANTH, K. V. 2012. SRSF1 regulates the assembly of pre-

mRNA processing factors in nuclear speckles. *Molecular Biology of the cell,* 23**,** 3694-3706.

VALENTE, E. M., ABOU-SLEIMAN, P. M., CAPUTO, V., MUQIT, M. M. K., HARVEY, K., GISPERT, S., ALI, Z., DEL TURCO, D., BENTIVOGLIO, A. R. & HEALY, D. G. 2004. Hereditary early-onset Parkinson's disease caused by mutations in PINK1. *Science,* 304**,** 1158-1160.

VAN DER VEEN, A. G. & PLOEGH, H. L. 2012. Ubiquitin-like proteins. *Annu Rev Biochem,* 81**,** 323-357.

VO, L., MINET, M., LACROUTE, F. & WYERS, F. 2001. Mpe1, a zinc knuckle protein, is an essential component of yeast cleavage and polyadenylation factor required for the cleavage and polyadenylation of mRNA. *Molecular and Cellular Biology,* 21**,** 8346–8356.

WALCZAK, H., IWAI, K. & DIKIC, I. 2012. Generation and physiological roles of linear ubiquitin chains. *BMC biology,* 10**,** 1.

WANG, J. & MALDONADO, M. A. 2006. The ubiquitin-proteasome system and its role in inflammatory and autoimmune diseases. *Cell Mol Immunol,* 3**,** 255-261.

WARD, J. 1988. DNA damage produced by ionizing radiation in mammalian cells: identities, mechanisms of formation, and reparability. *Progress in nucleic acid research and molecular biology,* 35**,** 95-125.

WARIS, S., CHARLES, M., WILCE, J. & WILCE, J. A. 2014. RNA Recognition and Stress Granule Formation by TIA Proteins. *Int. J. Mol. Sci.,* 15**,** 23377-23388.

WATKINS, J. F., SUNG, P., PRAKASH, L. & PRAKASH, S. 1993. The Saccharomyces cerevisiae DNA repair gene RAD23 encodes a nuclear protein containing a

135

ubiquitin-like domain required for biological function. *Molecular and cellular biology,* 13**,** 7757-7765.

WEI-FENG, L., SHAN-SHAN, Y., GUAN-JUN, C. & YUE-ZHONG, L. 2006. DNA damage checkpoint, damage repair, and genome stability. *Acta Genetica Sinica,* 33**,** 381-390.

WILSON, R. C., EDMONDSON, S. P., FLATT, J. W., HELMS, K. & TWIGG, P. D. 2011. The E2-25K ubiquitin-associated (UBA) domain aids in poly-ubiquitin chain synthesis and linkage specificity. *Biochemical and biophysical research communications,* 405**,** 662-666.

WILSON, R. C., HUGHES, R. C., FLATT, J. W., MEEHAN, E. J., NG, J. D. & TWIGG, P. D. 2009. Structure of full-length ubiquitin-conjugating enzyme E2-25K (huntingtin-interacting protein 2). *Acta Crystallographica Section F: Structural Biology and Crystallization Communications,* 65**,** 440-444.

WITTE, M. M. & SCOTT, R. E. 1997. The proliferation potential protein-related (P2P-R) gene with domains encoding heterogeneous nuclear ribonucleoprotein association and Rb1 binding shows repressed expression during terminal differentiation. *Proc Natl Acad Sci U S A,* 94**,** 1212-1217.

WOGAN, G. N., HECHT, S. S., FELTON, J. S., CONNEY, A. H. & LOEB, L. A. Environmental and chemical carcinogenesis. Seminars in cancer biology, 2004. Elsevier, 473-486.

WOLFFE, A. P. 1994. Structural and functional properties of the evolutionarily ancient Y-box family of nucleic acid binding proteins. *BioEssays,* 16**,** 245–251.

WU, C. 1995. Heat shock transcription factors: structure and regulation. *Annu Rev Cell Dev Biol,* 11**,** 441–469.

YOSHITAKE, Y., NAKATSURA, T., MONJI, M., SENJU, S., MATSUYOSHI, H., TSUKAMOTO, H., HOSAKA, S., KOMORI, H., FUKUMA, D., IKUTA, Y., KATAGIRI, T., FURUKAWA, Y., HIROMI, I., SHINOHARA, M., NAKAMURA, Y. & NISHIMURA, Y. 2004. Proliferation Potential-Related Protein, an ideal esophageal cancer antigen for immunotherapy, identified using complementary DNA microarray analysis. *Clinical Cancer Research,* 10**,** 6437–48.

YU, A., LI, P., TANG, T., WANG, J., CHEN, Y. & LIU, L. 2015. Roles of Hsp70s in Stress Responses of Microorganisms, Plants, and Animals. *Biomed Res Int,* 2015**,** 2015.

ZHANG, Y. F., HOMER, C., EDWARDS, S. J., HANANEIA, L., LASHAM, A., ROYDS, J., SHEARD, P. & BRAITHWAITE, A. W. 2003. Nuclear localization of Y-box factor YB1 requires wild-type p53. *Oncogene,* 22**,** 2782-2794.

ZHARKOV, D. 2008. Base excision DNA repair. *Cellular and molecular life sciences,* 65**,** 1544-1565.

ZHOU, B. S. & ELLEDGE, S. J. 2000. The DNA damage response: putting checkpoints in perspective. *Nature,* 408**,** 433-439.

APPENDIX I

LIST OF REAGENTS AND SUPPLIERS FOR *IN VITRO* STUDIES

Reagent	Supplier
Absolute ethanol	Merck
Agarose	Separations
Ammonium persulphate	BioRad
Ampicillin	Melford
Bovine serum albumin	Roche
Casein	Sigma
Dithiothreitol (DTT)	Melford
EDTA-free protease inhibitor cocktail	Roche
Fetal bovine serum	Roche
Formaldehyde	Merck
GeneJet Gel Purification Kit	Thermo Fisher Scientific
GeneJet Plasmid maxiprep Kit	Thermo Fisher Scientific
GeneJet Plasmid miniprep Kit	Thermo Fisher Scientific
Glacial acetic acid	Merck
Glycerol	Merck
Glycine	Merck
Isopropanol	Merck
Luria Bertani broth	Merck
MG132 (proteasome inhibitor)	Sigma

http://etd.uwc.ac.za/

N,N,N`,N`-Tetra methylene-diamine	BioRad
Nuclease free water	Qiagen
Nutrient agar	Merck
Polyethylene glycol 4000	Merck
Protease inhibitor cocktail	Roche
Reduced-L-glutathione (GSH)	Sigma
Restriction enzymes	Thermo Fisher Scientific
Snakeskin® Dialysis tubing	Separations
Sodium chloride	Merck
T4 DNA ligase	Thermo Fisher Scientific
Tris [Hydroxymethyl] aminomethane	Merck
Triton X-100	Merck
Tween® 20	Merck
Zinc sulphate	Merck

(B) LIST OF REAGENTS AND SUPPLIERS FOR *IN VIVO* STUDIES

Countess® Cell Counting Chamber Slides	Thermo Fisher Scientific
PBS	Lonza
DMEM F12	Lonza
DMEM	Lonza
Fetal bovine serum	The Scientific Group
Penicillin-streptomycin	The Scientific Group
Trypsin-Versene (EDTA) mixture 1X	Whitehead Scientific

Trypan Blue Solution, 0.4%	Thermo Fisher Scientific
Formaldehyde	Merck
Methanol	Merck
X-tremeGENE DNA Transfection Reagent	Roche

(C) LIST OF GENERAL STOCK SOLUTIONS, BUFFERS AND MEDIA

2X SDS gel sample buffer: 4% SDS, 0.125 M Tris pH 6.8, 15% glycerol and 1 mg/ml bromophenol blue. The buffer was stored at room temperature and 10% β-mercaptoethanol was added prior to use.

10 X PBS: 1.37 M NaCl, 0.027 mM KCl, 0.08 M Na2HPO4, 0.015 M KH_2PO_4 pH 7.4.

10 X running buffer: 25 mM Tris, 0.1 % (m/v) SDS and 250 mM Glycine.

Ampicillin: A 100 mg/ml solution was made in dH_2O water, filter sterilised and stored at -20 °C.

Ammonium persulphate: A 10 % stock solution was prepared in dH_2O. The solution was stored at -20 °C.

Cell lysis buffer: 5 mM β-mercaptoethanol, 0.5% Triton X-100 and Complete™ EDTA-free protease inhibitor cocktail in 1X PBS.

Binding buffer: 1 mM DTT, 5% BSA in 1X PBS.

Coomassie staining solution: 0.25 g Comassie Blue R-250, 40 % ethanol and 10 % acetic acid in 250 ml of dH_2O water.

DTT: 1M stock was prepared and stored at -20 °C.

Glutathione agarose cleansing buffer 1: 1 M boric acid, 0.5 M NaCl and adjusted to pH 8.5.

140

Glutathione agarose cleansing buffer 2: 1 M acetate and 0.5 M NaCl, adjusted to pH 4.5

IPTG: A 1M stock was prepared in distilled water, filter sterilized, aliqouted and stored and -20 °C.

Luria broth: 25g of Luria Bertani broth dissolved in 1 L of distilled water.

Luria Bertani Agar: 10 g/l tryptone, 5 g/l yeast extract, 5 g/l sodium chloride and 10 g/l agar in dH_2O

Protein Elution Buffer: 20 mM reduced glutathione in 1x PBS and used immediately.

Protein Wash Buffer: 1x PBS, 1 mM β-mercaptoethanol.

Transformation buffer 1 (Tfb1): 30 mM Potassium acetate, 50 mM MnCl2, 0.1 M KCl, 10mM $CaCl_2$ and 15 % (v/v) glycerol.

Transformation buffer 2 (Tfb2): 9 mM MOPS, 10 mM KCl, 50 mM $CaCl_2$, and 15 % (v/v) glycerol.

UNIVERSITY *of the*

WESTERN CAPE
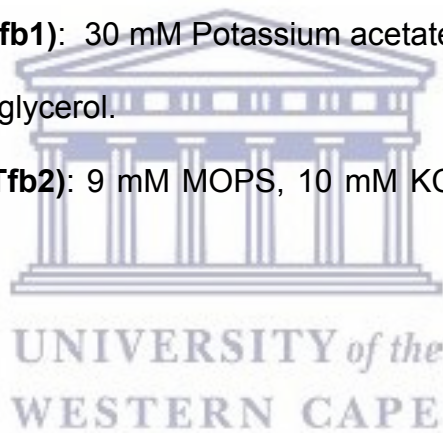
APPENDIX II: VERIFICATION OF CLONED GENE SEQUENCES OF VARIOUS CONSTRUCTS

(A) SEQUENCE VERIFICATION OF UBA CLONED INTO pGEX-6-P2 vector

```
Query  945   GGATCCAGTCCAGAATACACCAAAAAAATAGAAAACCTATGTGCTATGGGCTTTGATAGG   1004
             ||||||||||||||||||||||||||||||||||||||||||||||||||||||||||||
Sbjct  144   GGATCCAGTCCAGAATACACCAAAAAAATAGAAAACCTATGTGCTATGGGCTTTGATAGG   85

Query  1005  AATGCAGTAATAGTGGCCTTGTCTTCAAAATCATGGGATGTAGAGACTGCAACAGAATTG   1064
             ||||||||||||||||||||||||||||||||||||||||||||||||||||||||||||
Sbjct  84    AATGCAGTAATAGTGGCCTTGTCTTCAAAATCATGGGATGTAGAGACTGCAACAGAATTG   25

Query  1065  CTTCTGAGTAACTGATAACTCGAG   1088
             ||||||||||||||||||||||||
Sbjct  24    CTTCTGAGTAACTGATAACTCGAG   1
```

Restriction sites are highlighted in yellow (BamHI) and green (XhoI). 'Query' denotes the expected sequence and 'Sbjct' denotes the experimentally-determined sequence of the cloned insert. Stop codons TGA and TAA are highlighted in red.

142
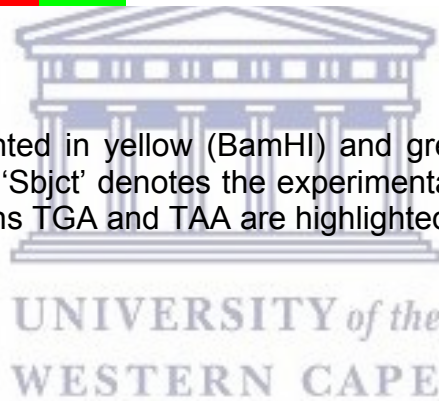
(B) SEQUENCE VERIFICATION OF DWNN13 CLONED INTO FLAG pcDNA3

```
Query   931   GGATCCATGTCCTGTGTGCATTATAAATTTTCCTCTAAACTCAACTATGATACCGTCACC   990
              ||||||||||||||||||||||||||||||||||||||||||||||||||||||||||||
Sbjct   1     GGATCCATGTCCTGTGTGCATTATAAATTTTCCTCTAAACTCAACTATGATACCGTCACC   60

Query   991   TTTGATGGGCTCCACATCTCCCTCTGCGACTTAAAGAAGCAGATTATGGGGAGAGAGAAG   1050
              ||||||||||||||||||||||||||||||||||||||||||||||||||||||||||||
Sbjct   61    TTTGATGGGCTCCACATCTCCCTCTGCGACTTAAAGAAGCAGATTATGGGGAGAGAGAAG   120

Query   1051  CTGAAAGCTGCCGACTGCGACCTGCAGATCACCAATGCGCAGACGAAAGAAGAATATACT   1110
              ||||||||||||||||||||||||||||||||||||||||||||||||||||||||||||
Sbjct   121   CTGAAAGCTGCCGACTGCGACCTGCAGATCACCAATGCGCAGACGAAAGAAGAATATACT   180

Query   1111  GATGATAATGCTCTGATTCCTAAGAATTCTTCTGTAATTGTTAGAAGAATTCCTATTGGA   1170
              ||||||||||||||||||||||||||||||||||||||||||||||||||||||||||||
Sbjct   181   GATGATAATGCTCTGATTCCTAAGAATTCTTCTGTAATTGTTAGAAGAATTCCTATTGGA   240

Query   1171  GGTGTTAAATCTACAAGCAAGACATATGTTATAAGTCGAACTGAACCAGCGATGGCAACT   1230
              ||||||||||||||||||||||||||||||||||||||||||||||||||||||||||||
Sbjct   241   GGTGTTAAATCTACAAGCAAGACATATGTTATAAGTCGAACTGAACCAGCGATGGCAACT   300

Query   1231  ACAAAAGCAGTATGTAAAAACACAATCTCACACTTTTTCTACACATTGCTTTTACCTTTA   1290
              ||||||||||||||||||||||||||||||||||||||||||||||||||||||||||||
Sbjct   301   ACAAAAGCAGTATGTAAAAACACAATCTCACACTTTTTCTACACATTGCTTTTACCTTTA   360

Query   1291  TAATGATCTAGA   1302
              ||||||||||||
Sbjct   361   TAATGATCTAGA   372
```
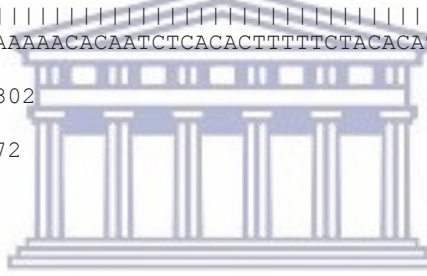
Restriction sites are highlighted in green (BamHI) and yellow (XbaI). 'Query' denotes the expected sequence and 'Sbjct' denotes the experimentally-determined sequence of the cloned insert. Stop codons TAA and TGA are highlighted in red.

(C) SEQUENCE VERIFICATION OF DWNN PI CLONED INTO pCMV-UWC VECTOR

```
Query  875   CTCGAGCTTCCTGTGTGCATTATAAATTTTCCTCTAAACTCAACTATGATACCGTCACCT   934
             ||||||||||||||||||||||||||||||||||||||||||||||||||||||||||||
Sbjct  248   CTCGAGCTTCCTGTGTGCATTATAAATTTTCCTCTAAACTCAACTATGATACCGTCACCT   189

Query  935   TTGATGGGCTCCACATCTCCCTCTGCGACTTAAAGAAGCAGATTATGGGGAGAGAGAAGC   994
             ||||||||||||||||||||||||||||||||||||||||||||||||||||||||||||
Sbjct  188   TTGATGGGCTCCACATCTCCCTCTGCGACTTAAAGAAGCAGATTATGGGGAGAGAGAAGC   129

Query  995   TGAAAGCTGCCGACTGCGACCTGCAGATCACCAATGCGCAGACGAAAGAAGAATATACTG   1054
             ||||||||||||||||||||||||||||||||||||||||||||||||||||||||||||
Sbjct  128   TGAAAGCTGCCGACTGCGACCTGCAGATCACCAATGCGCAGACGAAAGAAGAATATACTG   69

Query  1055  ATGATAATGCTCTGATTCCTAAGAATTCTTCTGTAATTGTTAGAAGAATTCCTATTTAAT   1114
             ||||||||||||||||||||||||||||||||||||||||||||||||||||||||||||
Sbjct  68    ATGATAATGCTCTGATTCCTAAGAATTCTTCTGTAATTGTTAGAAGAATTCCTATTTAAT   9

Query  1115  GAGGTACC   1122
             ||||||||
Sbjct  8     GAGGTACC   1
```

Restriction sites are highlighted in green (XhoI) and blue (KpnI). 'Query' denotes the expected sequence and 'Sbjct' denotes the experimentally-determined sequence of the cloned insert. Stop codons TAA and TGA are highlighted in red.

144

(D) SEQUENCE VERIFICATION OF DWNN13-AA CLONED INTO pCMV-UWC

```
Query   875   CTCGAGCTTCCTGTGTGCATTATAAATTTTCCTCTAAACTCAACTATGATACCGTCACCT   934
              ||||||||||||||||||||||||||||||||||||||||||||||||||||||||||||
Sbjct   371   CTCGAGCTTCCTGTGTGCATTATAAATTTTCCTCTAAACTCAACTATGATACCGTCACCT   312

Query   935   TTGATGGGCTCCACATCTCCCTCTGCGACTTAAAGAAGCAGATTATGGGGAGAGAGAAGC   994
              ||||||||||||||||||||||||||||||||||||||||||||||||||||||||||||
Sbjct   311   TTGATGGGCTCCACATCTCCCTCTGCGACTTAAAGAAGCAGATTATGGGGAGAGAGAAGC   252

Query   995   TGAAAGCTGCCGACTGCGACCTGCAGATCACCAATGCGCAGACGAAAGAAGAATATACTG   1054
              ||||||||||||||||||||||||||||||||||||||||||||||||||||||||||||
Sbjct   251   TGAAAGCTGCCGACTGCGACCTGCAGATCACCAATGCGCAGACGAAAGAAGAATATACTG   192

Query   1055  ATGATAATGCTCTGATTCCTAAGAATTCTTCTGTAATTGTTAGAAGAATTCCTATTGCTG   1114
              ||||||||||||||||||||||||||||||||||||||||||||||||||||||||||||
Sbjct   191   ATGATAATGCTCTGATTCCTAAGAATTCTTCTGTAATTGTTAGAAGAATTCCTATTGCTG   132

Query   1115  CCGTTAAATCTACAAGCAAGACATATGTTATAAGTCGAACTGAACCAGCGATGGCAACTA   1174
              ||||||||||||||||||||||||||||||||||||||||||||||||||||||||||||
Sbjct   131   CCGTTAAATCTACAAGCAAGACATATGTTATAAGTCGAACTGAACCAGCGATGGCAACTA   72

Query   1175  CAAAAGCAGTATGTAAAAACACAATCTCACACTTTTTCTACACATTGCTTTTACCTTTAT   1234
              ||||||||||||||||||||||||||||||||||||||||||||||||||||||||||||
Sbjct   71    CAAAAGCAGTATGTAAAAACACAATCTCACACTTTTTCTACACATTGCTTTTACCTTTAT   12

Query   1235  AATGAGGTACC   1245
              |||||||||||
Sbjct   11    AATGAGGTACC   1
```

Restriction sites are highlighted in yellow (XhoI) and green (KpnI). 'Query' denotes the expected sequence and 'Sbjct' denotes the experimentally-determined sequence of the cloned insert. Stop codons TAA and TGA are highlighted in red. Mutated bases are highlighted in cyan.

```
ctcgagcttcctgtgtgcattataaattttcctctaaactcaactatgataccgtcacctttt
   R  A  S  C  V  H  Y  K  F  S  S  K  L  N  Y  D  T  V  T  F
gatgggctccacatctccctctgcgacttaaagaagcagattatggggagagagaagctg
 D  G  L  H  I  S  L  C  D  L  K  K  Q  I  M  G  R  E  K  L
aaagctgccgactgcgacctgcagatcaccaatgcgcagacgaaagaagaatatactgat
 K  A  A  D  C  D  L  Q  I  T  N  A  Q  T  K  E  E  Y  T  D
gataatgctctgattcctaagaattcttctgtaattgttagaagaattcctattgctgcc
 D  N  A  L  I  P  K  N  S  S  V  I  V  R  R  I  P  I  A  A
gttaaatctacaagcaagacatatgttataagtcgaactgaaccagcgatggcaactaca
 V  K  S  T  S  K  T  Y  V  I  S  R  T  E  P  A  M  A  T  T
aaagcagtatgtaaaaacacaatctcacactttttctacacattgctttatacccttttataa
 K  A  V  C  K  N  T  I  S  H  F  F  Y  T  L  L  L  P  L  -
tgaggtacc
 -  G  T
```

Translated amino acid sequence of DWNN13-AA

145